Investigation of N-methyl-D-aspartate receptor autoimmunity

By

Brian E. Jones

A DISSERTATION

Presented to the Neuroscience Graduate Program

and the Oregon Health & Science University

School of Medicine

in partial fulfillment of the requirements for the degree of

Doctor of Philosophy

February 2019

School of Medicine

Oregon Health & Science University

CERTIFICATE OF APPROVAL

This is to certify that the Ph.D. dissertation of

Brian E. Jones

has been approved February 2019

Advisor, Gary L. Westbrook, MD

Member and Chair, Jacob Raber, PhD

Member, Dennis Bourdette, MD

Member, Eric Gouaux, PhD

Table of Contents

List of Figures

Acknowledgements

I would like to express my deepest appreciation to everyone who supported me during graduate education. I am indebted to my mentor Gary L. Westbrook for his guidance and patience. He gave me a place in the OHSU neuroscience graduate program and his lab, acting as my constant advocate even when my research endeavors floundered. Of course, without the assistant of Eric Gouaux and his lab members, April Goehring, Xianqiang Song, and Farzad Jalali-Yazdi none of this work would have been possible. I would like to give a special thanks to April Goehring who provided the bulk of the reagents used to generate our mouse model and offered technical support at every turn. Professor Jacob Raber not only served as my committee chair, he opened up his lab in order for me to conduct the behavioral assessments described in this work. Also invaluable to the behavioral component of this project was the training and assistance I received from Sydney Weber Boutros. Dr. Dennis Bourdette served as a member of my committee offer constructive criticism and support throughout. While his lab members, Gail Marracci and Priya Chaudhary were integral in planning the immunopathology assessments described in this work. The members of the OHSU microscopy core, Stefanie Kaech Petrie, Aurelie Snyder and Crystal Chaw provided invaluable training. Whereas Ken Tovar swept in at the eleventh hour to save me from spending another fruitless year trying to master electrophysiology. Lastly, my parents, wife and daughter never failed to provide unconditional love and support. This list is woefully incomplete representing a fraction of the people who offered friendship, support and love. To all those I have failed to recognize here I offer my sincere gratitude.

Abstract

Autoimmunity to membrane proteins in the central nervous system has been increasingly recognized as a cause of neuropsychiatric disease. A key recent development was the discovery of antibodies to NMDA receptors in some cases of encephalitis, characterized by cognitive changes, memory loss, seizures, and sometimes long-term morbidity or mortality. Treatment approaches and experimental studies have largely focused on the pathogenic role of these autoantibodies. Passive antibody transfer to mice has provided useful insights but does not produce the full spectrum of the human disease. Here we describe a unique *de novo* autoimmune mouse model of anti-NMDA receptor encephalitis. Active immunization of immune competent mice with conformationally-stabilized, native-like NMDA receptors induced a fulminant encephalitis with behavioral and pathologic characteristics similar to those observed in the human disorder. Our results provide evidence for neuroinflammation and immune cell infiltration as a component of the autoimmune response in mice. Use of transgenic mice indicated that mature T cells as well as antibody-producing cells were required for disease induction. Our results provide insights into disease pathogenesis as well as a platform for testing mechanisms of disease initiation and therapeutic approaches.

General Overview

The human experience is fundamentally emergent, arising from the complex interplay of external and internal stimuli as processed and interpreted in the central nervous system (CNS). As such, our ability to engage our environment, learn, think, and emote relies upon proper communication between the cellular constituents of the CNS (Nichols and Newsome, 1999). Neurotransmitter receptors and related synaptic proteins are essential to this process (Mayford et al., 2012; Newcomer and Krystal, 2001). Thus, perturbations to such proteins often result in profound behavioral and cognitive aberrations (Koob and Volkow, 2016; Lepeta et al., 2016; van Spronsen and Hoogenraad, 2010). In the past decade, autoimmunity to a variety of neuronal cell-surface proteins has been linked to encephalitides with neuropsychiatric symptoms (Dalmau et al., 2017; Zong et al., 2017). In a subset of these disorders the symptomatology, target antigen, and patient response to immunomodulatory therapies indicate a pathophysiological roll for the associated autoantibodies (Dalmau et al., 2017; Zong et al., 2017). This pattern is in contrast to several previously identified paraneoplastic syndromes of the CNS in which antibodies generated against onconeuronal antigens target intracellular proteins and are often considered diagnostic rather than pathogenic (Dalmau and Rosenfeld, 2008; Darnell and Posner, 2006). Instead, this new class of “autoimmune encephalopathies” appears to resemble the myasenthic syndromes of the peripheral nervous system in which the autoantibodies themselves are capable of directly disrupting synaptic proteins (Drachman et al., 1982; Nagel et al., 1988).

To date, sixteen such “autoimmune encephalopathies” have been recognized (Dalmau et al., 2017). The autoantibodies associated with these disorders target a variety of synaptic proteins including, but not limited to, ionotropic and metabotropic neurotransmitter receptors, voltage-gated ion channels, proteins involved in endocytosis, cell-adhesion molecules, and synaptogenic proteins (Dalmau et al., 2017; Zong et al., 2017). In a subset of these disorders the associated clinical syndrome is stereotyped, as in anti-*N*-Methyl-D-Aspartate (NMDA) receptor encephalitis in which a patient often presents with a prodromal flu-like malaise followed by rapid onset of psychiatric (e.g. confusion, aggressive behaviors) and neurologic signs (e.g., memory impairment, dyskinesias, seizures, autonomic instability). In other autoimmune encephalopathies the clinical course is less distinctive, with many of the disorders sharing similar signs and symptoms. For a few of these disorders, laboratory investigations have demonstrated a pathogenic potential for the associated autoantibodies via receptor internalization, altering clustering, or allosteric modulation (Dalmau et al., 2017; Zong et al., 2017). In the majority of autoimmune encephalopathies however, our knowledge of the role of autoantibodies in disease progression is incomplete. How, for example, does antibody mediated receptor internalization contribute to CNS inflammation?

In Chapter 1 I will review the unique nature of CNS immunity. I will then discuss autoantibody-associated diseases of the central nervous system with emphasis on the clinical and pathophysiological features of neuropsychiatric autoimmune disorders. Subsequently I will review the central role played by the NMDA receptor in the healthy

brain In Chapter 2, I describe our experiments developing a unique mouse model of the associated autoimmune encephalitis. Finally, in Chapter 3 I outline the limitations of the model and describe a set of future experiments aimed at its further characterization and application in translational medicine.

Chapter 1: *CNS Immunity and autoimmune encephalitis*

The central nervous system (CNS) is unique in terms of the structural and cellular components composing its immunological repertoire. Possessing a single macrophage population in the parenchyma proper, and sheathed in a complex physical barrier limiting peripheral immune cell access, the response of the CNS to infection or injury varies greatly from other organ systems. Exemplifying this difference, immunogenic agents administered directly into the parenchyma of the central nervous system fail to, or are very slow to, initiate the adaptive immune response that occurs in peripheral tissues. Thus, by definition, the CNS is a site of 'immune privilege' (Galea et al., 2007). However, the brain, spinal cord, and retinal tissues constituting the CNS are able to recruit peripheral immune players when confronted with immune challenges beyond the capacity of CNS-resident immune cells to resolve. Furthermore, constant surveillance by resident myeloid cells, located in parenchymal, meningeal, and perivascular tissues, as well as other leukocytes circulating in the cerebral spinal fluid that baths the CNS, aid in immunological defense of the brain. Despite the exquisite regulation of endemic immune players and highly selective barriers sequestering the CNS, the CNS is still susceptible to infection and autoimmunity. In the following sections I will review the elements of the CNS immune system governing its response to immunogens and its dysregulation in the context of autoimmune diseases.

Physical & biochemical barriers to CNS entry

The CNS possesses structural characteristics that help sequester it from peripheral immunogens and limit transit of peripheral leukocytes into the organ proper. The three

meningeal layers surrounding the CNS parenchyma represent a portion of the physical barrier separating and protecting the brain and spinal cord. Of mixed mesenchymal and neural crest origins, the outer most meningeal layer, the dura mater, is composed of tough connective tissue juxtaposed to the cranium. Next, the arachnoid and pia mater, or leptomeninges, are separated by arachnoid trabeculae to create the CSF-filled subarachnoid space (Fig. i;(Prinz and Priller, 2017)). Blood vessels entering the CNS are initially lined by the leptomeninges, creating perivascular spaces (Virchow-Robin spaces). In addition to the leptominigeal barrier blood vessels traversing, the CNS possess specialized junctional protein complexes between adjacent cells (zona occludens) that limit the passage of cells and large or polar molecules. Proteins such as occludin, claudin, and junctional adhesion molecules cooperate to make tight junctions. Whereas, cadherins-E, P, and N are responsible for generating adherens junctions (Dando et al., 2014; Lampron et al., 2013). These tight and adherens junctional complexes in the endothelium regulate paracellular transmigration between the periphery and CNS. On the abluminal side of the vessel, endothelial basement membrane combines with astrocytic end feet to create the laminin-rich glia limitans perivascularis, whereas the CNS parenchyma and adjacent astrocytic elements compose the glia limitans superficialis. Together, these structures form the blood-brain barrier (BBB), a major obstruction to the passage of peripheral immune cells as well as antigens circulating in the blood stream (Dando et al., 2014; Daneman and Prat, 2015). However, the BBB is not a static entity, as astrocytes, pericytes, and neurons communicate with each other and the vascular endothelium (neurovascular unit) to regulate blood flow, metabolite transfer, leukocyte entry, and the junctional complexes

themselves (Dando et al., 2014; Prinz and Priller, 2017). Under pathophysiological conditions, cytokines such as tumor necrosis factor α (TNF-α), interleukin-6 (IL-6), and interleukin-1β (IL-1β) mediate the disruption of junctional complexes creating a 'leaky' BBB. Microbes and other pathogens can also compromise the BBB via activation of a host of receptors expressed on the luminal side of the CNS endothelium. For example, chemokine receptors such as the C-C chemokine receptor type 5 (CCR5) and the C-X-C chemokine receptor type 4 (CXCR4), activated by the HIV virus, and the polarity complex Par3/Par6/PKCzeta, high-jacked by meningococcal bacteria, promote degradation of tight junctions to facilitate pathogen entry (Lampron et al., 2013). Transmigration of peripheral leukocytes requires the interaction of vascular cell adhesion molecules (CAMs) with their cognate ligands expressed on immune cells (Takeshita and Ransohoff, 2012). This process will be discussed in detail in future sections.

CNS-Antigen presentation

Under normal physiological conditions, the aforementioned selective barriers tightly regulate the entry of antigen presenting cell (APC) and leukocyte into the CNS parenchyma. Moreover, the healthy CNS is an unwelcoming environment for these peripheral immune cells expressing high levels of TGF-β, interleukin-10, and gangliosides that contribute to their suppression or destruction (Ransohoff and Brown, 2012). Thus, immunogens must leave the CNS to prime an immune response. Lacking a true lymphatic system, the route of egress for antigens in the CNS is via circulating cerebral spinal fluid (Prinz and Priller, 2017). The CSF-brain interface is more

permissive than the blood-brain barrier with interstitial fluid flowing into perivascular and ventricular spaces, where it ultimately enters the blood stream via arachnoid villi. Interstitial fluid may also drain through the perforations of the cribiform plate or by following the path of cranial nerves. Regardless of route, antigens move to the deep cervical lymph nodes where dendritic cells process and present them to lymphocytes, or they are intercepted by resident myeloid cells as they traverse the CSF-brain barrier (Prinz and Priller, 2017). In addition to allowing the immune system to sample foreign immunogens, the flow of interstitial fluid from the CNS to the periphery provides an opportunity for self-antigens to prime an autoimmune response (Dando et al., 2014). However, there are no naïve T-cells in these locations, and in the absence of a disease state, antigen mediated priming of lymphocytes does not occur in the CNS parenchyma (Galea et al., 2007).

In summary, anatomical features specific to the CNS prevent pathogen entry and control peripheral immune cell ingress; whereas, the flow of solutes from the CNS parenchyma into the CSF allows fixed populations of immune cells to surveil and respond to immune insults (Fig. i). During pathophysiological conditions, the BBB can be mechanically compromised, and leukocytes are actively recruited into the CNS. Furthermore, the CSF possesses populations of activated monocytes and memory T cells capable of honing in on regions of neuroinflammation or trafficking to secondary lymph organs to potentiate an adaptive immune response (Prinz and Priller, 2017). Thus, the CNS is far from a sequestered organ system, and rather is in constant communication with the peripheral immune system.

Fig. i The CNS immune system during homeostasis (Prinz and Priller, 2017)

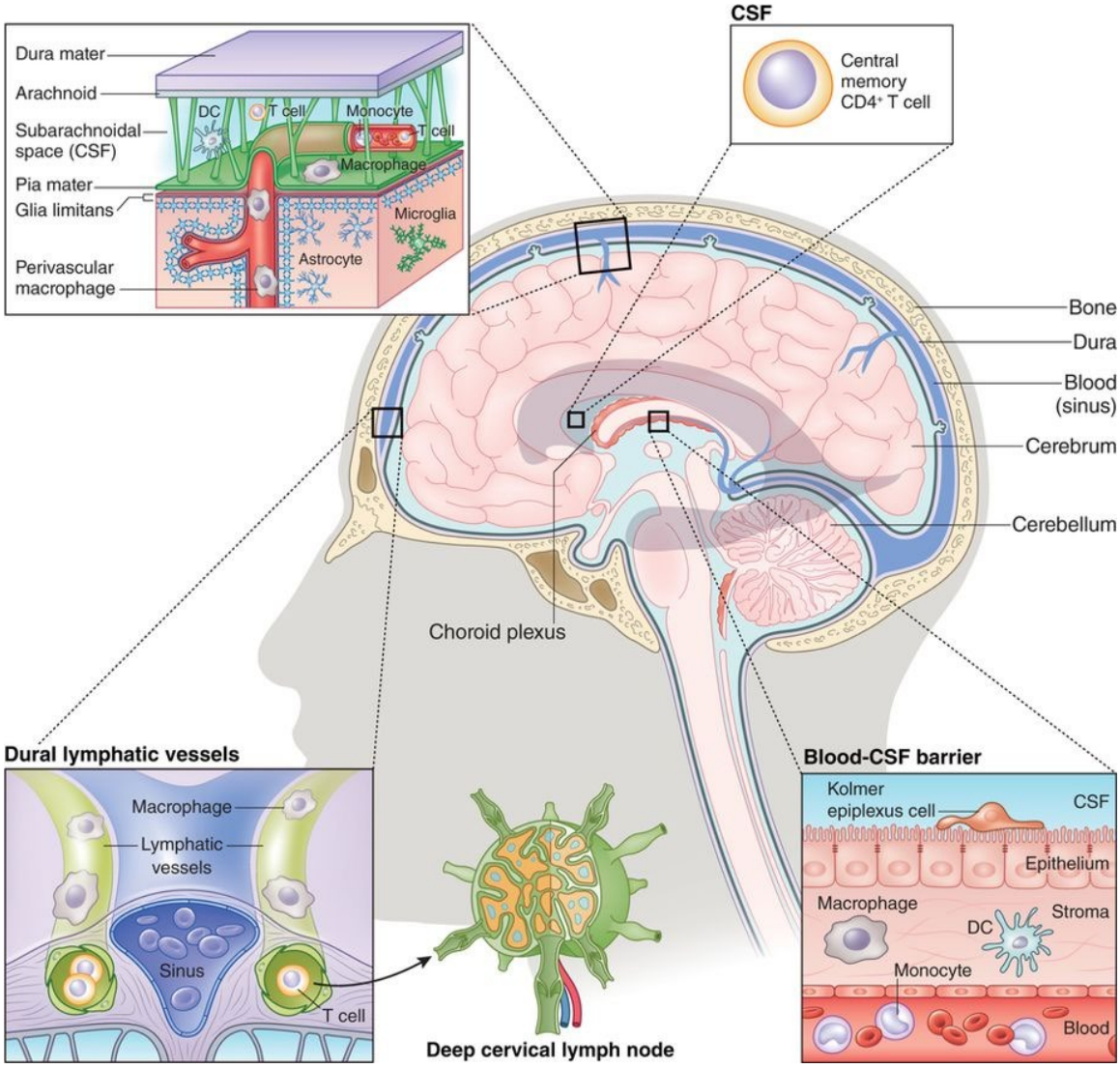

Fig i. "The CNS immune system during homeostasis" The following figure reproduced with permission from Prinz and Priller (2017) illustrates the physical barriers (Blood-Brain and Blood-CSF barriers) that protect the CNS from pathogen entry, the location of extra-parenchymal leukocytes functioning in immune surveillance, and the route of egress for CNS antigens to the deep cervical lymph nodes.

Myeloid cells & Innate Immunity

Cells of the myeloid lineage including tissue resident macrophages, dendritic cells, granulocytes, and monocytes play crucial roles in the defense of the CNS. Each of these cell types are located in particular anatomical niches and serve different functions in the maintenance of CNS health (Prinz and Priller, 2017).

Microglia

Microglia are the sole mononuclear phagocyte found in the CNS parenchyma. Unlike the above myeloid cells, microglia are derived from hematopoietic progenitors in the yolk sac, are long-lived, and undergo self-renewal locally with no further contribution from the bone marrow (Ajami et al., 2007). They enter the CNS at an early embryonic stage where they take up permanent residence. Microglia exist in close apposition to neurons, and under normal physiological conditions function in synaptic pruning, neural circuit development, and neurogenesis. They tile the CNS with highly motile ramified processes capable of dynamically sampling their environs using a host of surface receptors to sense changes in pH, cyto- and chemokine signals, amino acids, and other organic and inorganic moieties. In the absence of disease, microglia exist in an immunosuppressive environment, passively by dint of their isolation from plasma proteins but also through active cell-signaling mechanisms. Neuron-microglial inhibitory signals are mediated by cell-cell or receptor-soluble ligand interactions such as those between CD200-CD200R and CX3CL1-CX3CR1, respectively (Ransohoff and Cardona, 2010).

Under pathophysiological conditions such as a disrupted blood-brain barrier, microglia can sense plasma proteins such as fibronectin through their MAC1 receptor complex (CD11b-CD18 and $\alpha_M\beta_2$-integrin) to take on a more pronounced phagocytic character. Furthermore, microglia respond to Pathogen-Associated and Danger-Associated Molecular Patterns (PAMPs and DAMPs) via canonical pattern recognition receptors (PRRs). Toll-like receptors (TLRs), one family of PRRs, bind extracellular bacterial immunogens such as peptidoglycan triacyl-lipoproteins and lipopolysaccharides to induce proinflammatory cytokine release (e.g. interleukin-1β (IL-β), Tumor necrosis factor-α, and interleukin-12 (IL-12); whereas, bacterial and viral components in the cytoplasm are bound by members of the Nod-Like Receptor (NLR) and RIG-1-like receptor families. For example, the NLR, NOD2 can bind single-stranded viral DNA resulting in NF-κB induction and subsequent cytokine production (Lampron et al., 2013). A subset of both TLR and NLR receptors on microglia respond to endogenous DAMPs such as uric acid and heat-shock proteins released by distressed or dying neurons. In addition, microglia can sense excessive ATP in the interstitium via purinergic receptor-related channels like the p2x7 receptor (Ransohoff and Brown, 2012).

Activated microglia take on an amoeboid morphology indicative of their mononuclear phagocyte lineage. As with peripheral macrophages, an “M1/M2” phenotypic dichotomy is often applied to their CNS counterparts. Microglia are polarized to a cytotoxic “M1” state by proinflammatory cytokines such as TNF-α, IL-1β, and IFN-γ. Upon binding of two or more of these cytokines, microglia increase production of inflammatory mediators including TNF-α, IL-2, and IL-6, as well as cytotoxic agents such as nitric oxide and cyclooxygenase-2. In contrast, “M2” microglia are thought to be tissue-protective.

Activated by interleukin-10 (IL-10), interleukin-4 (IL-4), and interleukin-13 (IL-13), microglia of this phenotype release vascular endothelia growth factor (VEGF) and related cytokines that function in tissue remodeling and repair. However, as we learn more about the *in vivo* responses of microglia, this delineation likely represents the extremes of a continuum (Goldmann and Prinz, 2013).

The role of microglia in CNS autoimmunity is an area of intensive investigation. Early evidence of their involvement in an autoimmune disease stems from histopathological identification of activated microglia surrounding the nascent white-matter lesions in MS patients. Subsequent studies using the Experimental Autoimmune Encephalomyelitis (EAE) mouse model of MS demonstrated that microglia directly contributed to pathogenesis (Goldmann and Prinz, 2013). In these studies, suppression of microglia prior to EAE induction resulted in protracted onset and attenuated severity of the disease state. The polarization of microglia toward a cytotoxic “M1” phenotype has been implicated in EAE pathogenesis. Evidence for this hypothesis stems in part from intravenous treatment with miR-124, a regulatory microRNA suppressing transition to the “M1” state. In these experiments EAE induction and progression was inhibited in mice receiving mi-124. In a complementary set of experiments in which a suppressor of cytokine signaling (SOCS)-3, an inhibitor of proinflammatory cytokine production, was genetically ablated, microglia assumed a predominately M1 phenotype. These SOC3-deficient mice showed early onset of EAE, increased disease severity, and enhanced neuronal death. As mentioned above, “M1” microglia can induce cell death directly by releasing nitric oxide and reactive oxygen species. However, in the context of

autoimmune inflammation, microglia appear to act largely by signaling through leukocytes. For example, IL-12 released from microglia functions in the differentiation of T_H1 cells, considered a critical effector of EAE pathogenesis; whereas, T_H17 cells, a pro-inflammatory lymphocyte, is primed by microglia through IL-17 release. In addition, microglia release a host of chemoattractant chemokines capable of recruiting leukocytes to the CNS. For example, the deletion of CCL2, a chemotactic agent and disruptor of BBB stability, reduced disease severity in EAE. Finally, microglia are capable of direct priming or re-priming of T cell infiltrates. Under pathophysiological conditions microglia upregulate expression of MHC class I and II proteins, as well as the co-stimulatory receptors CD80/86 and CD40. These protein complexes allow microglia to act as antigen presenting cells directing T cells toward an encephalitogenic fate (Goldmann and Prinz, 2013).

Extra-parenchymal macrophages

A second group of macrophages, ontogenetically related to microglia, reside just outside the CNS parenchyma in perivascular spaces, the choroid plexus (Kolmer's cells), and the meninges (Prinz et al., 2017). Unlike microglia, homeostasis of this macrophage population is in part regulated by blood monocytes. In addition, these cells can extravasate into the blood stream to interact with peripheral lymphocytes and move to secondary lymph organs. Perivascular macrophages reside in the glia limitans perivascularis, meningeal macrophages near fibroblast-like cells lining the meninges, and Kolmer cells in the stroma of the choroid plexus. Both parenchymal (microglia) and extra-parenchymal macrophage populations express a common set of surface receptors

such as Iba1, CD11b, CX3CR1, and F4/80 (Prinz et al., 2017). In addition, both cell types express, to varying degrees, receptors involved in antigen-presentation including major histocompatibility complex II (MHCII) and other costimulatory molecules. Under normal physiological conditions only the extraparenchymal macrophage? group of myeloid cells express these receptors at sufficient levels to function in antigen presentation (Ransohoff and Perry, 2009). However, in the context of an autoimmune disease, these cells function in the priming of naïve T cells facilitating T cell transit into the CNS.

Mast Cells

Apart from microglia, mast cells are the only other myeloid derivative extant in CNS parenchyma. Typically found in tissues with significant exposure to external immunogens such as the skin, gastrointestinal tract, and respiratory system, mast cells are classically defined by their antimicrobial function and role in allergic disorders. In both contexts, stimulation of mast cells can induce rapid vesicular degranulation releasing histamine, proteases, and TNF-α, with mediators of inflammation such as eicosanoids and prostaglandins immediately following. The canonical pathway for mast cell activation is antigen-induced IgE aggregation leading to FcεRI receptor cross-linking and subsequent second messenger signaling. However, IgG-specific Fc receptors are also found in abundance, and have been shown in mice to have activating and inhibiting roles (Galli and Tsai, 2012; Sibilano et al., 2014; Urb and Sheppard, 2012). Defined by the expression of C-kit and FcεRI, mast cells take up residence in the CNS early in development and are primarily of the tryptase-chymase phenotype (Ribatti, 2015).

These cells are widely dispersed, residing in the parenchyma of the thalamus, hypothalamus, area postrema, and outside the brain parenchyma in the choroid plexus (Nelissen et al., 2013; Ribatti, 2015). Although sparse in population, mast cells have been implicated in a number of neurologic disorders including Alzheimer's disease, autism, and multiple sclerosis. Vasoactive agents such as histamine and TNFα allow mast cells to directly alter BBB integrity. Mast cells also directly stimulate pro-inflammatory responses in microglia and astrocytes via the release of tryptase and leukotrienes, respectively (Hendriksen et al., 2017). In the context of autoimmunity, the role of mast cells is controversial. Histologically, mast cells accumulate around the demyelinated lesions of MS patients, but experimental evidence is mixed with reports of mast cell potentiation and amelioration of EAE pathology (Hendriksen et al., 2017). However, their involvement in directing various immune cells to sites of injury and infection support an integral role for mast cells in CNS immunity and autoimmunity (Bartholomäus et al., 2009; Kivisäkk et al., 2009).

Astrocytes as immune cells

Derived from neuroepithelial stem cells, astrocytes are the most prevalent glial cell in the CNS. Their myriad roles include maintenance of the BBB, trophic support of neurons, regulation of synaptogenesis, neurotransmitter recycling, and homeostasis of extracellular ions amongst others. As players in CNS immunity, astrocytes express a number of receptors and soluble mediators typically restricted to cells of the innate and adaptive immune system. Their role in innate immunity is exemplified by their expression of the Toll-like receptor-3, a PRR activated by double-stranded viral RNA.

Interestingly, *in vivo* and *in vitro* experiments demonstrate that astrocytic TLR3 activation results in the release of proinflammatory (e.g., nitric oxide, CCL2 and CXCL10) and neuroprotective (e.g., VEGF, NT-4 and CNTF) mediators, reflecting astrocytes dual-role in defense and preservation of the delicate CNS environment (Farina et al., 2007). In addition to anti-viral PRRs, astrocytes possess an extensive antibacterial armament. For example, expression of the intracellular NOD1 and NOD2 proteins allow astrocytes to recognize bacterial peptidoglycan and respond by releasing the proinflammatory interleukin, IL-6; whereas, the SR-MARCO scavenger protein facilitates the recognition of gram-positive and gram-negative bacteria. Astrocyte-microglial interactions also appear critical to innate immune responses. The complex intercommunication between the two glial cells is illustrated by CXCL12/TNFα signaling. Release of CXCL2 by astrocytes prompts microglia to generate significant amounts of TNF-α, which in turn reduces astrocytes' capacity to take up excess glutamate. The resultant excitotoxicity caused by glutamate-induced calcium entry can potentiate neuroinflammation and neuronal loss (Bezzi et al., 2001).

Astrocytes, like microglial and mast cells, bridge the gap between the innate and adaptive immune response, perhaps best illustrated by their role in regulating neuroinflammation. In this context, current evidence points to distinct "protective" and "detrimental" signaling pathways. As an example of the protective role of astrocytes, binding of the normally proinflammatory cytokine IL-6 to the glycoprotein gp130 reduces recruitment of T cells and limits inflammation in a STAT3 dependent mechanism (Colombo and Farina, 2016). *In vivo* studies reveal that genetic ablation of gp130

exacerbates behavioral deficits and immunopathology in EAE models. TGFβ signaling represents another means by which astrocytes modulate neuroinflammation. Activation of TGFβ receptors results in inhibition of proinflammatory cytokine/chemokine production by preventing NFκB nuclear translocation. Thus, the loss of TGFβ signaling in astrocytes increases T cell infiltration, gliosis, and neuronal loss during infection (Colombo and Farina, 2016).

In contrast to their role as mitigators of neuroinflammation, astrocytes express several chemokines that function in recruitment of leukocytes. NFκB-dependent CXCL10 expression by astrocytes is a potent chemoattractant for macrophages, APCs, and T cells. The detrimental effects of CXCL10/CCL2-mediated leukocyte recruitment has been demonstrated indirectly in injury and EAE models. *In vivo* experiments in which production of these chemokines is blocked via NFκB inhibition indicate reduced leukocyte infiltration and improved clinical outcomes (Brambilla et al., 2005; van Loo et al., 2006). In other studies, inflammatory cytokines (i.e. IFN-γ and TNF-α) induced secretion of B cell survival factor (BAFF) by astrocytes and BAFF expression was elevated in astrocytes in demyelinated lesions in MS patients (Krumbholz et al., 2005). In addition to leukocyte recruitment, astrocytes are capable of production and release of pro-inflammatory mediators thus directly contributing to tissue damage. In response to the interleukin IL-17 released by T_H17^+ T cells, astrocytes can upregulate a number of pro-inflammatory cytokines/chemokines and metalloprotease genes, as well as increase iNOS activity. Not surprisingly, blockade of IL-17 mediated signaling leads to reduction of EAE severity (Qian et al., 2007; Trajkovic et al., 2001).

In summary, astrocytes are mediators of CNS immunity with demonstrated roles in both innate and adaptive immune responses. As discussed above, astrocytes are capable of interfacing with other CNS mediators of innate immunity as well as recruiting peripheral leukocytes. Finally, derangement of astrocyte signaling can exacerbate autoimmune responses leading to increased neuroinflammation and tissue damage (Colombo and Farina, 2016; Farina et al., 2007; Liddelow and Barres, 2017).

Adaptive Immunity & the CNS

As mentioned in the introduction to this chapter, the CNS is considered a site of "immune privilege". This concept has led to the misconception that the brain is completely sequestered from the peripheral immune system. The CNS is actually an immunologically active organ in continuous communication with the bodies' greater immune panoply. In the previous sections, I discussed the physical/biochemical barriers (BBB and anti-inflammatory environs), endemic immune cells (microglia, astrocytes and mast cells), and cells involved in immune surveillance (perivascular, meningeal and choroid plexus macrophages) that constitute the unique immunological environment of the CNS. I also considered the afferent pathways (interstitial fluid and CSF drainage) that facilitate communication with the periphery. In this section I discuss the means by which the peripheral immune system accesses the CNS and once there, functions in its protection and at times its derangement.

The vasculature in the meninges and choroid plexus are the most probable routes of peripheral immune cell entry. In the non-pathophysiological state, vascular endothelial cells express cell adhesion molecules (CAMs) only at low levels, preventing the robust adhesion needed by leukocytes for transmigration. In response to a variety of “distress signals,” vascular endothelial cells upregulate expression of CAMs such as intracellular adhesion molecule-1 (ICAM-1) and vascular cell adhesion molecule-2 (VCAM-1). Activated/memory lymphocytes in turn express lymphocyte function-associated antigen-1 (LFA-1) and α4-integrin that recognize the aforementioned CAMs. Although the exact mechanisms of entry remain unknown, evidence points to cytoskeletal rearrangement following leukocyte adhesion, leading to degradation of endothelial tight junctions and subsequent paracellular transmigration. In addition, the BBB is highly responsive to cytokine/chemokine signals such as TNF-α and IL-6, both of which can modulate junctional complexes (Kipnis, 2016; Lampron et al., 2013). In traversing the choroid plexus, leukocytes must first cross the highly fenestrated vascular endothelium and stromal matrix before transmigrating through the tight junctional complexes of the epithelium composing the CSF-Brain barrier. These epithelial cells express the same array of adhesion molecules as described above and thus are likely to mediate leukocyte crossing in a similar manner (Meeker et al., 2012). Our knowledge of mechanisms of entry has outpaced our understanding of the signals involved in recruiting specific immune cell subtypes. Some evidence exists for the expression of major histocompatibility complexes (MHC) on endothelial cells capable of presenting specific antigens to peripheral immune cells (Monso-Hinard et al., 1997; Wheway et al., 2013), although these MHCs do not appear to play a role in the activation of leukocytes.

The types of CAMs expressed by endothelial cells, as well as the milieu of cytokines and chemotactic molecules released by CNS resident immune cells, also appear to function in the selection of specific immune cells (Lampron et al., 2013; Takeshita and Ransohoff, 2012).

Our understanding of the pathologic mechanisms of infiltrating leukocytes comes largely from the study of EAE. In this context, autoreactive leukocytes initially activated and expanded in the periphery, enter the CNS where they are re-primed by resident APCs. For decades, one of the primary effectors of autoimmunity in EAE was considered to be the $CD4^+$ T_H1 cell. Although a preponderance of new evidence has forced a revision of the established CD4+ T_H1 paradigm, a brief review of its presumed role is informative (Goverman, 2009; Wu and Alvarez, 2011). $CD4^+$ T_H1 cells require IL-12, a product of activated microglia, for differentiation and are characterized by their expression of TNFα, IL-2, and IFNγ. High levels of TNFα in the CNS have been linked to chronic inflammation, white matter degeneration, and seizures (Probert et al., 1997); whereas, IFNγ has been shown to increase MHC class II expression and attract macrophages of the cytotoxic M1 phenotype. Thus, $CD4^+$ T_H1 certainly process the biochemical armament required to damage the CNS.

In the last decade $CD4^+$ T_H17 cells have taken center stage in discussion of CNS autoimmunity. Their contribution to CNS inflammation is suggested by their ability to "produce the pro-inflammatory cytokines IL-17A and IL-7F, and their ability to either directly synthesize or induce other cell types to produce many pro-inflammatory

mediators such as IL-6, granulocyte/macrophage colony-stimulating factor (GM-CSF), matrix metalloproteinases and CXC chemokines including CXCL8 (a potent neutrophil chemoattractant)" (Goverman, 2009). Their involvement in CNS autoimmunity is underscored by a number of studies using the EAE model. For example, IL-23 deficient mice, a critical cytokine for T_H17 activation, are resistant to EAE induction; whereas, the "neutralizing IL-17 activity ameliorated EAE" (Goverman, 2009).

$CD8^+$ T cell responses in the CNS are linked to a number of paraneoplastic autoimmune encephalopathies as well as having a demonstrated role in EAE and MS pathogenesis. In the latter disorders, $CD8^+$ T cells outnumber $CD4^+$ T cells in active white matter tract lesions. In the former diseases, areas of profound cell death are commonly inundated with cytotoxic $CD8^+$ T cells. Priming of these cytotoxic lymphocytes requires MHC class I antigen presentation. Interestingly, there is some evidence of a predisposition to MS linked to expression of the MHC class I HLA-A3 genetic variant. $CD8^+$ T cells are traditionally associated with defense against intracellular pathogens. When primed, these cells have three primary means of destroying the instigating pathogen. First, they express the pro-inflammatory cytokines TNF-α and IFN-γ. Second, they release cytotoxic granules containing perforin and granzymes. Perforins are pore-forming proteins capable of punching holes in the plasma membrane. Granzymes, are serine proteases that enter the target cell through the pores created by perforins. Finally, they express FasL which binds to the Fas receptor expressed on the surface of compromised cells. The FasL/Fas interaction induces a caspase cascade inducing apoptosis (Zhang and Bevan, 2011). Each of these mechanism can induce cell death

and axonal degeneration in the aforementioned autoimmune disorders (Goverman, 2009; Korn and Kallies, 2017; Wu and Alvarez, 2011).

B and plasma cells, along with the immunoglobulins they produce, are typically involved in many autoimmune disorders of the CNS. Despite this fact, the mechanisms by which these immunoglobulins contribute to CNS damage is a subject of some controversy. In MS, mixed reports of autoantibodies directed against myelin constituents have been reported; however, a pathogenic mechanism remains elusive. Complement and IgG deposits in MS plaques suggest opsonization, antibody-mediated phagocytosis, as one means of B cell-initiated tissue damage. Modulation of T cells represents another, albeit indirect, means by which B cells may contribute to autoimmune pathogenesis. For example, pharmacological depletion of B cells has been shown to reduce IFN-γ expression in T cells. Conversely, B cells from MS patients produced more TNF-α and lymphotoxin when stimulated by T cells. Thus, the interplay between the two lymphocyte populations may reinforce pro-inflammatory signals creating a cytotoxic environment (Wu and Alvarez, 2011). I will discuss direct antibody-mediated pathogenesis in the next section.

In summary, although diverse in their pathogenesis, all CNS autoimmune diseases represent a derangement of the innate and adaptive immune systems (Fig. ii). CNS resident immune cells may directly cause tissue damage, recruit peripheral effectors, or function in both roles; whereas, peripheral immune cells must be primed outside of the

CNS, traverse the brains physical and biochemical barriers, and be re-activated upon entry to participate in disease progression.

Fig. ii "Histopathological characteristics of neuroinflammation versus neurodegeneration in humans" (Prinz and Priller, 2017)

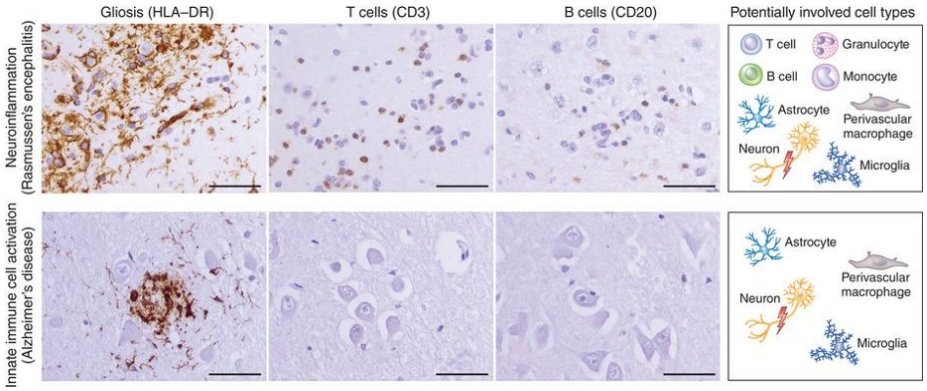

Fig. ii "Histopathological characteristics of neuroinflammation versus neurodegeneration in humans" reproduced with permission from Prinz and Priller (2017) illustrates the different roles of glia and peripheral immune cells in neuroinflammation as compared to neurodegeneration.

Autoimmune encephalitides

Perhaps the best known autoimmune diseases of the nervous system, myasthenia gravis and multiple sclerosis, involve reaction to autoantigens of muscle and glia, respectively. However, a subset of CNS autoimmune disorders involve loss of self-tolerance to neuronal proteins. In many such diseases, the antibodies produced serve a diagnostic role without proven pathogenic potential. However, as outlined in the introduction, the autoantibodies observed in a expanding list of autoimmune encephalopathies appear to have direct pathophysiological effects. In the following section, I review the reported pathology, instigating factors underling loss of self-

tolerance, and role of autoantibodies prior to describing CNS autoimmunity characterized by expression of anti-NMDA receptor antibodies.

Paraneoplastic neurologic syndromes (PNS)

Paraneoplastic neurologic syndromes represent a broad category of diseases in which neurological dysfunction results from an autoimmune reaction to a peripheral tumor (Darnell and Posner, 2006). The mechanisms of neurologic dysfunction in these disorders are distinct from those caused by “metastases, metabolic or nutritional deficits, infections, coagulopathy, or side effects of cancer treatments,” (Dalmau and Rosenfeld, 2019; UpToDate) with damage to the nervous system isolated to a single cell-type or spanning the neuraxis. As such, the signs and symptoms associated with paraneoplastic neurologic syndromes are heterogeneous, ranging from neuromyopathies, to specific ataxias, to cognitive and personality deficits, often reflecting the part of the nervous system most affected (Pelosof and Gerber, 2010). These syndromes are distinct from paraneoplastic endocrine syndromes in which the associated tumors produce hormones or peptides that alter normal metabolic activities, as in cancer-mediated Cushing’s syndrome, in which ectopically produced adrenocorticotropic hormone leads to excessive cortisol levels and subsequent neurologic aberrations (Kaltsas et al., 2010; Pelosof and Gerber, 2010). Paraneoplastic neurologic syndromes frequently precede detection of the underlying malignancy and result in severe, progressive disorders that can take on a relapse-remitting character (Darnell and Posner, 2006). The neoplasms associated with these syndromes are found anywhere in the body; however, cancers producing neuroendocrine proteins (e.g., small

cell lung cancers), teratomas containing neural tissue common to the ovaries and testes, and tumors found in organs with a immunoregulatory function (e.g., thymus) predominate (Dalmau and Rosenfeld, 2008). These cancers produce onconeural antigens with homologous protein structures to their native counterparts (Dalmau and Rosenfeld, 2008). Although the immunologic mechanisms leading to the immune-cross reaction are not completely understood, evidence suggests that dendritic cells phagocytose cellular debris sloughed from the cancer process, and present these antigens to effector B and T cells, reflecting a breakdown of self-tolerance (Arina et al., 2002; Darnell and Posner, 2006). The mechanisms' underlying loss of self-tolerance is unknown; however, the abnormal characteristics of the associated cancer cells may prime the autoimmune reaction (Darnell and Posner, 2006). In fact, research suggests that the initial recruitment of leukocytes is adaptive, aimed at destroying the neoplasm and autoimmunity is an unintended sequelae (Darnell and DeAngelis, 1993).

Autoantibodies are found in the serum and cerebral spinal fluid of seventy percent of patients exhibiting a paraneoplastic neurologic syndrome (Pelosof and Gerber, 2010). These antibodies are broadly grouped based on the intra- or extracellular location of their target. They can be further classified according to: "(1) those that are molecularly well characterized with a strong cancer association (anti-amphiphysin, anti-CV2 [CRMP5], anti-Hu [ANNA-1], anti-Ma2, anti-recoverin, anti-Ri [ANNA-2], anti-Yo [PCA-1]); (2) those that are partially characterized (ANNA-3, anti-mGluR1, anti-Tr, anti-Zic4, PCA-2); or (3) those occurring in both cancer- and non–cancer-associated syndromes

(anti-acetylcholine receptor [AchR], anti–nicotinic AchR, anti-VGCC, anti-VGKC)" (Pelosof and Gerber, 2010).

Intracellular antigens in PNS

In many cases of paraneoplastic autoimmune encephalitis, the self-antigens are intracellular proteins and the resulting autoantibodies possess limited pathogenic capacity (Dalmau and Rosenfeld, 2008; Darnell and Posner, 2006). By contrast, CSF pleocytosis and paraenchymal infiltration of autoreactive T cells are a prominent pathologic finding in many of these paraneoplastic neurologic disorders (Albert and Darnell, 2004). As such, the mechanism of pathogenesis in this class of disorders is thought to be immune (i.e. T) cell-mediated.

One such disorder is paraneoplastic cerebellar degeneration associated with Yo antibodies, targeting the cerebellar degeneration related protein 2. Patients with this condition develop vestibular symptoms followed by rapid onset of cerebellar ataxia, dysarthria, and dysphagia (Dalmau and Rosenfeld, 2008). Anti-Yo antibodies are highly diagnostic of the underlying malignancy. but do not enter neurons and are not directly involved in cell death (Tanaka et al., 1995, 1998). Autopsy samples from these patients do, however, show cytotoxic T cell infiltrates capable of inducing neuronal degeneration via perforin and granzyme B action, clustered around affected cells (Dalmau et al., 2017). Thus, the significant degeneration of cerebellar Purkinje cells observed in patients with this disease is thought to be mediated by cytotoxic T cells rather than autoantibodies.

Anti-Ma2 encephalitis is another paraneoplastic neurologic disorder associated with antibodies to intracellular antigens. Encoded by the paraneoplastic antigen Ma2 gene (PNMA2), the Ma2 protein resides in the nucleus of neurons and germ cells of the testis. Not surprising, testicular tumors are commonly associated with this disorder (Dalmau and Rosenfeld, 2008). The function of Ma2 is unknown; however, sequence homology with the Modulator of Apoptosis 1 (MOA1/PNMA4) protein suggests a pro-apoptotic function (Behr et al., 2007; Tan et al., 2001). Limbic, hypothalamic, and brainstem structures are often involved in this disorder. Thus the clinical presentations have been described as: “in addition to limbic dysfunction, some patients present with excessive daytime sleepiness, narcolepsy, cataplexy, REM-sleep abnormalities, hyperphagia, decrease in CSF concentrations of hypocretin-1, and hypothalamic–pituitary hormonal deficits…” (Dalmau and Rosenfeld, 2008). And, “…other patients present with severe hypokinesis and supranuclear gaze palsy that predominantly involves vertical gaze, and can develop to affect horizontal gaze and cranial nerve nuclei…,”(Dalmau and Rosenfeld, 2008), reflecting involvement of brainstem nuclei. As with Yo-antibodies, Ma2 antibodies do not readily cross the plasma membrane and thus appear diagnostic rather than pathogenic; whereas, perivascular lymphocytic cuffing and perineuronal cytotoxic T-cell infiltrates are common pathological feature of this disorder suggesting a cell-mediated pathogenesis.

The limited pathogenicity of intracellular autoantibodies is not universal. For example, one cancer-associated retinopathy, in which the loss of photoreceptors causes a progressive visual impairment, is thought to be mediated by anti-recoverin antibodies

that directly enter the cell. Once inside photoreceptors, these antibodies may inhibit normal recoverin function leading to a hypo-phosphorylation of rhodopsin and subsequent apoptosis (Ohguro and Nakazawa, 2002). Similarly, autoantibodies against the intracellular BAR-domain protein amphiphysin are thought to play a direct pathophysiologic role in a paraneoplastic variant of stiff-person syndrome (Werner et al., 2016). In this disease patients experience progressive onset of muscle rigidity, thought to be mediated by disruptions in gamma-aminobutyric acid (GABA)-mediated synaptic transmission. Ultrastructural studies using patient-derived amphiphysin antibodies indicate their capacity to impede endocytosis at GABAergic synapses resulting in vesicular depletion (Werner et al., 2016). However, antibody-mediated pathogenesis appears to be the exception rather than the rule for paraneoplastic neurologic disorders associated with intracellular autoantibodies.

Extracellular antigens in PNS

By contrast, antibody-mediated pathogenesis appears to be a relatively common feature of paraneoplastic neurologic disorders associated with autoantibodies to extracellular proteins. Three other characteristics of these disorders further differentiate them from paraneoplastic neurologic syndromes associated with intracellular antigens. First, patients with these disorders tend to be more responsive to immunotherapies. Second, the disruption of the target antigen appears to directly underlie the signs or symptoms. Finally, cell death is a less prominent finding in neuropathological assessment. (Lancaster and Dalmau, 2012).

An archetypic disorder in this category is paraneoplastic Lambert-Eaton myasthenic syndrome (LEMS). Patients with this condition often present with hip-girdle weakness that progresses in a caudocranial direction. The absence of muscle reflexes, myalgias, and autonomic abnormalities can also be present. Nearly 15%of LEMS patients have an associated malignancy. Small cell lung cancers expressing voltage-gated calcium channels (VGCCs) are found in the majority of cases (Kesner et al., 2018). The predominant immunoglobulin associated with the disease targets presynaptic P/Q-type VGCCs (Kesner et al., 2018). These antibodies have been shown experimentally to induce VGCC cross-linking and internalization (Fukuda et al., 2003; Nagel et al., 1988). The resultant reduction in calcium influx at the presynaptic terminal decreases the release probability of acetylcholine laden vesicles leading to impairments of synaptic transmission at the neuromuscular junction (Fukuda et al., 2003; Motomura and Fukuda, 2011; Nagel et al., 1988).

Another well-characterized disorder of the neuromuscular junction commonly associated with autoantibodies is myasthenia gravis (MG). Ptosis (i.e. eye-lid droop) and diplopia (i.e. double vision) are early clinical features of MG often followed by facial and bulbar muscle involvement leading to difficulty chewing and swallowing. The subsequent weakening of proximal limb muscles and the diaphragm can be life-threatening. Together these symptoms reflect the characteristic fatigability of skeletal muscles found in MG (Drachman, 1994; Drachman et al., 1982). Nearly eighty-five percent of myasthenia gravis patients produce antibodies against the nicotinic acetylcholine receptor (AChR) located on the post-synaptic side of the neuromuscular

junction. In approximately fifteen percent of MG cases a thymic epithelial tumor is thought to underlie the autoimmune reaction although Hodgkin's lymphoma and cancers of the lung and breast have also been associated with the disorder (Wirtz et al., 2003). As with paraneoplastic LEMS, autoantibodies in myasthenia gravis compromise synaptic transmission by inducing receptor internalization and degradation (Drachman et al., 1982). Alternatively, a significant proportion of anti-AChR antibodies in MG patients alter receptor function by directly occluding the ligand-binding site (Howard et al., 1987). In addition, complement-mediated destruction of the motor end plate is a third mechanism by which anti-AChR antibodies interrupt normal NMJ function (Engel and Arahata, 1987).

Paraneoplastic neurologic disorders involving antibodies to extracellular proteins are not limited to the peripheral nervous system. In fact, malignancies associated with antibodies to CNS synaptic proteins predominately underlie many variants of autoimmune encephalitis. As in myasthenic syndromes, the autoantibodies associated with these disorders appear to be directly pathogenic. Similarly, the autoantibodies and symptomatology in both categories of neurologic syndromes are also found in patients with no cancer association. Given the parallels between paraneoplastic and non-neoplastic autoimmune encephalitides associated with extracellular antigens I will treat them simultaneously in the following section.

'Non-paraneoplastic' *autoimmune encephalitides*

In our discussion of disorders associated with autoantibodies to extracellular neuronal proteins I will use the term autoimmune encephalopathies (AE), coined by Dr. Josep

Dalmau as a group designation for these diseases (Dalmau et al., 2017). In the past decade, sixteen such AEs have been identified that overlap clinically with paraneoplastic neurologic syndromes yet lack an underlying malignancy. The neuronal antigens targeted in these disorders serve myriad functions although many are involved in synaptic transmission and plasticity. Patients with these disorders can present with a stereotyped array of symptoms indicative of target antigen or with a more generalized constellation of symptoms. In the following section we will review characteristics of exemplar autoimmune encephalopathies, modeled on the excellent review by Dalmau and colleagues (2017), before an in-depth description of anti-NMDA receptor encephalitis.

Limbic system associated disorders

Inflammation of the medial temporal lobes, hippocampus, amygdala, frontobasal cortex, and cingulate cortex defines limbic encephalitis. Although the term has a strong association with paraneoplastic neurological disorders, other causes include autoimmune encephalopathy and viral infection (Tüzün and Dalmau, 2007). The clinical onset is rapid and progressive involving severe memory deficits, mood derangements, and anxiety. Impairments of memory are more often anterograde although limited retrograde amnesia of weeks to months has been reported. Temporal lobe seizures, MRI enhancement of the mesotemporal lobe, and abnormal EEGs often accompany the telltale memory impairments (Tüzün and Dalmau, 2007).

Perhaps the best characterized examples of autoimmune limbic encephalitis involve pathogenic antibodies to AMPA receptors, $GABA_B$ receptors, and LGI-1 (Dalmau et al., 2017). In each of these disorders the hippocampus and other temporal lobe structures are disproportionately affected. Each disorder has unique symptomatology, likely reflecting the divergent physiological role played by the particular antigen as well as differential involvement of brain regions.

***AMPA receptor*:** The α-amino-3-hydroxy-5-methyl-4-isoxazolepropionic acid (AMPA)-sensitive ionotropic glutamate receptor is expressed widely throughout the central nervous system with high expression in the hippocampus, subiculum, striatum, cerebellum, and neocortex (Sprengel, 2006). As a mediator of fast excitatory synaptic transmission, AMPA receptors are essential for normal nervous system development and plays key roles in synaptic plasticity (Dingledine et al., 1999; Shepherd and Huganir, 2007). The receptor is a member of the ionotropic glutamate receptor family and is composed of four subunits (GluA1-4), each containing extracellular amino-terminal and ligand-binding domains, a transmembrane pore-forming region, and an intracellular C-terminal domain (Gouaux, 2004).

Antibodies directed against extracellular epitopes of the GluA1 and GluN2A subunits are pathognomonic of anti-AMPA receptor autoimmune encephalitis. These subunits are highly expressed in the CA3-CA1 regions of the hippocampus likely explaining the disproportionate involvement of the area (Lai et al., 2009). Patients with this disorder are often older (mean age 62 years), predominately female (62%), with 70% associated

having underling cancers of the lungs, breasts, or ovaries (Dalmau et al., 2017). Whereas the majority of patients present with the aforementioned “limbic” symptoms, a subset show progressive dementia or psychosis.

Although the neuropathology associated with anti-AMPA receptor encephalitis is poorly characterized, a potential pathogenic role for anti-GluA1/2 antibodies has been demonstrated experimentally in cell-culture based studies. Immunocytochemistry and western blot assays indicate that autoantibodies can induce receptor clustering and internalization. In addition, incubation of cultured neurons in serum or CSF derived from patients reduced AMPA receptor-mediated excitatory post-synaptic currents (Lai et al., 2009; Peng et al., 2015). Viewed in concert with the positive response of patients to therapies aimed at reducing autoantibody load, these findings have been used to support a largely antibody-mediated pathophysiology.

***$GABA_B$ receptor*:** Another interesting subtype of autoimmune encephalitis is associated with antibodies to gamma-aminobutyric acid (GABA) receptors. In this disorder, autoantibodies to $GABA_B$ receptors are linked to a syndrome of limbic encephalitis accompanied by severe seizures or status epilepticus, and in limited cases, opsoclonus-myoclonus syndrome (Höftberger et al., 2013). $GABA_B$ receptors are heterodimers consisting of a GABA-B1 subunit, containing the ligand binding domain, and a GABA-B2 subunit which interacts with G-proteins to mediate intracellular signaling (Bettler et al., 2004). Isoforms of the GABA-B1 subunit function in compartmentalization of the receptor to pre- (B1a) or post-synaptic (B1b) domains. In

general, $GABA_B$ receptors inhibit synaptic signaling. For example, presynaptic $GABA_B$ receptors can decrease neurotransmitter release probability by inhibiting voltage-gated calcium channels; whereas, the post-synaptic $GABA_B$ receptors can hyperpolarize the cell by activating G protein-activated inward-rectified potassium (GIRK) channels (Vigot et al., 2006).

The putative pathogenic epitope is an extracellular region of the GABA-B1 subunit (Lancaster et al., 2010). Interestingly, cell-based assays do not indicate internalization as the pathogenic mechanism of $GABA_B$ receptor autoantibodies. Electrophysiological experiments conducted in cultured hippocampal neurons instead suggest that the antibodies are allosteric modulators of the receptor. Specifically, application of patient-derived CSF has been shown to block the effects of a $GABA_B$ receptor agonist, baclofen. These data have been used to extrapolate the potential of autoantibodies to block $GABA_B$ receptor mediated inhibition (Jain, 2015). Thus, antibody mediated $GABA_B$ receptor antagonism has been suggested as a mechanism for the severe seizures observed in these patients.

***LGI-1 protein*:** The third autoimmune limbic encephalitis I will discuss derives its name from autoantibodies to the leucine-rich glioma inactivation-1 protein (LGI-1), or epitempin. This disorder was initially associated with voltage-gated potassium channels based on co-immunoprecipitation experiments (Shillito et al., 1995). Subsequent studies revealed the actual target of patients' antibodies to be the aforementioned LGI-1 with a subset of patients developing autoimmunity to the contactin-associated protein-like2

(CASPR2) protein (Irani et al., 2010; Lai et al., 2010). Unlike the two previously described diseases, the anti-LGI-1 encephalitis patients are generally older males with limited cancer association (Irani et al., 2010). Further differentiating this disorder clinically is the tendency for facio-brachial seizures to precede limbic symptoms (Irani et al., 2011). In addition, MRI and EEG investigations indicate basal ganglia and frontal cortex involvement (López Chiriboga et al., 2017; Navarro et al., 2016). Another seemingly unique feature of this disorder is the persistence of neurological impairments following immunotherapies (Ariño et al., 2016; van Sonderen et al., 2016).

LGI-1 incorporates into VGKCs complexes providing a possible explanation for VGKC co-immunoprecipitation in early investigations of the disorder (Schulte et al., 2006). Electrophysiological evidence suggests that association of LGI-1 with VGKC complexes decreases neurotransmitter release probability (Seagar et al., 2017). LGI-1 also interacts with ADAM22, a catalytically inactive member of the metalloprotease family, via a C-terminal epitempin-repeat domain (Yamagata et al., 2018). This LGI1-ADAM22 ligand-receptor complex appears to enhance AMPA receptor-mediated synaptic transmission via interactions with PSD-95 and stargaze proteins (Fukata et al., 2006). Mutations to LGI-1, ADAM22/23 and Kv channels have all been linked to a similar epileptic phenotype suggesting a mechanistic nexus by which antibodies to LGI-1 could mediate the disease state (Morante-Redolat et al., 2002; Owuor et al., 2009; Smart et al., 1998). Preliminary data suggests downregulation of AMPA receptors via antibody interactions may play a part in the disorder's pathophysiology as well. However, the dominant antibody isotype IgG4 possesses limited capacity for crosslinking and

internalization (Ariño et al., 2016), thus differentiating a potential antibody-mediated mechanism distinct from that proposed for anti-AMPA receptor encephalitis.

Extra-limbic disorders

Most autoimmune encephalitides can be heterogeneous in both autoantigen identity and clinical presentation making simple categorization difficult. In the following section I will explore a subset of disorders selected for their unique constellation of symptoms, the additional involvement of extra-limbic structures, and interesting pathophysiology.

***$GABA_A$ receptors*:** Autoimmune encephalitis associated with antibodies to $GABA_A$ receptors is characterized by multifocal MRI enhancement in cortical and subcortical regions, treatment-refractory seizures, and status epilepticus (Petit-Pedrol et al., 2014; Spatola et al., 2017). In addition, a subset of patients with cognitive abnormalities and focal neurological signs, such as hemiparesis, dyskinesias, aphasia, or oculomotor disturbances have been reported (Dalmau et al., 2017). Heteropentameric $GABA_A$ receptor are ionotropic chloride channels mediating fast inhibitory synaptic transmission and as such are pharmacological targets of anticonvulsants, anxiolytics, and sedatives (Rudolph and Knoflach, 2011). The dominant composition of $GABA_A$ receptors consists of 2α , 2β , 1δ , and 1γ subunit(s) with numerous other subunits and subunit isoforms contributing in particular cell types (Sigel and Steinmann, 2012). The primary autoantibodies in this disorder target the alpha, beta, and to a lesser extent, gamma subunits (Petit-Pedrol et al., 2014; Spatola et al., 2017). Limited evidence for a direct pathogenic role for anti- $GABA_A$ antibodies exists; however, at least one study

demonstrated synapse-selective loss of $GABA_A$ receptor immunoreactivity following incubation in patient CSF. Interestingly, non-synaptic $GABA_A$ receptors were not affected (Petit-Pedrol et al., 2014). Although an in-depth investigation of the pathogenic potential of anti-$GABA_A$ antibodies is needed, a similar loss of synaptic $GABA_A$ receptors can occur in experimental models of epilepsy suggesting parallel mechanisms (Naylor et al., 2005). As $GABA_A$ are inhibitory in most neurons, it is clear that an understanding of the affected circuits will be required to explain hyperexcitability states such as seizures.

***Dopamine-2 Receptor*:** Dopamine receptors are expressed widely throughout the central nervous system playing critical roles in voluntary movement and reward among myriad other functions. Multiple human diseases are associated with dysfunction in dopaminergic signaling, including but not limited to, Parkinson's disease, tourette's syndrome, and schizophrenia (Jaber et al., 1996). G protein-coupled dopamine receptors can be broadly divided into two subfamilies (D1 and D2) based on the associated G protein effector. D1-like dopamine receptors (D1 and D5) stimulate cAMP production via $G\alpha_{s/olf}$ mediating activation of adenylyl cyclase (AC) and are located post-synaptically. By contrast, the D2-lik (D2-D4) inhibit AC through their $G\alpha_{i/o}$ effector proteins and can be located both pre- and post-synaptic (Beaulieu and Gainetdinov, 2011).

Patients that develop antibodies to the D2 receptor present as a variant of basal ganglia encephalitis. The antibodies appear to be conformationally-specific, recognizing extracellular epitopes on the receptor; however, the rarity of this disorder has limited

investigations of the pathophysiological effects of the related antibodies (Dale et al., 2012). Given the receptors robust expression in basal ganglia nuclei, for example on GABAergic medium spiny neurons in the striatum, it is not surprising that the clinical features of the disorder include dystonia, parkinsonism, and chorea, in addition to psychiatric symptoms observed in schizophrenia (Dale et al., 2012). Interestingly, autoantibodies to the D2 receptor have also been identified in patients experiencing isolated psychiatric symptoms; however, the similarity of these autoantibodies to those involved in basal ganglia encephalitis are unknown (Pathmanandavel et al., 2015).

***Neurexin-3α*:** This cell-adhesion protein is part of a family of neurexins involved in synapse development, maintenance, and neurotransmission. Neurexins are the product of alternative splicing of mRNA from three genes (NRX1,2, and 3) encoding two long α and two short β isoforms. The protein is composed of a large extracellular domain, transmembrane region, and short cytoplasmic tail. Neuroligins, another protein family involved in synaptogenesis, are one of several post-synaptic cell-adhesion binding partners for neurexins (Krueger et al., 2012). The extracellular domain of neurexins has been shown to regulate postsynaptic AMPA receptors; whereas, the cytoplasmic tail interacts with vesicular machinery to modulate neurotransmitter release, as demonstrated in GABAergic neurons (Aoto et al., 2015). Schizophrenia and autism have been linked to mutations of the neurexin gene.

Patients with this form of autoimmune encephalitis initially develop a prodromal flu-like condition that include gastrointestinal symptoms. As the disorder progresses, confusion, loss of consciousness, and seizures have been reported with a subset of patients

displaying facial dyskinesias and others requiring ventilation (Gresa-Arribas et al., 2016). The pathogenic nature of anti-neurexin3α antibodies is unique as compared to the other autoimmune encephalitides discussed. *In vitro* assays with rat neurons (DIV7-17) showed that antibody exposure reduced overall synapse numbers. By contrast, 24hr incubation of neurons at DIV18 had no discernable effect. In both experiments, no structural changes were observed in exposed cells. Interpretation of these results is complicated by a history of systemic autoimmunity in 4 of the 5 patient studies as well as the presence of antinuclear antibodies (Gresa-Arribas et al., 2016).

***NMDA receptor*:** The *N*-methyl-D-aspartate receptor is a ligand-gated ion channel functioning in excitatory neurotransmission throughout the CNS. It is unique amongst ionotropic receptors in its requirement of two different agonists and voltage-dependent relief of magnesium block to initiate cation conductance (Hansen et al., 2018; Tovar and Westbrook, 2017). Thus, this receptor acts as a coincidence-detector with extrinsic voltage sensitivity. NMDA receptors are assembled as heterotetrameric complexes consisting of two obligate GluN1 subunits and two GluN2 (A-D) subunits. The GluN3 (A-B) subunit represents a third family member capable of being substituted for GluN2; however, its physiological role is controversial (Pachernegg et al., 2012). The specific subunit composition of NMDA receptors has developmental, cellular, and regional specificity and provides unique biophysical and pharmacological properties. Structurally, the receptor is divided into four domains: 1) the extracellular amino-terminal domain (ATD) with several sites for binding of allosteric modulators such as Zn^{2+}; 2) the “clam shell-like” ligand binding domain (LBD) with the GluN1 subunits binding glycine;

whereas, the GluN2 subunits recognize glutamate; 3) the transmembrane (TMD) domain consisting of three membrane spanning alpha helices (M1, M3 and M4) and a reentrant loop (M2) with elements of M3 and M2 forming the pore region; whereas, all four helices are involved in pore opening; and 4) a large cytoplasmic tale with numerous phosphorylation sites and regions capable of interacting with cytoplasmic proteins like PSD-95 and calmodulin (Hansen et al., 2018; Lee et al., 2014a; Lü et al., 2017; Tovar and Westbrook, 2017).

NMDA receptor dysfunction has been implicated in a number of CNS disorders including stroke, neurodegenerative diseases, psychiatric illness, and autoimmune encephalitis (Paoletti et al., 2013). The pathophysiology of each disease suggests either NMDA receptor hyperactivity or hypofunction as a contributing factor. For example, in stroke and traumatic brain injury (TBI), NMDA receptor mediated calcium toxicity is thought to underlie much of the resultant tissue damage. In models of ischemia and TBI, treatments aimed at tamping down NMDA receptor mediated hyperactivity, such as antagonism of GluN2B containing receptors, have been shown to prevent excitotoxic cell death. Similarly, in models of Huntington's disease, in which death of striatal medium spiny neurons is a major pathological finding, overactive NMDA receptors have been suggested to play a disproportionate role in excitotoxicity. Conversely, reduced function of NMDA receptors, particularly on GABAergic interneurons, is implicated in aspects of schizophrenia. This "NMDA receptor hypofunction hypothesis" is rooted in the observation that NMDA receptor antagonists cause dissociative symptoms in humans and that postmortem analysis of brain tissue from schizophrenic patients

indicates a reduction in NMDA receptor expression in a subset of GABAergic neurons (Paoletti et al., 2013; Zhou and Sheng, 2013).

Hypofunction has also been proposed as the dominant pathophysiologic mechanism of anti-NMDA receptor encephalitis (Dalmau et al., 2017). Initially identified as a paraneoplastic syndrome, epidemiological investigations now indicate that the disorder occurs more frequently in the absence of an associated neoplasm (Dalmau et al., 2007, 2011, 2017). In fact, in pediatric populations it is considered a leading cause of non-infectious encephalitis (Gable et al., 2012). The etiology of this non-paraneoplastic variant is unknown; however, previous HSV-1 infections have been reported in a number of cases (Salovin et al., 2018). Patients with this disorder often experience a prodromal flu-like malaise followed by acute onset of neuropsychiatric symptoms. The constellation of psychiatric symptoms as enumerated by Dalmau and colleagues include "…anxiety, insomnia, delusional thinking (e.g. grandiose delusions, hyper-religiosity), hallucinations, paranoid thoughts, pressured speech, mood disorder (predominately manic), or aggressive behavior, with alternating episodes of agitation and catatonia…" (Dalmau et al., 2017). Neurological manifestations rapidly follow dominated by "…seizures, reduced verbal output, decreased level of consciousness, highly characteristic orofacial and limb dyskinesias, choreoathetosis, dystonic postures, rigidity, and autonomic dysfunction…" (Dalmau et al., 2017). Patients often lapse into coma requiring respiratory support and medical management of cardiac or autonomic abnormalities such as tachycardia or bradycardia.

A significant proportion of patients have an abnormal EEG reading in the course of the disorder. This often consists of slow disorganized waveforms, epileptic activity, or bursts of rhythmic beta frequencies overriding slower delta oscillations (e.g. “extreme delta brush”). Although hyperintensities on MRI indicative of focal inflammation do occur, normal or diffuse enhancement is more common. Pleocytosis and oligoclonal bands are common CSF findings. However, the clinical diagnosis is made when anti-GluN1 antibodies are identified in the context of the aforementioned neuropsychiatric symptoms (Dalmau et al., 2017; Graus et al., 2016a; Titulaer et al., 2013a). Investigations of the neuropathology associated with anti-NMDA receptor encephalitis are limited and the findings are heterogenous. One consistency is gliosis to a greater or lesser extent (Bien et al., 2012a; Camdessanché et al., 2011a; Martinez-Hernandez et al., 2011a; Tüzün et al., 2009a). Activated microglia and astrocytes have been reported in multiple brain regions including the hippocampus, basal ganglia, and neocortex. Perivascular infiltrates are common, being dominated by B and plasma cells. Not surprisingly, IgG deposits are prominent in anatomical regions with dense NMDA receptor expression. Complement however is a rare finding. $CD4^+$ T cells have been observed lining vessels and in the brain parenchyma. In at least one case report, pro-inflammatory $CD4^+$ T_H17^+ T cell infiltrates were associated with poor response to immunomodulatory therapies (Filatenkov et al., 2017). There is scant evidence for cytotoxic CD8+ T cell involvement or cell death. However, CT scans have shown reversible atrophy, and functional imaging suggests long-term changes that correlate with learning and memory impairments (Finke et al., 2013). The standard treatment regimen involves a course of anti-inflammatory drugs with intravenous immunoglobulins

(IV Ig), plasmaphoresis, and immunosuppressive agents to follow (Titulaer et al., 2013a). Nearly eighty percent of patients recover after protracted hospitalization often lasting several months, followed by extensive physical and cognitive therapies. A relapse-remitting variant is reported in the remaining patient population, with death a rare outcome (Dalmau et al., 2011, 2017).

The antibodies observed in a patient's CSF are typically of the IgG1-3 subclasses. Immunoreactivity to the conformational intact GluN1 subunit is pathognomonic. However, a subset of patients also produces antibodies to the GluN2A and GluN2B subunits (Dalmau et al., 2008). The pathogenic potential of these anti-NMDA receptor antibodies has been demonstrated by *in vitro* cell-based assays and *in vivo* passive-transfer studies (Dalmau et al., 2017; Gleichman et al., 2012a; Hughes et al., 2010a; Planagumà et al., 2015a). Cultured neurons exposed to a patient's CSF show signs of antibody-mediated receptor internalization with corresponding reductions in NMDA receptor currents (Hughes et al., 2010a). Intraventricular infusion of CSF from affected patients can lead to progressive impairments in learning and memory in mice, with a concomitant decrease of NMDA receptor immunoreactivity in the hippocampus (Planagumà et al., 2015a). These data, along with positive responses to immunomodulatory therapies aimed at reducing antibody load, support a disease mechanism involving antibody-mediated NMDA receptor hypofunction. However, antibodies alone do not account for the neuroinflammation, dyskinesias, or spontaneous seizures common to the disorder (Planagumà et al., 2015a). As such, a *de novo*

autoimmune animal model of the disorder would be valuable to further our understanding of the pathophysiology of anti-NMDA receptor encephalitis.

In the next chapter I describe a *de novo* mouse model of autoimmune NMDA receptor encephalitis generated by active immunization with native-like NMDA receptor holoprotein embedded in a lipid bilayer. This combination of lipid and protein (i.e. proteoliposome) has been used for several decades to study the biophysical properties of membrane bound protein complexes as well as in the generation of antibodies (Banerjee and Datta, 1983; Casad and Volkova, 1999; Drachev et al., 1976; Pérez et al., 2004; Suharni et al., 2014). Yet, prior to this study there were no reports of proteoliposome-induction of autoimmunity. Its use in our model was serendipitous emerging from observations following immunization of a llama with *Xenopus laevis* GluN1-GluN2B proteoliposomes by the laboratory of Eric Gouaux. The llama in question was immunized for the purpose of generating anti-NMDA receptor antibodies to be used in crystallography experiments. Unfortunately, shortly after inoculation with the NMDA receptor proteoliposome preparation the animal developed a hyperactive locomotor phenotype with continuous circling, followed by death. On the suggestion of Dr. Gary Westbrook, encephalitis was suspected and the llama's brain was preserved for histological assessment. Dr. Randy Woltjer in neuropathology at Oregon Health & Science University confirmed the presence of CNS inflammation showing that the llama's hippocampus contained perivascular cuffing and $CD3^+$ T cell infiltrates (Fig. iii).

Fig. iii Neuropathology in llama immunized with NMDA receptor proteoliposomes

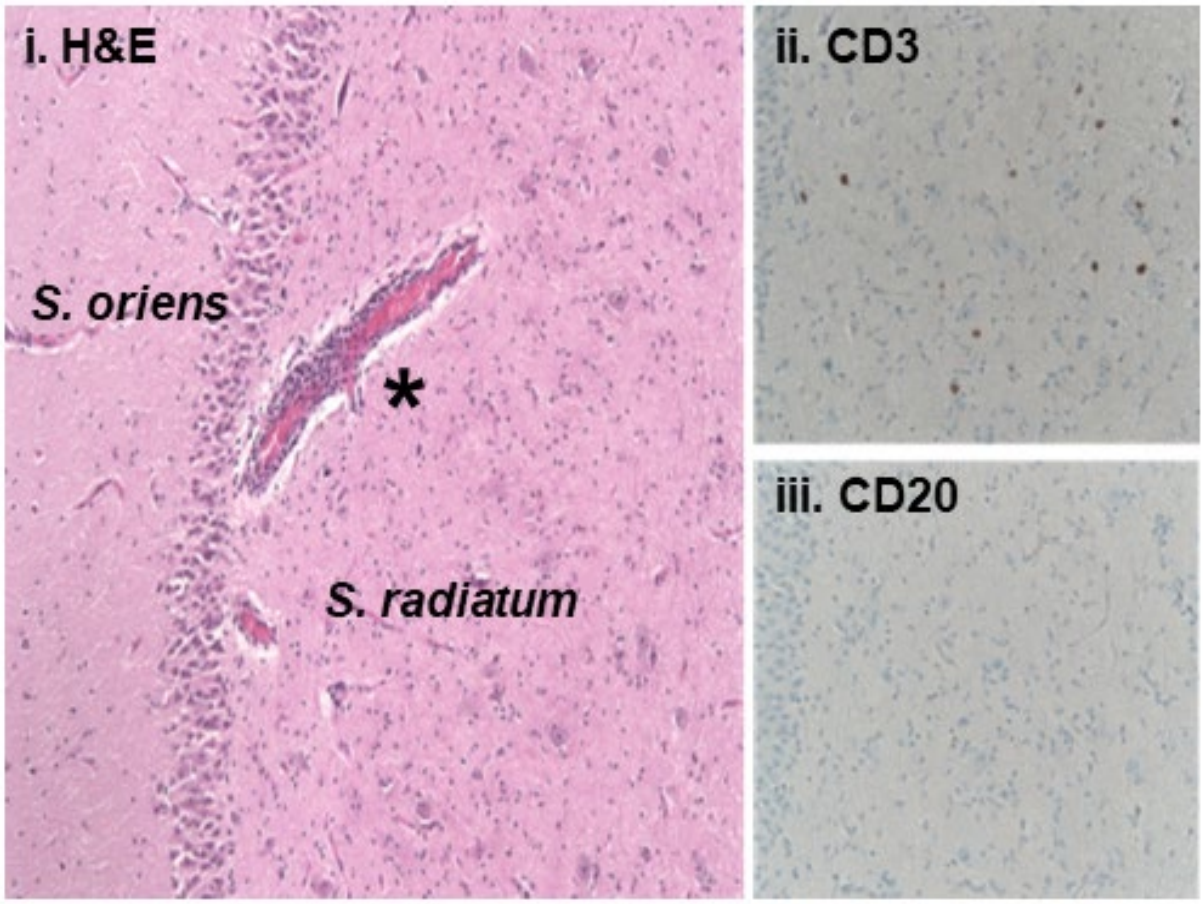

Panel i) H&E histology showing perivascular cuffing (black asterisk) in llama hippocampus. Panel ii) $CD3^+$ T cell immunolabeling in the stratum radiatum of the llama. Panel iii) Sparse $CD20^+$ B cell immunolabeling observed in llama brain (images provided by Dr. Randy Woltjer).

Without serum or CSF samples however, no definitive relationship to anti-NMDA receptor antibodies could be determined. Still, the nature of the behavioral phenotype, neuropathology, and immunogen suggested an autoimmune encephalitis.

Thus we hypothesized that the NMDA receptor proteoliposomes could be used to develop an animal model of the disease in mice. For my initial investigations I used the same *X. laevis* GluN1-GluN2B proteoliposome preparation that induced a disease state

in the llama. In a complementary set of experiments I used rat GluN1-GluN2A proteoliposomes. The amino acid sequences from the human, frog, llama, mouse and rat GluN1 subunit are strikingly similar (Table i). Thus, it is not surprising that the disease phenotype observed in mice immunized with the xenopus or rat NMDA receptor proteoliposome preparation was nearly identical (See Chapter 2).

This mouse model allowed us to explore the nature of the immunogen (e.g. conformational state, subunit composition, species specificity) responsible for generating an autoimmune reaction. In addition we were able to identify the immune cell repertoire activated early in the disorder as well as during fulminate disease. It is our hope that this model will provide valuable information regarding the pathophysiology underlying anti-NMDA receptor encephalitis as well as serve as a platform for the development of novel therapeutics.

Table i. Species specific GluN1 amino acid sequence alignment

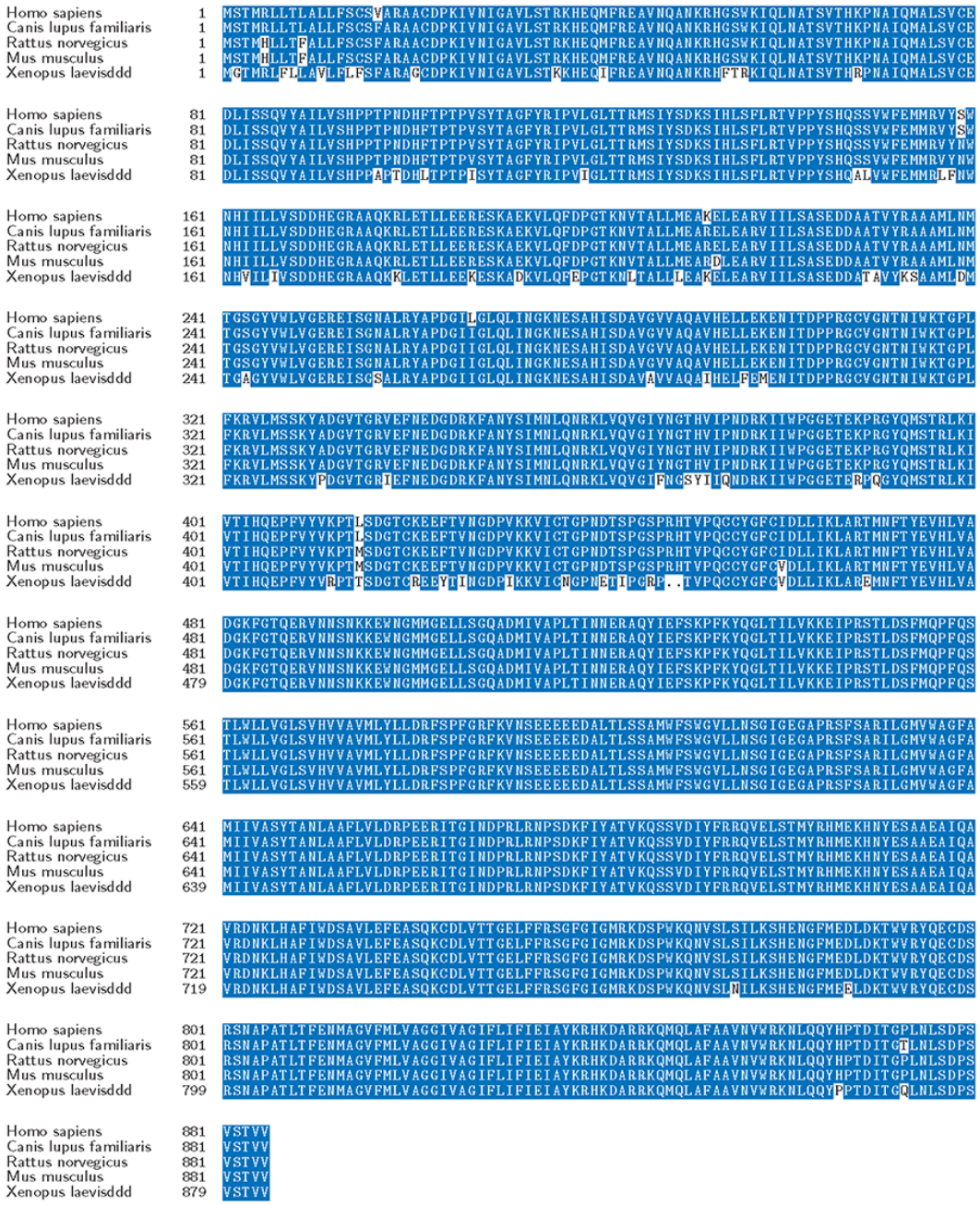

Table i. Species specific GluN1 amino acid sequence alignment. Wild-type GluN1-1b a.a. (1-881) sequences for H. sapien, C. lupus familiaris, R. norvegicus, M. musculus, X. laevis. Blue highlights indicate a.a. sequence homology.

Chapter 2: Autoimmune receptor encephalitis in mice induced by active immunization with conformationally-stabilized holoreceptors[¥]

[¥] In revision at Science Translational Medicine (March 2019)

BioRxiv link: https://www.biorxiv.org/content/10.1101/467902v1

Authors: Brian E. Jones, Kenneth R Tovar[†], April Goehring, Farzad Jalali-Yazdi, Nana J. Okada[#], Eric Gouaux, Gary L. Westbrook[*]

Affiliations:

Vollum Institute, Oregon Health and Science University

To whom correspondence should be addressed: [*]Gary L. Westbrook, Vollum Institute, L474, Oregon Health & Science University 3181 SW Sam Jackson Park Road Portland OR 97239. email: westbroo@ohsu.edu

[†] current address: Neuroscience Research Institute, University of California, Santa Barbara, Santa Barbara, CA 93016

[#] current address: Department of Psychology, 16 Barker Hall, University of California, Berkeley, Berkeley, CA 94720

One Sentence Summary: We report an active immunization model of autoimmune NMDA receptor encephalitis in mice that recapitulates the features of the clinical disease, provides insights into the pathophysiology, and offers a platform for investigation of new therapeutic interventions.

Abstract: Autoimmunity to membrane proteins in the central nervous system has been increasingly recognized as a cause of neuropsychiatric disease. A key recent development was the discovery of antibodies to NMDA receptors in some cases of encephalitis, characterized by cognitive changes, memory loss, seizures and at times long-term morbidity or mortality. Treatment approaches and experimental studies have largely focused on the pathogenic role of these autoantibodies. Passive antibody transfer to mice has provided useful insights, but does not produce the full spectrum of the human disease. Here we describe a unique *de novo* autoimmune mouse model of anti-NMDA receptor encephalitis. Active immunization of immune competent mice with conformationally-stabilized, native-like NMDA receptors induced a fulminant encephalitis, consistent with the behavioral and pathologic characteristics of human cases. Our results provide evidence for neuroinflammation and immune cell infiltration as a component of the autoimmune response in mice. Use of transgenic mice indicated that mature T cells as well as antibody-producing cells were required for disease induction. This active immunization model may provide insights into disease induction as well as a platform for testing therapeutic approaches.

Introduction

Behavioral changes, psychosis, memory impairment, and seizures have been recognized as a pattern in several forms of encephalitis (Dalmau et al., 2017). In some cases, this discrete clinical syndrome has been attributed to Herpes simplex virus, but the underlying cause in other cases has remained unknown. In 2007, autoantibodies targeting *N*-methyl-D-aspartate (NMDA) receptor were discovered in a subset of these patients (Dalmau et al., 2007; Sansing et al., 2007). With recognition of anti-NMDA receptor encephalitis as a clinical syndrome, diagnostic tests have revealed that the disease is surprisingly common in patients of all ages. Initially considered as one of the paraneoplastic disorders, it is now clear that many patients do not have detectable tumors (Dalmau et al., 2008; Titulaer et al., 2013b), underscoring our lack of understanding of the underlying etiology. Patient-derived samples suggest a role for antibodies directed at NMDA receptor subunits in the pathogenesis, leading to treatments to reduce antibody titers with plasmapheresis or immunosuppression (Dalmau et al., 2011). However, recovery following standard treatments can be prolonged and incomplete (de Bruijn et al., 2018; Finke et al., 2013, 2016; Titulaer et al., 2013b).

Passive transfer of antibodies from affected patients to mice have indicated that NMDA receptor antibodies can cause hypofunction in NMDA receptor-mediated synaptic transmission (Dalmau et al., 2008; Hughes et al., 2010b; Planagumà et al., 2015b; Tüzün et al., 2009b). Yet, the initiating immunological factors as well as the potential role of immune cell infiltrates and neuroinflammation in the disease process are difficult

to determine using existing models (Bien et al., 2012b; Camdessanché et al., 2011b; Martinez-Hernandez et al., 2011b; Tüzün et al., 2009b). A robust animal model of the disease has the potential to address such issues.

To develop a mouse model of autoimmune encephalitis, we postulated that immunization with fully assembled receptors could be important in triggering the disease. Thus we used active immunization with intact native-like NMDA receptors composed of GluN1-GluN2B tetramers embedded in liposomes. Subcutaneous injection of these NMDA receptor-containing proteoliposomes induced fulminant encephalitis within 4 weeks in young adult mice. The mice demonstrated behavioral changes, seizures as well as histological features of neuroinflammation and immune cell infiltration that were most prominent in the hippocampus. The presence of NMDA receptor antibodies was confirmed by immunohistochemistry and western blot. $CD4^+$ T cell infiltration was an early feature, and both mature T and B cells were required for disease induction.

Results

Active immunization with NMDA receptor holoprotein induced encephalitis

We used purified GluN1/GluN2B NMDA fully-assembled tetrameric receptors (holoreceptors) as described in methods to immunize C57Bl6 adult mice (Fig. 1A). Subcutaneous immunization with NMDA receptors in proteoliposomes was followed by a booster two weeks later. Littermate control cohorts were injected only with liposomes or with saline. Overt neurological signs began to appear by four weeks, and by six weeks post-immunization nearly all of the proteoliposome-treated mice (86%) exhibited abnormal home cage behavior (Fig. 1B), indicating the high incidence of disease following holoprotein immunization. The most prominent behavioral changes were hyperactivity (86%) followed by tight circling (50%), overt seizures (21%) and hunched back/lethargy (11%), (Fig. 1C & Movie S1-S5). Cumulative clinical scores (described in methods) were significantly higher in proteoliposome-treated mice (proteoliposome v. liposome $p < 0.0001$, proteoliposome v. saline $p < 0.0001$, liposome v. saline $p < 0.9999$; Kruskal-Wallis, Dunn's multiple comparisons post hoc; n=28/treatment group). Because the presence of clinical signs was assessed with two-minute daily observation periods, seizure prevalence in particular was likely underestimated. Proteoliposome-treated mice also had increased mortality by six weeks post-immunization (n=8/56 proteoliposome, n=0/56 controls; $p < 0.0005$; Log-rank test), which was likely seizure-related.

To assess behavioral phenotype, we used a battery of standardized tests. Open field testing (Fig. 2A) confirmed a hyperactive locomotor phenotype with nearly double the

distance traveled in proteoliposome-treated mice (proteoliposome. 5472 ± 525.4 cm, n =26; liposome = 3207 ± 111 cm, n = 28; saline = 3093 ± 84.9 cm; n=28; proteoliposome v. liposome p = 0.0002; proteoliposome v. saline p < 0.0001; liposome v. saline p > 0.9999; Kruskal-Wallis test with Dunn's multiple comparisons post hoc). Proteoliposome-treated mice also showed a high degree of variability in the open field ranging from near immobility to extreme hyperactivity. Nest building, indicative of complex stereotyped behavior, was severely compromised in the proteoliposome-treated mice (Fig. 2B). At six weeks post-immunization, control mice created precise nests whereas proteoliposome-treated mice barely disturbed the nestlets as indicated by a lower nesting score: proteoliposome (24 and 48 hours) = 1 ± 0.29 and 1.48 ± 0.39, n=27; liposome = 4.60 ± 0.14, and 4.78 ± 0.11, n = 28; saline = 4.21 ± 0.14 and 4.75 ± 0.12, n = 28. proteoliposome v. liposome p < 0.0001; proteoliposome v. saline p < 0.0001; liposome v. saline p = 0.3603 (24 hours); proteoliposome v. liposome. p < 0.0001; proteoliposome v. saline p < 0.0001; liposome v. saline p > 0.9999 (48 hours); Kruskal-Wallis with Dunn's multiple comparisons post hoc). In the zero maze, often used as a measure of anxiety-like behavior, proteoliposome-treated mice spent more time in the normally aversive open-area (% time open-area: proteoliposome = 27.90 ± 3.70, n = 18; liposome = 16.08 ± 0.71, n = 28; saline = 16.32 ± 0.96, n = 28; proteoliposome v. liposome. p = 0.0065; proteoliposome v. saline. p = 0.0081; liposome. v. saline. p > 0.9999; Kruskal-Wallis with Dunn's multiple comparisons post hoc). There was no statistical difference in the total distance moved in the open or closed areas indicating that hyperactivity could not explain the observed phenotype ([Open area: proteoliposome: 175.4 ± 26.18 cm; liposome: 118.7 ± 9.41 cm; saline; 130.4 ± 15.67

cm; proteoliposome v. liposome p = 0.0786; proteoliposome v. saline. p = 0.0629; liposome. v. saline. p = >0.9999]; [Closed area: proteoliposome: 572.6.4 ± 27.29 cm; liposome: 494.8 ± 17.83 cm; saline; 524.1 ± 22.17 cm; proteoliposome v. liposome p = 0.1140; proteoliposome v. saline. p = 0.4312; liposome. v. saline. p = >0.9999], Kruskal-Wallis with Dunn's multiple comparisons post hoc). These results indicated that immunization with NMDA receptor holoprotein induces a striking behavioral phenotype consistent with encephalitis. The results were not limited to the specific holoprotein as we observed a similar phenotype in mice immunized with rat GluN1-GluN2A holoprotein (Fig. S5).

Neuroinflammation and peripheral leukocyte infiltration

Interestingly, the histopathology of reported cases of anti-NMDA receptor encephalitis is heterogeneous, and can include immune cell infiltrates, neuroinflammation and occasionally neuronal loss (Bauer and Bien, 2016; Bien et al., 2012b; Camdessanché et al., 2011b; Martinez-Hernandez et al., 2011b). In proteoliposome-treated mice, hematoxylin-labeled perivascular cuffing was prominent in multiple CNS regions including the hippocampus and neocortex (Fig. 3A, right panels). Patchy areas of cell death were rare, occurring in one of six mice included in the analysis (Fig. 3B, right panels). No evidence of inflammation or cell death were present in controls (Fig. 3A, B, left panels). Immunolabeling with GFAP and Iba1 revealed an inflammatory response in many of the proteoliposome-treated mice (Fig. 4A,B, right panels). Total GFAP immunoreactivity in the hippocampus was much higher than controls (proteoliposome: $42.5 \times 10^8 \pm 8.80 \times 10^8$; control: $6.33 \times 10^8 \pm 1.64 \times 10^8$; proteoliposome v. control. p =

0.0022; Mann Whitney test; n=6 mice /group). Iba1 labeling revealed foci of microgliosis compared to scattered diffuse labeling in controls (Fig. 4B). Total Iba1 immunoreactivity in the hippocampus was 60.9 x 10^8 ± 14.3 x 10^8; in proteoliposome-treated mice compared to 28.5 x 10^8 ± 1.64 x 10^8 in controls: 28.5 x 10^8 ± 1.64 x 10^8 ($p = 0.0022$, Mann Whitney test; n=6 / group).

In severely affected mice, there was also pronounced CNS infiltration by peripheral immune cells. Labeling with the pan-leukocyte marker CD45R was robust in the hippocampus (Hipp), striatum (Str), thalamus (Thal), amygdala (Amyg) and neocortex (Ctx), (Fig. 5A, right panel). Control mice showed sparse CD45R labeling (Fig. 5A, left panel). Mean $CD45R^+$ cell densities for control- and proteoliposome-treated mice are summarized in Table 1. Peripheral immune cells including activated macrophages/microglia ($Galectin3^+$), plasma cells ($CD138^+$), helper T cells ($CD4^+$), B cells ($CD20^+$) were strikingly increased in the brains of proteoliposome-treated mice, whereas cytotoxic T cells ($CD8^+$) were sparse or absent (Fig. 5B, right panel). In contrast liposome- or saline-treated mice lacked immunoreactivity to the same immune cell markers (Fig. 5B, left panel). Quantification of immune cell subtypes in the hippocampus is summarized in Table 1. Although mice at 3 weeks post-immunization did not show prominent clinical features, neuroinflammation and immune cell infiltration could be detected in some animals at this early time point (Table 1 and Fig. S3).

Receptor autoantibodies in serum from proteoliposome-treated mice

Staining for mouse IgG as a proxy for the presence of autoantibodies, essentially outlined the hippocampus (Fig. S1), consistent with patterns observed in anti-NMDA receptor encephalitis. Serum from proteoliposome-treated mice showed bands on Western blots corresponding to purified recombinant rat and *Xenopus* GluN1 subunit protein as well as *Xenopus* GluN2B. Although a putative pathogenic epitope on the GluN1 amino-terminal domain (ATD) has been identified in the human disease, immunoreactivity to GluN2A and GluN2B subunits has been reported in a subset of cases (Dalmau et al., 2007, 2008; Gleichman et al., 2012b; Kreye et al., 2016a). For the mouse shown in Figure 6A, serum also labeled a *Xenopus* GluN1 subunit that lacked the ATD domain, indicating the presence of polyclonal antibodies in at least some of the mice. Serum from liposome or saline-treated mice did not recognize NMDA receptor subunits (Fig. 6A, middle panel). Serum from proteoliposome-treated mice collected at three weeks post-immunization did not label NMDA receptor subunits on western blot, but labeling was present in cell-based assays (Fig. S4), perhaps indicating a lower antibody titer at this early time point.

Hippocampal NMDA receptors are triheteromeric, composed of GluN1, GluN2A and GluN2B subunits (Hansen et al., 2014; Tovar et al., 2013), and are widely distributed in the neuropil. To assess the distribution of labeling with purified IgG from proteoliposome-treated mice, we compared the IgG labeling to a GluN2A subunit-specific antibody that was highly effective in floating tissue sections (Fig. 6B, 6 weeks post-immunization). Purified IgG from controls showed no labeling. In cultured mouse

hippocampal neurons (DIV14-21), only the IgG isolate from proteoliposome-treated mice co-localized with the GluN1 subunit specific antibody (Fig. 6C). The punctate labeling along dendrites and at dendritic spines follows the expected distribution of NMDA receptors at synapses. To further assess subunit specificity of the IgG isolates, we used HEK293 cells to express and stain for NMDA receptor subunits. HEK cells were transfected with single subunit constructs or combinations of GluN1/2A and GluN1/2B. As observed in the primary hippocampal cultures, proteoliposome IgG co-localized with cells labeled with a GluN1 subunit-specific antibody (Fig. 6D). Immunolabeling of HEK cells expressing only the GluN1 subunit further confirmed the presence of GluN1-specific antibodies in proteoliposome-treated mice (Fig. S2). In the cell based assays, 100% of proteoliposome-treated mice were positive for GluN1 antibodies by six weeks post-immunization. All but one proteoliposome treated-mouse showed immunoreactivity to GluN1 at three weeks post-immunization, indicating the presence of antibodies before overt clinical signs.

Serum from proteoliposome-treated mice did not acutely block NMDA receptor function, as assessed by whole-cell currents in cultured hippocampal neurons (Fig. 7A & B). NMDA (50 μM) was co-applied by local flow pipes either with serum from liposome-treated mice or serum from proteoliposome-treated mice (1:100 dilution). The NMDA-evoked current in the presence of serum from proteoliposome-treated mice was 95.9 ± 6.8% of that evoked by NMDA + serum from liposome-treated mice in the same neuron (n=8; p=0.23, paired t-test; Shapiro-Wilk normality test, proteoliposome serum: p = 0.2231; liposome serum: p = 0.1413). In contrast, a 24-hour incubation with serum from

proteoliposome-treated mice reduced synaptically-activated NMDA receptors, which underlie the slow components of EPSCs and drive overall network activity. As shown in Figure 7C (top left), the slow components of EPSC barrages from neurons incubated in serum from liposome-treated mice were greatly reduced by the NMDA receptor antagonist, D-AP5, as indicated by the rapid decay of the spontaneous EPSCs (Fig 7C, top right). However, after 24-hour incubation in serum from proteoliposome-treated mice, spontaneous EPSCs had reduced NMDA receptor-mediated currents and thus were less sensitive to block by D-AP5 (Fig. 7C, bottom right). For neurons incubated in serum from liposome-treated mice total charge from spontaneous EPSCs was reduced to 44.1 ± 7.9% of control charge by D-AP5 (Fig. 7D). In contrast, D-AP5 reduced total charge to only 85.6 ± 6.0% of control charge in neurons incubated with serum from proteoliposome-treated mice (n=8 per group; $p < 0.005$, paired t-test; Shapiro-Wilk normality test, proteoliposome serum: $p = 0.3893$; liposome serum: $p = 0.5722$ Fig. 7D). These results demonstrate a marked reduction in NMDA receptor function after 24 hour incubation with serum from proteoliposome-treated mice. We also stained the same 24-hour treated cultures for PSD-95, as a proxy for synapses, and GluN1 to assess their colocalization (Fig. 7E). The 24-hour incubation did not affect total synaptic puncta, but did result in a >50% decrease in GluN1 immunoreactivity (Fig. 7E), entirely consistent with the reduction in functional measures of NMDA receptor activity ([PSD-95 puncta per μm: proteoliposome, 0.54 ± 0.019; liposome, 0.62 ± 0.059; $p = 0.4244$, Mann-Whitney test]; NR1+PSD-95 puncta per μm: proteoliposome, 0.18 ± 0.034; liposome, 0.56 ± 0.064; $p = 0.0003$, Welch's t-test; Shapiro-Wilk normality test: proteoliposome, p

= 0.8788; liposome, p = 0.9482)]. Thus antibodies in the mouse model contribute to NMDA receptor hypofunction.

T cells as well as B cells are necessary for proteoliposome-induced encephalitis

Studies of anti-NMDA receptor encephalitis in human cases have focused on the role of antibodies (Dalmau et al., 2007; Hughes et al., 2010b; Tüzün et al., 2009b). Our results in proteoliposome-treated mice are consistent with the presence of B cell infiltrates as well as NMDA receptor autoantibodies. However, we saw evidence of B and T cell in the brains of proteoliposome-treated mice. In human cases perivascular T cell infiltrates, primarily CD4+ helper T cells, have been reported however, parenchymal infiltrates appear infrequent (Camdessanché et al., 2011b; Tüzün et al., 2009b). To distinguish the roles of B and T cells in the mouse disease, we used two well-characterized mutant mouse lines that lack mature B cells or mature T cells (Kitamura et al., 1991; Mombaerts et al., 1992). Consistent with a role for B cells in the pathophysiology, proteoliposome treatment of MuMt$^-$ mice, which lack the capacity to generate an antigen specific antibody response, showed no behavioral or histological abnormalities at 6 and 12 weeks post-immunization (Fig. S6). To evaluate the role of mature T cells we used Tcrα$^-$ ("CD4, CD8 cell KO") mice, which lack mature helper T and cytotoxic T cells. All proteoliposome-treated Tcrα$^-$ mice survived to 12 weeks without clinical signs of disease (Fig. 8A). Likewise Tcrα$^-$ mice did not show histopathological evidence of gliosis or cell infiltrates and serum lacked detected anti-NMDA receptor antibodies (Fig. 8B-D). A cohort of immune competent wild-type mice immunized in parallel with the MuMt$^-$ and Tcrα$^-$ showed the expected phenotype, indicating the potency of the immunogen. These

results confirm the expected role of B cells, but also indicate a requirement for mature T cells in disease pathogenesis.

Discussion

Our results demonstrate that active immunization with NMDA receptor holoproteins induces a disease state in mice that recapitulates the core features of human anti-NMDA receptor encephalitis including the presence of pathogenic anti-GluN1 autoantibodies (Graus et al., 2016b). In general, active immunization animal models have played an important role in the study of neurological disorders including autoimmune diseases such as myasthenia gravis and multiple sclerosis (Amor et al., 1994; Patrick and Lindstrom, 1973). For example, peptide fragments from myelin have long been used to generate experimental autoimmune encephalomyelitis (EAE) with its incumbent clinical signs to test the molecular basis and therapeutic approaches in MS (Amor et al., 1994; Bjelobaba et al., 2018; Croxford et al., 2011). Likewise, active immunization with neuromuscular junction proteins can cause myasthenic-like features in mice (Viegas et al., 2012). Although synaptic membrane proteins have been implicated in autoimmune encephalitis, studies of these diseases have largely been limited to passive transfer approaches (Dalmau et al., 2017). Our *de novo* autoimmune anti-NMDA receptor encephalitis model represents an additional approach to examine the pathophysiology and developing novel treatment approaches for the human disease.

Comparison to reported human cases of anti-NMDA receptor encephalitis and study limitations

The etiology in some cases of encephalitis was an enigma for decades. The discovery of NMDA receptor antibodies in a subset of these patients was not only a surprise, but

also provided an opportunity for a better understanding of the causes and also treatment strategies (Dalmau et al., 2008). The diagnostic criteria used to identify anti-NMDA receptor encephalitis (Graus et al., 2016a) includes a number of features that were also present in our mouse model including: behavioral changes, movement abnormalities, seizures, and the presence of antibodies to the GluN1 subunit of NMDA receptors. Interestingly, the clinical signs and histopathology ranged from mice with marked behavioral impairments to other mice that lacked clinical signs but had histological features and anti-NMDA receptor antibodies. Our mice all had antibodies to GluN1, but in some cases we also saw immunoreactivity to GluN2B or to a construct that lacked the ATD of GluN1. This pattern is consistent with a polyclonal response in our mice, which had fulminant disease symptoms at the time of serum collection. However, consistent with the human disease, a GluN1 epitope was predominant.

It will be interesting to examine immunized mice at earlier time points to look for specific memory deficits, more subtle cognitive impairments as well as the evolution and atomic localization of autoantibody epitopes. We did not examine some other aspects that have been reported in the human disease such as autonomic dysfunction or the cause of death in some of our mice, which likely was due to seizures. Furthermore we did not investigate aberrant electrophysiological activity at the network and synaptic level *in vivo* or in brain slices derived from affected mice. However, these questions are all addressable using this mouse model, which offers significant advantages for further exploration of such issues. Interestingly, antibodies recognizing NMDA receptor subunits have been observed in some other contexts. For example, systemic lupus

erythematosus (SLE) is associated with a with a range of antibodies to nuclear antigens as well as antibodies recognizing the NMDA receptor GluN2A subunit (Husebye et al., 2005; Tay and Mak, 2015). However, unlike the NMDA receptor antibodies found in our mouse model and human anti-NMDA receptor encephalitis patients, anti-GluN2A/B antibodies derived from SLE patients do not appear to alter synaptic responses but rather induce cell death (Husebye et al., 2005; Tay and Mak, 2015). Furthermore, although limited cell death is observed in a few mice in our model and a subset of anti-NMDA receptor encephalitis patients it was not major contributor to pathogenesis.

Although histopathological reports are available for only a small fraction of human cases of anti-NMDA receptor encephalitis, immune cell infiltrates and neuroinflammation have been observed in severely affected patients (Camdessanché et al., 2011b; Tüzün et al., 2009b) but were less prominent in other cases (Bien et al., 2012b). The presence or absence of inflammatory cell infiltrates thus likely depends on the time point at which the tissue is examined. Notably, neuroinflammation in our mice was most prominent during the fulminant stages of the disease (6 weeks post-immunization). In the human disease and in our mouse model, cytotoxic T cell involvement can occur, but was not a prominent feature. Also consistent with human cases, IgG infiltration, especially prominent in the hippocampus, was present in our mice (Fig. S1).

Prior experimental studies of anti-NMDA receptor encephalitis used passive transfer approaches with patient-derived CSF/IgG (Hughes et al., 2010b; Moscato et al., 2014; Planagumà et al., 2015b; Tüzün et al., 2009b). These studies provide compelling

evidence for the involvement of NMDA receptor antibodies in pathogenesis (Hughes et al., 2010b; Kreye et al., 2016a; Moscato et al., 2014; Planagumà et al., 2015b). Intraventricular infusion of human NMDA receptor antibodies in mice decreased NMDA receptor density in the hippocampus (Malviya et al., 2017; Planagumà et al., 2015b), but these mice did not exhibit movement disturbances or spontaneous seizures (Malviya et al., 2017; Planagumà et al., 2015b; Rosch et al., 2018; Wright et al., 2015). These observations suggest that passive infusion of NMDA antibodies is not sufficient to fully mimic the clinical syndrome. Although no animal model is expected to perfectly mimic a human disease, our results indicate that active immunization of immune competent mice with NMDA receptor holoproteins induces a fulminant encephalitis with the definitive features of the human disease. The active immunization model also allows an examination of the time course of the disease process from the point of induction.

The pathophysiological elements

The current hypothesis for the clinical phenotype is that antibody-mediated internalization of NMDA receptors leads to hypofunction at a network level. The available evidence convincingly demonstrates that antibodies from human cases cause internalization of NMDA receptors *in vitro* and reduce NMDA responses (Hughes et al., 2010b; Ladépêche et al., 2018; Tüzün et al., 2009b). Thus therapies in use or proposed have been directed at removing antibodies, immunosuppression, or preventing receptor internalization (Dalmau et al., 2017). The hypofunction hypothesis gains further support from the behavioral side-effects observed with use of NMDA receptors antagonists, but general NMDA receptor hypofunction does not easily account for the presence of

unprovoked, spontaneous seizures given the presence of NMDA receptors on both excitatory and inhibitory neurons and the complexity of the circuits involved (Rosch et al., 2018). More analysis will be necessary to relate receptor internalization to neurological signs and whether other factors contribute to the spectrum of clinical signs and histopathology.

Although prior studies of anti-NMDA receptor encephalitis have largely focused on the role of B cells and antibodies, the role of $CD4^+$ T cells in autoimmune encephalitis is an area of growing interest (Pilli et al., 2017). T cells could promote neuroinflammation as well as potentiate B cell- and plasma cell-mediated antibody responses. In human cases, CSF cytokine/chemokine profiles support a role for $CD4^+$ T cell involvement (Byun et al., 2016; Kothur et al., 2016; Liba et al., 2016; Ulusoy et al., 2012). For example, interleukin-17, a pro-inflammatory cytokine produced by Th17 $CD4^+$ T cells, is prominent in the CSF of human cases and may perform the dual role of blood-brain barrier disruption and upregulation of IL-6, a pro-B cell and plasma cell cytokine (Byun et al., 2016; Huppert et al., 2010; Kebir et al., 2007). Although cytotoxic T cells were not a prominent histological feature in our mice, the absence of disease in the $TCR\alpha^-$ mice lacking mature $CD4^+$ or $CD8^+$ cells support an important role for at some population of T cells in disease pathogenesis. Thus therapies designed to reduce T cell-mediated inflammation (e.g. blocking interleukin 17 signaling) as well as those aimed at reducing B cell activation are worthy of further investigation.

Conformationally-restricted triggers

The trigger for an autoimmune reaction to NMDA receptors remains unclear. Immunization using peptide fragments to produce NMDA receptor antibodies have not resulted in reports of clinical disease. In a recent study, mice immunized with NMDA receptor peptides did not show clinical signs, but the authors suggested that blood-brain barrier integrity may prevent circulating NMDA receptor antibodies from entering the CNS (Pan et al., 2018). The immunogens in our case were the tetrameric *X. laevis* GluN1/GluN2B or rat GluN1/GluN2A receptor in native-like heteromeric assembly (Lee et al., 2014b). The *X. laevis* subunits had been altered to maximize protein stability, e.g. by removal of the intracellular C-termini (Lee et al., 2014b), and were capable of binding glutamate or glycine, which may also have improved protein stability. Importantly, the rat subunits we used had no mutations except for removal of the intracellular C-termini and thus unaltered topology in the ATD, one of the putative sites of pathogenic antibody interactions in human cases (Gleichman et al., 2012b; Kreye et al., 2016a). The use of immunogens with intact extracellular domains likely played a role in the high incidence of disease in our mice, and may be relevant considerations for other membrane proteins implicated as causes of encephalitis. Our results strongly suggest that disease induction depends on conformationally restricted epitopes. This idea is consistent with prior studies in HEK293 cells, which showed an assembled NMDA receptor was necessary for reactivity of antibodies from human cases (Dalmau et al., 2007, 2008). In human cases, the source of intact NMDA receptors to trigger the autoimmune response is unknown, but could be ectopic expression from a tumor, or membrane debris following an insult causing neuronal cell loss. For example, anti-NMDA receptor encephalitis has

been reported following viral infection (Armangue et al., 2013; Titulaer et al., 2013b). An association with viral infection was also suggested in the case report of Knut, a polar bear at the Berlin zoo (Prüss et al., 2015).

Significance to human disease

Despites the prevalence of anti-NMDA receptor encephalitis, many experimental questions remain unanswered given the lack of a *de novo* autoimmune animal model that recapitulates the signs and symptoms. The mouse model described here provides such a platform and has already provided several new insights. For example, use of conformationally-stabilized holoproteins appears to be a critical component of immunogenicity, and our results already indicate a complex pathogenesis. Thus the initial steps in disease induction, the roles of specific immune components, and potential new therapies can now be tested.

Methods

Study Design: We examined the effect of active immunization with NMDA receptor native-like holoproteins on normal adult mice. The aim of the study was to investigate autoimmunity to NMDA receptors in the context of anti-NMDA receptor encephalitis. Littermate controls (liposome or saline) of both sexes were used for all interventions. Results from liposome and saline controls did not differ and were thus combined for statistical analysis of "control" in some experiments as indicated. Criteria were established in advance based on pilot studies for issues including data inclusion, outliers, selection of endpoints, and sample size (see statistics section). All analyses were blinded. Observations within each animal were averaged and the value for N replicates reflects the number of animals. Details for each experimental technique and analysis are included in the text and figure legends.

Animals: We used the following mouse strains: C57BL/6J (Jax #000664), BALB/cJ (Jax #000651), MuMt^{-} (B6.129S2-Ighm^{tm1Cgn}/J; Jax #002288), and Tcrα^{-} (B6.129S2-Tcrα^{tm1Mom}/J; Jax #002116). BALB/cJ mice were used only in pilot studies and all reported data are from C57BL/6J mice. Homozygous MuMt^{-} and Tcrα^{-} were obtained directly from Jax for immediate use in experiments and were not bred in-house. Genotyping of homozygous mutant MuMt^{-} and Tcrα^{-} breeder mice was conducted by Jax prior to shipping of offspring. MuMt^{-} and Tcrα^{-} were housed in the OHSU super barrier facility whereas other strains were housed in standard OHSU mouse facilities. All mice were housed under a 12hr light/dark cycle at 75°F, 60% humidity, with ad libitum

access to food and water (Picolab Rodent Diet 20, no.5053). The OHSU Institutional Animal Care and Use Committee approved all procedures.

NMDA receptor expression and purification: NMDA receptor holoprotein production and purification followed previously described procedures (Lee et al., 2014b), with modifications, as described below. The subunits from *Xenopus laevis* used in these experiments show 92% amino acid identity (96% similarity) with rat NMDA receptor subunits. The *X. laevis* constructs were optimized for stability, by site directed mutagenesis, to facilitate purification of holoprotein complexes (Lee et al., 2014b). The rat constructs used were unmutated apart from a C-terminal truncation. To generate receptor protein HEK293 GnTI$^-$ cells were grown in suspension and transduced with P2 BacMam viruses the for GluN1 and GluN2 subunits at a multiplicity of infection (M.O.I.) of 1:1 (GluN1:GluN2) and incubated at 37 °C. At 14 h post-transduction, 10 mM sodium butyrate was added to the cultures and the temperature was shifted to 30°C. Cells were collected 60 h post-transduction and disrupted by sonication. Membranes were collected by centrifugation and homogenized in buffer composed of 150 mM NaCl, 20 mM Tris-HCl pH 8.0 (TBS buffer) and solubilized in TBS buffer supplemented with 1% lauryl maltose neopentyl glycol (MNG-3) detergent, 0.8 μM aprotinin, 2 μg/ml leupeptin, 2 mM pepstatin A, 1 mM glutamate, 1 mM glycine, and 2 mM cholesterylhemisuccinate (CHS) for 1.5 hours at 4 °C. The soluble fraction was bound to streptactin resin and eluted in a TBS buffer containing 0.02% MNG-3, 0.2 mM CHS and 5 mM desthiobiotin. The receptor-containing solution was concentrated and digested with 3C protease overnight at 4 °C. The receptor was further purified by size-exclusion chromatography

(SEC) in buffer containing 400 mM NaCl, 20 mM MES pH 6.5, 1 mM *n*-dodecyl β-D-maltoside (DDM), and 0.2 mM CHS. Peak fractions were pooled and concentrated to 250-500 µL using a 100kDa molecular weight cutoff centrifuge protein concentrator to a protein concentration of approximately 2 mg/mL.

NMDA receptor proteoliposome preparation and immunization: Purified holoprotein was reconstituted into proteoliposomes for immunization as described previously (Coleman et al., 2016; Lü et al., 2017). Liposomes were prepared using a lipid mixture composed of asolectin:cholesterol:lipid A:brain polar lipid (molar ratio 60:17:3:20). Lipids (40 mg of total lipid) were dissolved in 5 mL of chloroform in a 100 mL glass round bottom flask. Chloroform was evaporated using a rotary evaporator and lipids were rehydrated in 10 mL TBS and subjected to at least 10 freeze/thaw cycles by immersing the flask in liquid N_2 and thawing the flask in a 30 °C water bath. The resuspended lipid mixture was extruded through two 200 nm filters 10 times or until the lipid appeared translucent. Lipids were centrifuged at 100,000xg for 45 minutes and resuspended in TBS at a concentration of 40 mg/mL. Purified holoprotein was added to lipids at a ratio of 1:80 protein to lipid (w/w) and incubated on ice for 10 minutes. The solution was brought to a final concentration of 400 mM NaCl and 0.8% sodium deoxycholate and incubated on ice for 30 minutes. Excess salt and detergent was removed using a PD-10 desalting column and the proteoliposomes were collected, by centrifugation, by way of a 45 minute 100,000xg centrifugation step. For immunization, the NMDA receptor proteoliposome pellet was resuspended in sterile saline by gentle pipetting. Adult mice (PND60) received a subcutaneous injection, proximal to the right inguinal lymph node,

with proteoliposome (25µg total NMDA receptor protein/200µl saline), liposome, or saline, followed by a booster at two weeks. Mice were observed daily (2 min duration) in their home cage for overt signs of encephalitis. Observer was blinded to treatment condition using a 0-5 scoring scale: *hyperactivity* (0=normal exploratory movement, 1=continuous running); *circling* within the long body axis (absent=0, 1=present); *hunched back & lethargy* (0=absent, 1=present); *clinical seizure* (0=absent, 1=present); *death* (0=absent, 1=present), modified from a scoring scale used for a mouse model of HSV-1 encephalitis (Anglen et al., 2003; Sellner et al., 2005).

Behavioral assessments: Behavioral assessment mice were performed at 5-6 weeks post-immunization in the OHSU behavioral research core. Fourteen male and 14 female mice, housed individually, from each treatment group (proteoliposome, liposome, saline) were tested. Mice were acclimated to the behavioral suite for three days prior to testing. Researchers were blinded to experimental conditions. Behavioral testing was conducted between 7am-12pm during the light-on period. The planned behavioral test battery included zero maze, nesting, open-field, novel-object recognition, and context-cued fear conditioning. However, the profound locomotor phenotype made results from novel-object recognition and context-cued fear condition difficult to interpret. Thus only open-field, nesting behavior and zero maze were used. *Open Field:* Mice freely exploring a 40 x 40 cm Plexiglas arena. Ethovision (Noldus, Netherlands) video tracking software was used to trace and quantify movement. Mice were acclimated to the arena for 5 min on day 1. On Days 2 and 3 mice were recorded for 10 min. We assessed total distance moved (cm) and percent time spent exploring the central region (interior 20 x 20 cm) of

the arena (Davis et al., 2012), *Nesting Behavior:* Assessment of nest building, a complex stereotyped behavior (Deacon, 2006). At time point zero two new pressed cotton nestlets were weighed, placed in the home cage of an individually housed mouse, and photographed. At 24 hours, a new photograph was taken and any untorn nesting material (pieces > 0.1 grams) was weighed and returned to the cage. A photograph was repeated at a 48 hours. Scoring of the nest was based on a 1-5 scale per Deacon et al (2006 from untouched nestlets (score 1) to a fully constructed nest with central cavity and surrounding wall (score 5). *Zero Maze:* The zero maze (Kinder Scientific, Poway, CA) consisted of four sections alternating between closed and open areas. Mice were placed in an open area of the maze and allowed to explore for 10 min. Movement and location of the mice was tracked by an automated photo beam detection system. Outcome measures were total distance moved (cm) and percent time spent in open and closed areas of the maze (Davis et al., 2012).

Histology and immunohistochemistry: Brain tissue for histology and immunohistochemistry was prepared as follows: terminally anesthetized mice were transcardially perfused with 10 ml phosphate buffered saline (PBS) followed by 10ml of 4% paraformaldehyde (PFA) in PBS, and brains post-fixed in 4% PFA/PBS overnight. For hematoxylin & eosin (H&E) PFA fixed brains were transferred to 70% ethanol, paraffin embedded, and 6 µm microtome sections were mounted and stained. For Immunohistochemistry, floating vibratome sections (40-100 µm) were permeabilized, and nonspecific staining blocked in 0.4% Triton + 10% normal horse serum (NHS) in PBS for 2 hours at room temperature. Sections were incubated overnight (4ºC) with

primary antibody in 1.5% NHS-PBS, washed in PBS (3 x 15 min) prior to incubation with secondary antibodies (Invitrogen AlexaFluor, 1:300) in 1.5% NHS-PBS for 2hrs at room temperature. Sections were counterstained with DAPI (1 x15 min; Sigma # 28718-90-3, 1:20K in PBS) and mounted on slides using Fluoromount-G (SouthernBioTech # 01001). The following primary/secondary antibody pairings were used to label floating brain section: CD45R (BD Biosciences #550539, 1:25; Invitrogen #A21208, AlexaFluor488), CD4 (BD Biosciences #550280, 1:25; Invitrogen #A21208, AlexaFluor488), CD8 (BD Biosciences #550281, 1:25; Invitrogen #A21208, AlexaFluor488), CD20 (Santa Cruz Biotechnology #7735, 1:50; Invitrogen #A21447, AlexaFluor647), CD138 (R&D Systems #AF3190, 1:100; Invitrogen #A11057, AlexaFluor568), Galectin3 (R&D Systems #AF1197, 1:500; Invitrogen #A21447, AlexaFluor647), Iba1 (Wako Laboratory Chemicals #019-19741, 1:500; Invitrogen #A21206, AlexaFluor488), GFAP-Cy3 (Millipore Sigma #C9205, 1:500), GluN2A (Invitrogen #480031; Invitrogen #A11008 AlexaFluor488).

Immune cells ($CD45^+$, $CD4^+$, $CD8^+$, $CD20^+$, $CD138^+$, $Galectin3^+$) and inflammatory cells (Iba1, GFAP) were quantified in three representative brain sections spanning -0.9 mm to -2.3 mm from bregma (Franklin and Paxinos, 2012) from six randomly chosen mice (3♀; 3♂) per group. The observer was blinded to experimental conditions. Images were captured using a Zeiss/Yokogawa CSU-X1 Spinning Disk microscope (10x 0.45 numerical aperture). A 4x4 tiled z-stack consisting of 26, 1.39 um, optical sections was collected. Exposure time and laser intensity settings were held constant during image collection. Fused max intensity projections were constructed using Zen Blue software

(Zeiss) and Fiji-Image J software. Cells/μm^3 reported reflect mean density values across sampled sections. Iba1 and GFAP immunofluorescence intensity measurements were plotted as arbitrary units of pixel intensity (Image J) using the following formula: fluorescence intensity = integrated density – (ROI area X mean background fluorescence).

Serum collection, IgG purification and Western blots: For serum collection, blood from transcardial puncture was allowed to clot at room temperature for 15min, centrifuged (2000rpm) at 4ºC for 15 min and supernatant aliquots stored at -20ºC and 4ºC. A Nab Protein A/G spin kit (ThermoFisher Sci. #89950) was used for IgG isolation. IgG concentration was determined using the Bradford dye-binding method (Bio-Rad #5000002). Serum and IgG isolates were tested against the following purified NMDA receptor subunits with C-terminal deletions as indicated: *Xenopus laevis*: GluN1-3a, GluN1-3aΔATD (Lee et al., 2014b; Song et al., 2018), GluN2A (AAI70552.1) residues 1-834, GluN2B (NP_001104191.1) residues 1-839; rat: GluN1-1a (U08261) residues 1-847, GluN1-1b (U08263) residues 1-868, GluN2A (AF001423) residues 1-866, and GluN2B (NP_036706) residues 1-868. NMDA receptor subunit constructs were cloned into pEGBacMam for transfection of tsA201 adherent cells (HEK 293T, ATCC CRL-11268) (Goehring et al., 2014). All constructs had a green fluorescent protein (GFP) tag at the carboxyl terminus. Transfected tsA201 cells were solubilized in 200 µl of lysis buffer (150 mM NaCl, 20 mM Tris pH 8.0, 40 mM *n*-dodecyl-β-D-maltoside, 1 mM phenylmethylsulfonyl fluoride, 2 mg/ml leupeptin, 0.8 mM aprotinin, and 2 mM pepstatin A) for 1 hr. The extracts were centrifuged for 40 minutes at 40000 rpm at 4°C and the

supernatants were collected, resolved by sodium dodecyl sulfate polyacrylamide gel electrophoresis using a 4-15% gradient gel and transferred to nitrocellulose. Anti-GFP antibody (Invitrogen, A11122), and serum samples were used at dilutions of 1:5000 and 1:100, respectively. The secondary antibodies (LI-COR IRDye 680, 926-68071 and IRDye 800CW, 926-32210) were used at a dilution of 1:10000.

in vitro assays and immunocytochemistry: HEK293FT cells (ThermoFisher Sci. #R70007) were cultured on poly-D-lysine (0.2mg/ml PDL; Sigma # P6407) coated glass coverslips (1mm; Bellco Glass #1943-10012A) in DMEM medium (DMEM Gibco #11965-092; 10% HI-FBS Gibco #10082-139; 1% Pen/Strep ThermoFisher Sci #15140122; 1% MEM NEAA Gibco #11140-050; 1% Glutamax Gibco #35050-061). At 30% confluence, cells were transfected with rat wild-type GluN1-1a/pCI-neo and GluN2A/pCI-neo or GluN2B/pCI-neo constructs (a gift from Dr. Weinan Sun) via calcium-phosphate precipitation in a 1:1 ratio (Sun et al., 2017). Transfected cells were incubated at 37ºC. After four to six hours, the transfection solution was exchanged for fresh DMEM medium containing 10 µM (R)-3-(2-Carboxypiperazin-4yl)propyl-1-phosphonic acid (CPP; Abcam #ab120159), returned to the incubator for twelve hours followed by fixation in 4% PFA-PBS (10 min). For immunocytochemistry (ICC) HEK cells were permeabilized and blocked for non-specific labeling as described above. We tested both whole serum and purified IgG in all ICC experiments and observed no difference in specific labeling. When using purified IgG, protein concentrations from all samples were matched. The following primary/secondary antibody combinations were used for colabeling experiments: GluN1 (Abcam #ab9864R; 1:100; Invitrogen #A11008

AlexaFluor488, 1:400) co-incubated with serum or purified IgG from liposome- or proteoliposome-treated mice (0.00625mg/ml; Invitrogen #A21236 AlexaFluor647, 1:400). A z-stack spanning a single cell layer was captured using a Zeiss/Yokogawa CSU-X1 Spinning Disk microscope (63x oil immersion 1.4 numerical aperture) with Zen Blue software (Zeiss) and Fiji-Image J software used for post-imaging processing.

For primary neuronal cultures, Hippocampi were dissected from C57BL/6 wildtype mice between post-natal days 0 and 2. Hippocampi were then dissociated with papain (Worthington LS003126; 200 U in 37ºC dissection saline, 35 minutes) followed by trituration. Cultures were maintained in a tissue culture incubator at 37ºC and 5% CO2 in media made with MEM (Gibco #11090-081), 5% heat inactivated fetal bovine serum (Gibco #10082-139), 2 mM Glutamax (Gibco #35050-061), 1ml/L Mito+ serum extender (Corning #CB50006) and 21 mM added glucose. Media was maintained in the tissue culture incubator and cultures had half the media volume changed every three days. All cultures were made in two cell plating stages. The first plating seeds the poly-D-lysine-coated coverslips (Neuvitro #GG-12-PDL) with glia (300,000-400,000 cells/35 mm dish) that were allowed to proliferate for at least two weeks. Neurons were then plated (100,000 - 200,000 cells/35 mm dish) in the second stage then grown on a glial substrate. For electrophysiological experiments, neurons were used after 7 - 10 days *in vitro*. Neurons were fixed in 100% methanol (-20º; 15min) for immunocytochemistry experiments. Staining protocols as described above were followed without additional permeabilization. NMDA receptor colabeling experiments were conducted at DIV14 and DIV21 using the following primary/secondary antibody combinations: GluN1 (Abcam

#ab9864R, 1:100; Invitrogen #A11011 AlexaFluor568, 1:400), Map2 (Novus Biologicals #NB300-213, 1:500; Invitrogen #A11039 AlexaFluor488, 1:400), purified IgG from liposome- or proteoliposome-treated mice (0.00625mg/ml; Invitrogen #A21236 AlexaFluor647, 1:400). A Zeiss 880 laser scanning confocal microscope was used to acquire a z-stacked image (63x oil immersion 1.4 numerical aperture). Zen Blue software (Zeiss) and Fiji-Image J software used for image processing.

Electrophysiology and quantification of synaptic puncta: For whole-cell voltage clamp recording, we used cultured mouse hippocampal neurons after 7 - 10 days *in vitro*. Recordings were done at room temperature, in external solution containing (in mM): 158 NaCl, 2.4 KCl, 10 HEPES, 10 D-glucose, 1 - 2 $CaCl_2$, and 0.01 SR95531 (Abcam #ab120042). Solution pH was adjusted to 7.4 and osmolality adjusted to 320 mosmol/kg H_2O. The pipette solution contained the following (in mM): 140 cesium methanesulfonate, 4 NaCl, 0.5 $CaCl_2$, 5 EGTA, 10 HEPES, 4 magnesium-ATP, 0.3 sodium-ATP (pH 7.4; 320 mosmol/kg H_2O). Neurons were continuously perfused through gravity-fed flow pipes which were placed within 100 micrometers of the recorded neuron during recordings. Cells were voltage clamped at -70 mV. Recording electrodes had resistances of 1.5 - 2.5 MOhm. The recording series resistance was always <8 mOhm and was compensated by at least 80% using the amplifier circuitry. Tetrodotoxin (1 μM) and NBQX (2.5 μM) were used in NMDA application experiments and drugs were applied via custom flow pipes that were translated with a computer-controlled piezo-electric bimorph. Computer-controlled solenoid-gated flow pipes were used for delivery of NMDA. In a different set of experiments, neurons were incubated

with either serum from proteoliposome or liposome-treated mice for 24 hours and spontaneous excitatory postsynaptic currents (sEPSCs) were recorded at a holding potential of -70 mV with or without D-AP5 (50μM; Abcam #ab120003). Axopatch 1C amplifiers and AxoGraph acquisition software (Axograph X) were used for data acquisition. Data were low-pass filtered at 2.5-5 kHz and acquired at 5-10 kHz. The same hippocampal neuronal cultures used in the chronic serum exposure electrophysiology experiments were fixed in 100% methanol and stained with PSD95 (Abcam #ab12093, 1:250; Invitrogen #A21447 AlexaFluor488, 1:400), GluN1 (Abcam #ab9864R, 1:100; Invitrogen #A10042 AlexaFluor568, 1:400), and MAP2 antibodies (Novus biotechne #nb300-213, 1:500; Jackson Immuno #703-545-155 AlexaFluor488, 1:400). A Zeiss 780 laser scanning confocal microscope was used to acquire a z-stacked image (63x oil immersion 1.4 numerical aperture). Zen Blue software (Zeiss) and Fiji-Image J software used for image processing. PSD-95 and GluN1 labeled extra-luminal puncta located within 3μm of dendrite plasma membrane were considered synaptic and included in quantification. Punta were counted along 100μm MAP2 positive dendritic sections from 8 individual cells from each incubation condition. Experimenters were blinded to experimental conditions for quantification.

Statistics: Sample size were determined based on prior experiments of this type with an effect size of 20% and power = 0.8. Tests of normality were used to determine the appropriate test. Multiple comparisons used 1- or 2-way ANOVA or nonparametric ANOVA as indicated for each experiment. Exact p values are provided and both the

number of animals and the number of observations are indicated as appropriate. Data unless other indicated are plotted as mean ± SEM. All statistical analyses were completed using Prism 7 software (GraphPad).

Acknowledgments: This work was supported by NS080979 and Ellison Medical Foundation (GLW), the NINDS imaging core facility (P30NS061800) and by NS038631 (EG). E.G. is an Investigator of the Howard Hughes Medical Institute. We thank the OHSU histology core for processing of samples, Randy Woltjer for advice concerning interpretation of the histology, Jacob Raber and Sydney Weber Boutros for assistance with the behavioral assessments, Gail Marracci and Priya Chaudhary for advice on immune cell markers, Weinan Sun for wild-type NMDA receptor subunit constructs, and Farzad Jalali-Yazdi for NMDA receptor amino acid sequence alignments. Competing interests: All authors declare that they have no competing interests. Data and materials availability: All summary data and individual measurements are included in the paper, associated supplementary figures and tables.

Keywords: autoimmunity, NMDA receptors, hippocampus, encephalitis, autoantibodies, neuroinflammation

Fig. 1

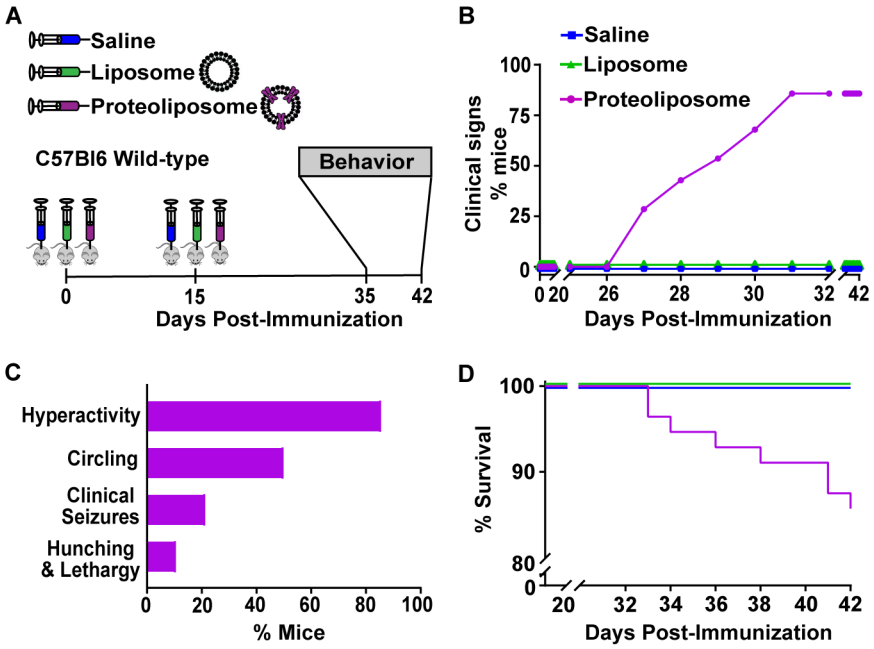
A
Saline
Liposome
Proteoliposome
C57Bl6 Wild-type
Behavior
0
15
35
42
Days Post-Immunization
B
Saline
Liposome
Proteoliposome
Clinical signs
% mice
100
75
50
25
0
0 20
26
28
30
32
42
Days Post-Immunization
C
Hyperactivity
Circling
Clinical
Seizures
Hunching
& Lethargy
0
20
40
60
80
100
% Mice
D
% Survival
100
90
80
0
20
32
34
36
38
40
42
Days Post-Immunization

Figure 1. Proteoliposome-treated mice show a pronounced phenotype (A) Timeline of treatment and behavioral testing. Adult wild-type received subcutaneous injections at day 0 and at day 15 with proteoliposome (purple) or control - liposome (green) or saline (blue). (B) Clinical signs were plotted from the first injection. Only proteoliposome-treated mice displayed clinical signs by six weeks post-immunization. (C) Clinical signs in proteoliposome-treated mice included locomotor hyperactivity and circling as well seizures and abnormal posture. (D) Kaplan-Meier survival plot revealed a marked increase in mortality in proteoliposome treated-mice.

Fig. 2

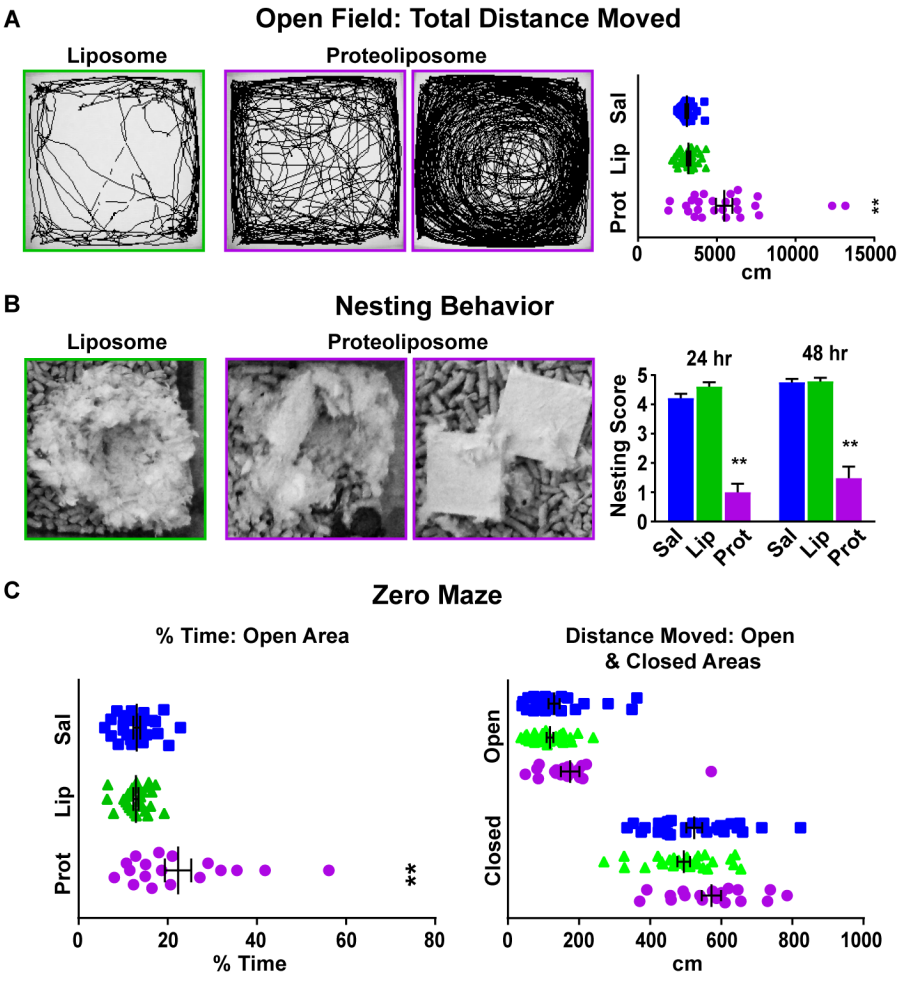
A
Open Field: Total Distance Moved
Liposome
Proteoliposome
Sal
Lip
Prot
**
0
5000
10000
15000
cm
B
Nesting Behavior
Liposome
Proteoliposome
24 hr
48 hr
Nesting Score
0
1
2
3
4
5
**
**
Sal
Lip
Prot
Sal
Lip
Prot
C
Zero Maze
% Time: Open Area
Sal
Lip
Prot
**
0
20
40
60
80
% Time
Distance Moved: Open & Closed Areas
Open
Closed
0
200
400
600
800
1000
cm

Figure 2. Behavioral assessment (A) Representative movement traces in the open field from a control mouse (field outlined in green) and two proteoliposome treated-mice (field outlined in purple) illustrate the hyperactivity phenotype. Total distance moved in the treatment groups are plotted at right: proteoliposome (purple), liposome (green) and saline (blue) purple. (B) Representative images of a normal nest created by a control mouse compared to the partial or incomplete nests in two proteoliposome treated-mice. Nests were scored at 24 and 48 hours and quantified as shown at right. (C) Mice were assessed in the zero maze for time spent in the open area (left) and for the total distance moved in the open and closed areas.

Fig. 3

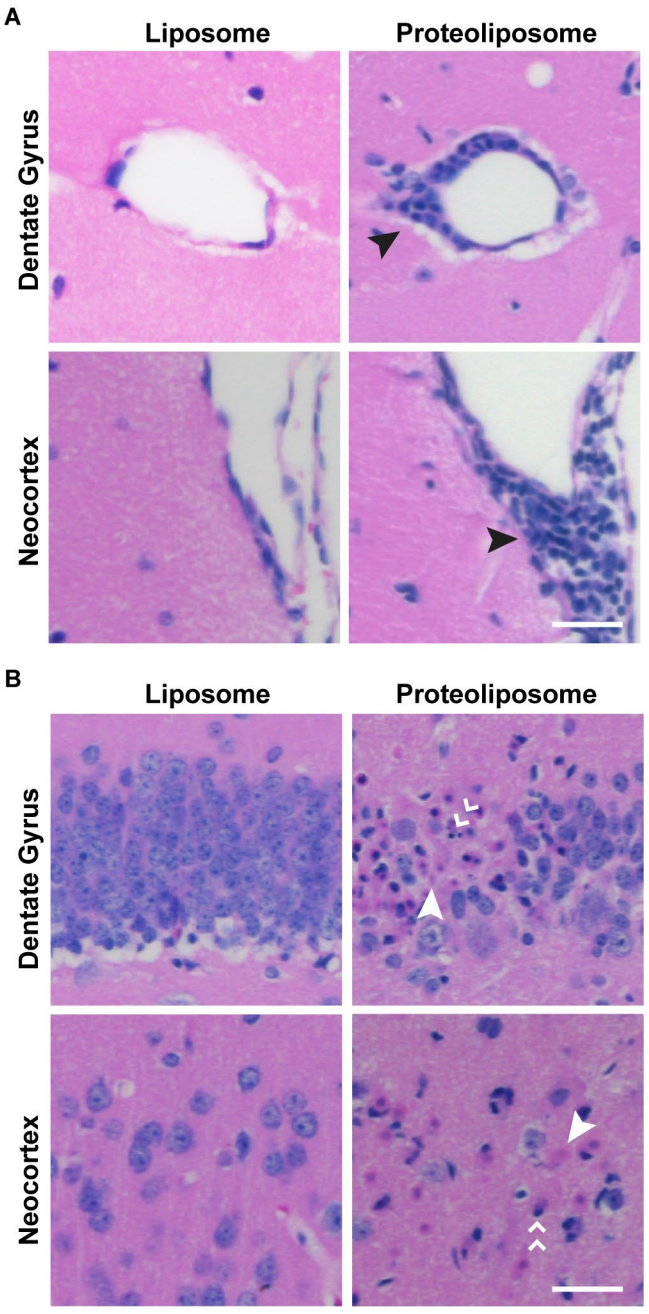
A
Liposome
Proteoliposome
Dentate Gyrus
Neocortex
B
Liposome
Proteoliposome
Dentate Gyrus
Neocortex

Figure 3. Histological evidence of CNS inflammation (A) Representative Images of perivascular cuffing (black arrow, right panels) in hippocampal and neocortical tissue from a proteoliposome-treated mouse. Matched samples from liposome-treated controls are shown at left. (B) Representative tissue sections also showed discrete areas of cell loss including karyolysis (single white arrow) and pyknosis (double white arrow) in a proteoliposome- treated mouse (right), but not in a control (left). Scale bar: 100μm.

Fig. 4

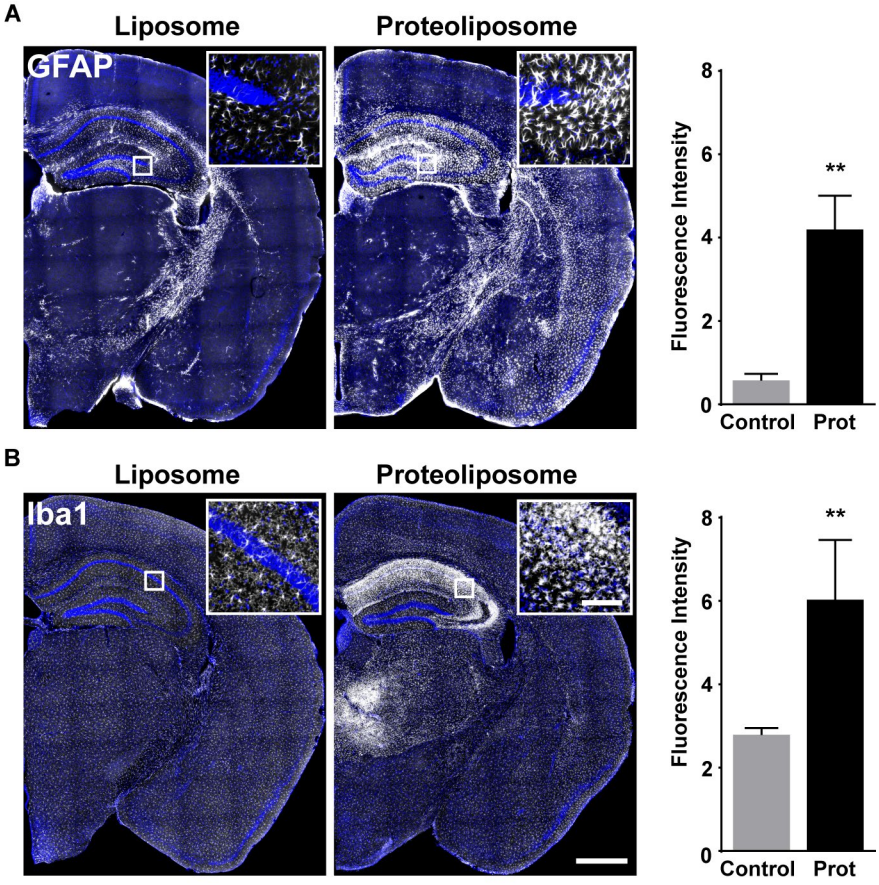
A
Liposome
Proteoliposome
GFAP
Fluorescence Intensity
8
6
4
2
0
**
Control
Prot
B
Liposome
Proteoliposome
Iba1
Fluorescence Intensity
8
6
4
2
0
**
Control
Prot

Figure 4. Evidence for reactive gliosis (A) Immunofluorescence for GFAP (white) was markedly enhanced in proteoliposome-treated mice (right) compared to controls (left). The insets are higher magnification images from the hippocampus to show individual astrocytes. The histogram shows quantification of GFAP immunofluorescence (see methods). (B) Labeling with the microglial marker Iba1 (white) was also greatly increased in proteoliposome-treated mice (right) compared to control (left), particularly in the hippocampus and thalamus. Higher magnification inset show intense microglia in the hippocampus of proteoliposome-treated mouse compared to the scattered microglial labeling in control. Immunofluorescence was quantified in the histogram as for GFAP. Scale bar: 1000μm (inset 100μm).

Fig. 5

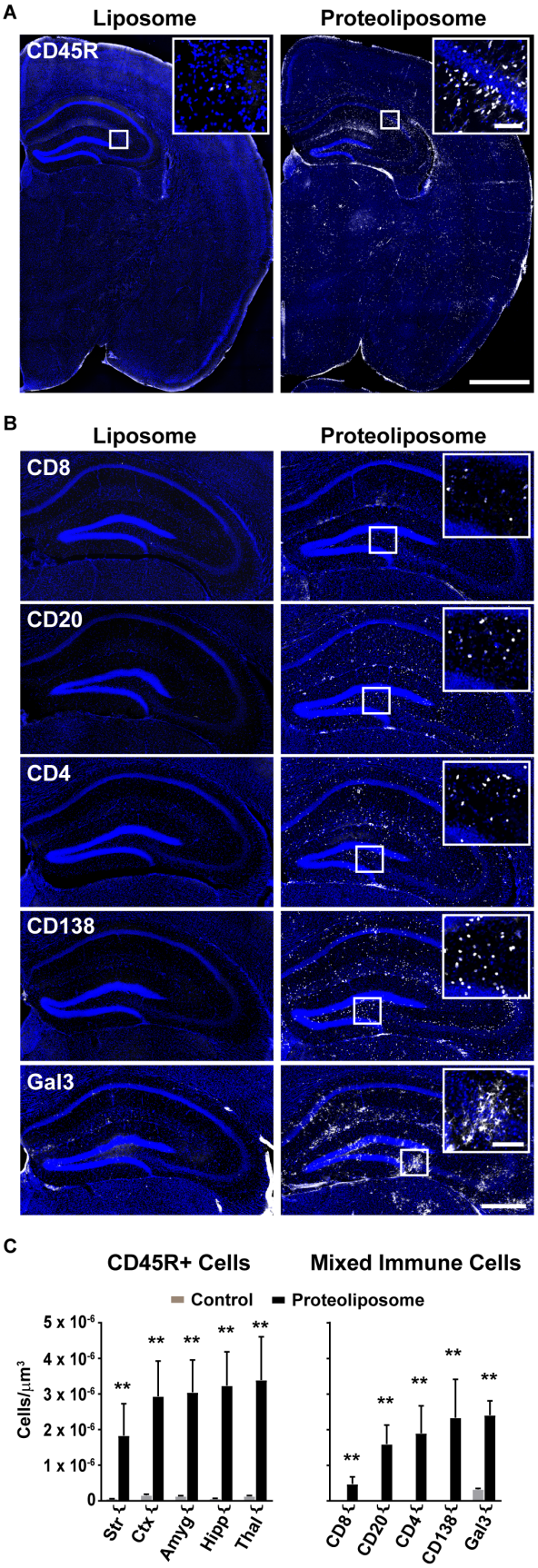
A
Liposome
Proteoliposome
CD45R
B
Liposome
Proteoliposome
CD8
CD20
CD4
CD138
Gal3
C
CD45R+ Cells
Mixed Immune Cells
Control
Proteoliposome
Cells/μm³
5 x 10⁻⁶
4 x 10⁻⁶
3 x 10⁻⁶
2 x 10⁻⁶
1 x 10⁻⁶
0
**
Str
Ctx
Amyg
Hipp
Thal
CD8
CD20
CD4
CD138
Gal3

Figure 5. Prominent immune cell infiltration (A) Robust expression of the pan-leukocyte marker, CD45R in a proteoliposome treated-mouse (right). Insets show labeling of individual $CD45R^+$ cells (white) from the indicated region of the hippocampus. Coronal sections from control mice had few if any $CD45R^+$ cells (left). Scale bar: 1000μm (inset 100μm). (B) Control mice (left) had sparse or absent labeling for a battery of immune cell markers ($CD8^+$, $CD4^+$, $CD20^+$, $CD138^+$, $Gal3^+$). Proteoliposome treated-mice showed marked increases in immune cell infiltrates as indicated with the insets from the hippocampal region; [Scale bar: 500μm (inset 200μm). (C) Left: $CD45R^+$ density (cells/μm^3) in striatum (Str), cortex (Ctx), amygdala (Amyg), hippocampus (Hipp) and thalamus (Thal) in proteoliposome-treated (black) and control mice (gray). Right: $CD8^+$, $CD4^+$, $CD20^+$, $CD138^+$, $Galectin3^+$ cell densities (cells/μm^3) in the hippocampus of proteoliposome treated (black) and control mice (gray). Only $Gal3^+$ cells were of sufficient density to be seen on the histogram in control mice.

Table 1.

Mean CD45R cell densities by anatomical region: 6 weeks post-immunization		
Anatomical Region	Control (cells/μm^3; $x10^{-7}$)	Proteolip. (cells/μm^3; $x10^{-7}$)
Striatum	0.57 ± 0.05	18.3± 8.94 **
Cortex	1.54 ± 0.32	29.3± 9.92 **
Amygdala	1.32 ± 0.13	30.4± 9.07 **
Hippocampus	0.59 ± 0.15	32.3± 9.50 **
Thalamus	1.30 ± 1.89	33.9± 12.1 **
**p = 0.0022, Mann Whitney test; n=6 mice/group		
Mean CD45R cell densities by anatomical region: 3 weeks post-immunization		
Anatomical Region	Control (cells/μm^3; $x10^{-7}$)	Proteolip. (cells/μm^3; $x10^{-7}$)
Striatum	1.16 ± 0.15	108.0 ± 54.5
Cortex	2.33 ± 0.44	46.7 ± 16.9
Amygdala	0.85 ± 0.19	47.3 ± 34.4
Hippocampus	0.97 ± 0.16	88.1 ± 17.5 *
Thalamus	1.53 ± 0.36	28.9 ± 13.7
*p = 0.0286, Mann Whitney test; n=4 mice/group		

Mean Immune cell subtype densities in hippocampus: 6 weeks post-immunization		
Immune Cell Subtype	Control (cells/μm^3; $x10^{-7}$)	Proteolip. (cells/μm^3; $x10^{-7}$)
CD8	0.026 ± 0.014	4.74 ± 2.00 **
CD20	$0 \times 10^0 \pm 0 \times 10^0$	15.9 ± 5.33 **
CD4	0.007 ± 0.006	18.9 ± 7.69 **
CD138	0.007 ± 0.007	23.3 ± 10.7 **
Galectin3	3.21 ± 0.265	24.0 ± 4.05 **
**p = 0.0022, Mann Whitney test; n=6 mice/group		
Mean Immune cell subtype densities in hippocampus: 3 weeks post-immunization		
Immune Cell Subtype	Control (cells/μm^3; $x10^{-7}$)	Proteolip. (cells/μm^3; $x10^{-7}$)
CD8	0.009 ± 0.006	0.10^{7} ± 0.03
CD20	0.03 ± 0.03	13.2 ± 9.47 *
CD4	0.38 ± 0.11	35.9 ± 16.5
CD138	0.07 ± 0.04	13.9 ± 11.4
Galectin3	2.81 ± 0.34	39.8 ± 14.0
*p = 0.0476, Mann Whitney test; n=5 mice/group		

Table 1. Quantification of immune cell infiltration Mean $CD45R^{+}$ cell densities across sampled anatomical regions in control and proteoliposome-treated mice at 6 and 3 weeks post-immunization (± SEM). Mean immune cell subtype densities in the hippocampus of control and proteoliposome treated mice at 6 and 3 weeks post-immunization (± SEM).

Fig. 6

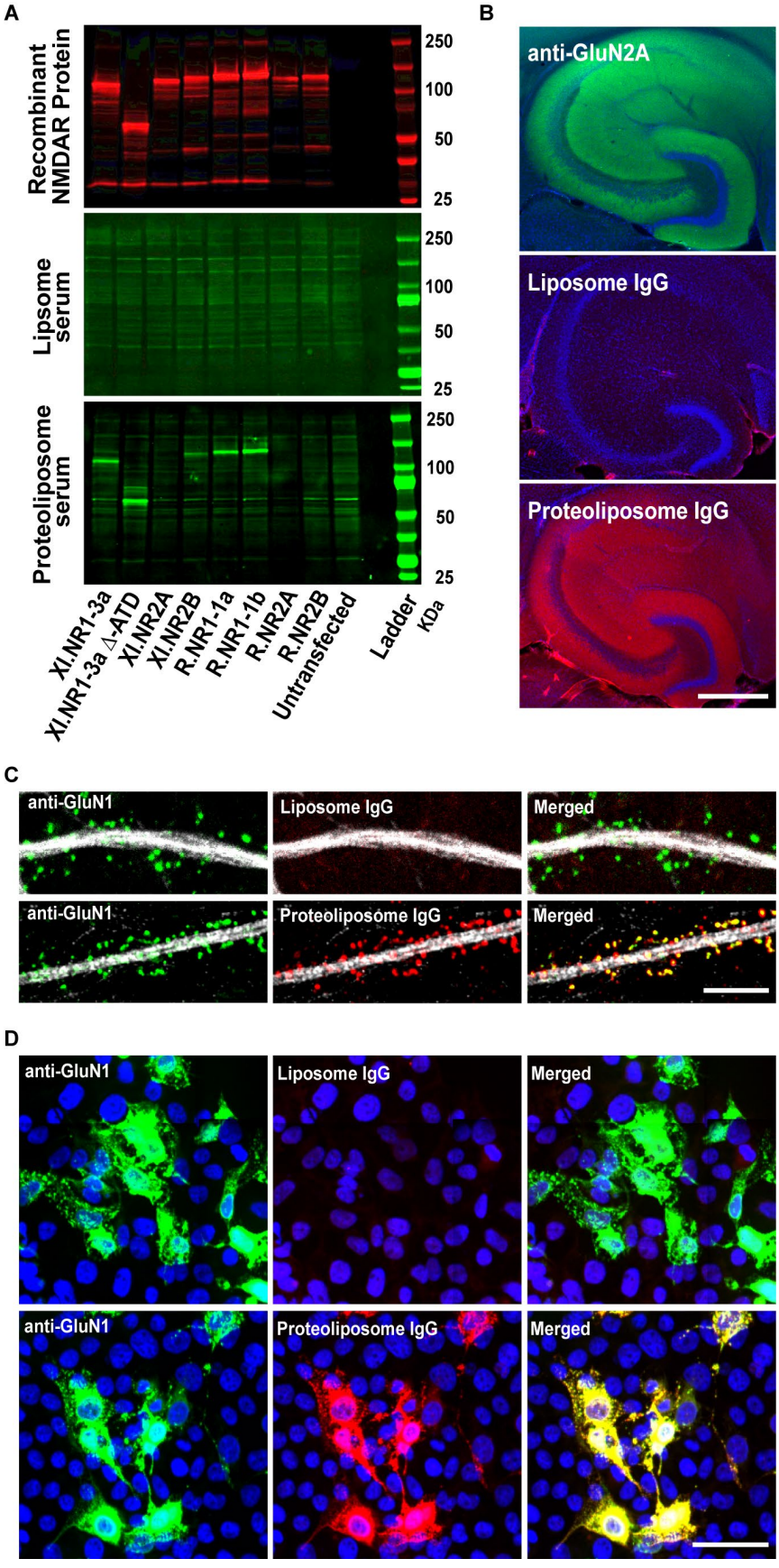
A
Recombinant NMDAR Protein
Lipsome serum
Proteoliposome serum
250
100
50
25
Xl.NR1-3a
Xl.NR1-3a Δ-ATD
Xl.NR2A
Xl.NR2B
R.NR1-1a
R.NR1-1b
R.NR2A
R.NR2B
Untransfected
Ladder
KDa
B
anti-GluN2A
Liposome IgG
Proteoliposome IgG
C
anti-GluN1
Liposome IgG
Merged
anti-GluN1
Proteoliposome IgG
Merged
D
anti-GluN1
Liposome IgG
Merged
anti-GluN1
Proteoliposome IgG
Merged

Figure 6. Detection of NMDA receptor subtype-specific serum antibodies and localization of IgG binding to NMDA receptors (A) A battery of recombinant GFP-tagged NMDA receptor subunits from *Xenopus* (Xl) and Rat (R) were blotted and detected with anti-GFP antibodies (red, top panel). Incubation with serum (1:100) derived from a liposome-treated mouse showed no specific labeling (green, middle panel). Serum (1:100) derived from a proteoliposome-treated mouse showed bands corresponding to GluN1 subunit isoforms in *Xenopus* and rat (Xl.GluN1-3a, R.GluN1-1a, R.GluN1-1b), *Xenopus* GluN2B as well as a *Xenopus* GluN1 lacking the ATD domain (Xl.NR1-3a ΔATD). Blots are from representative liposome-treated and proteoliposome-treated mice showing clinical signs of disease. (B) The pattern of immunoreactivity in hippocampal tissue sections for a commercial NMDA receptor antibody (GluN2A) in a wildtype mouse (left) matched that for purified IgG derived from proteoliposome-treated mice (right). IgG from liposome-treated mice had no labeling (middle). (Scale bar: 500μm). (C) Dendrites of cultured hippocampal neurons showed the expected punctate pattern of synapses using an anti-GluN1 antibody (green, left). IgG from proteoliposome-treated mice also showed punctate labeling along dendrites (bottom row, middle, red) that exactly matched anti-GluN1 labeling in the merge (bottom row, right, yellow). IgG from liposome-treated mice showed no labeling (top row, middle) although synapses were present as labeled with anti-GluN1 (top row, left and right, green).Dendritic shafts were labeled with anti-MAP2 antibody (gray) to enhance visualization, Scale bar: 5μm. (D) HEK293FT cells transfected with rat GluN1/2A subunits were labeled with anti-GluN1 antibody (left, top and bottom, green) as did IgG from proteoliposome-treated mice (bottom, middle, red). Merge panel shows

colocalization (bottom, right, yellow). IgG derived from control mice (top middle panel, red) showed no labeling. Scale bar: 15μm.

Fig. 7

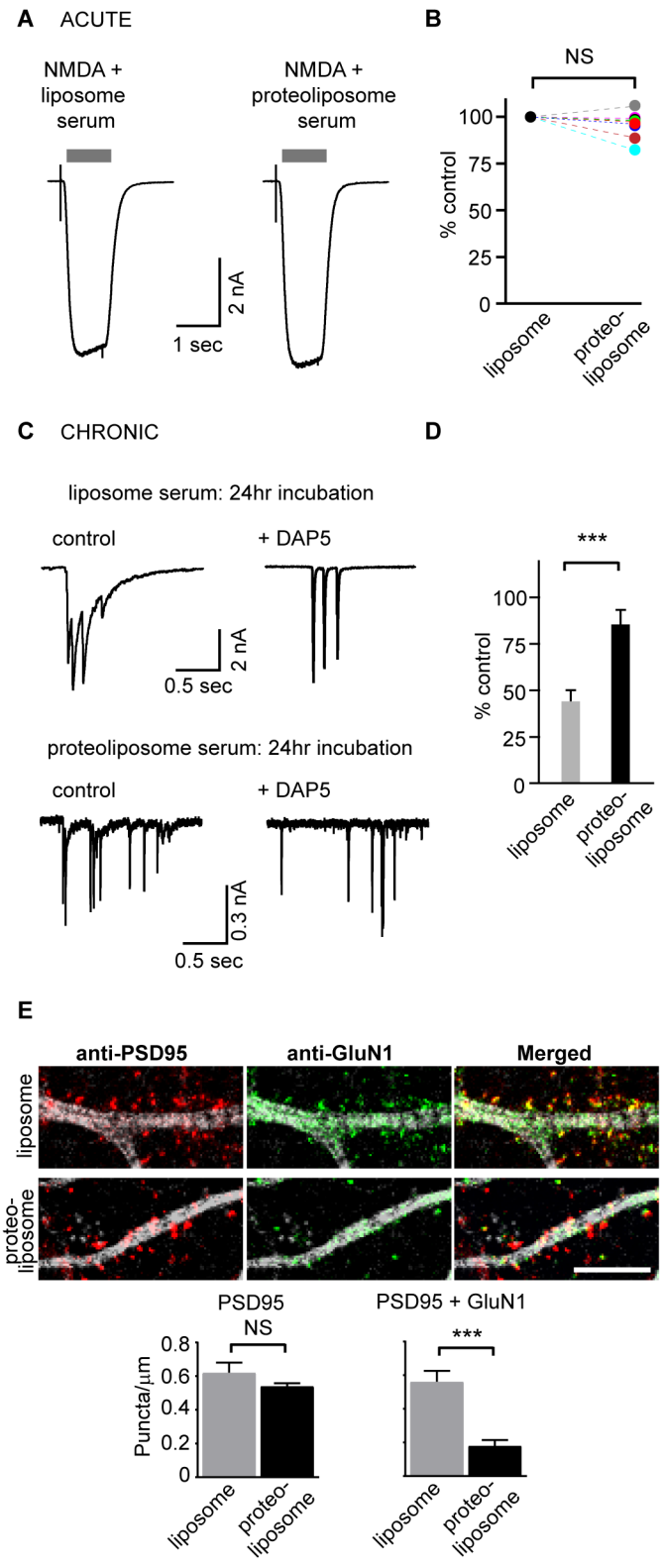
A ACUTE
NMDA + liposome serum
NMDA + proteoliposome serum
2 nA
1 sec
B
NS
100
75
50
25
0
% control
liposome
proteo-liposome
C CHRONIC
liposome serum: 24hr incubation
control
+ DAP5
2 nA
0.5 sec
proteoliposome serum: 24hr incubation
control
+ DAP5
0.3 nA
0.5 sec
D
***
100
75
50
25
0
% control
liposome
proteo-liposome
E
anti-PSD95
anti-GluN1
Merged
liposome
proteo-liposome
PSD95
NS
PSD95 + GluN1
***
Puncta/μm
0.8
0.6
0.4
0.2
0
liposome
proteo-liposome
liposome
proteo-liposome

Figure 7. Serum-induced reduction in NMDA receptor function and GluN1 immunoreactivity (A) Representative whole-cell currents in a neuron evoked by acute flow-pipe application of NMDA + serum from liposome-treated, or NMDA + serum from proteoliposome-treated mice, respectively. Serum dilution was 1:100. (B) Evoked whole-cell NMDA currents for 8 neurons revealed no measurable effect of proteoliposome serum on current amplitudes. (C, D) Spontaneous excitatory postsynaptic currents were recorded following 24-hour incubation ("chronic") in serum from liposome or proteoliposome-treated mice. EPSCs in cells treated with serum from liposome-treated mice showed prolonged bursts of inward currents that were reduced by the NMDA receptor antagonist, D-AP5 (top left and right). The slow components of the NMDA receptor-mediated currents were less prominent after incubation with serum from proteoliposome-treated mice (bottom left) and were markedly less sensitive to block by D-AP5 (bottom right) as quantified by total charge transfer in the histogram in panel D. (E) Dendrites of cultured hippocampal neurons incubated in serum from liposome and proteoliposome-treated mice show no change in synaptic puncta as indicated by PSD-95 immunoreactivity (left, top & bottom, red). The same dendrites showed a measurable reduction in GluN1 labeled synapses when incubated in serum from proteoliposome-treated mice (middle, bottom, green) whereas incubation in serum from control mice showed no reduction (middle, top, green). Right panels show overlap of GluN1 and PSD-95 immunolabeling (right, top and bottom, yellow) illustrating the reduction of GluN1 positive synapses in cells incubated in serum from proteoliposome treated mice. Dendrites are labeled with anti-MAP antibody (gray). Scale bar: 10μm. Quantification of PSD-95 and GluN1 positive synaptic puncta per μm of dendrite shown

in left and right histograms (liposome = gray; proteoliposome = black). Quantification of PSD-95 and GluN1 positive synaptic puncta per μm of dendrite shown in left and right histograms (liposome = gray; proteoliposome = black).

Fig. 8

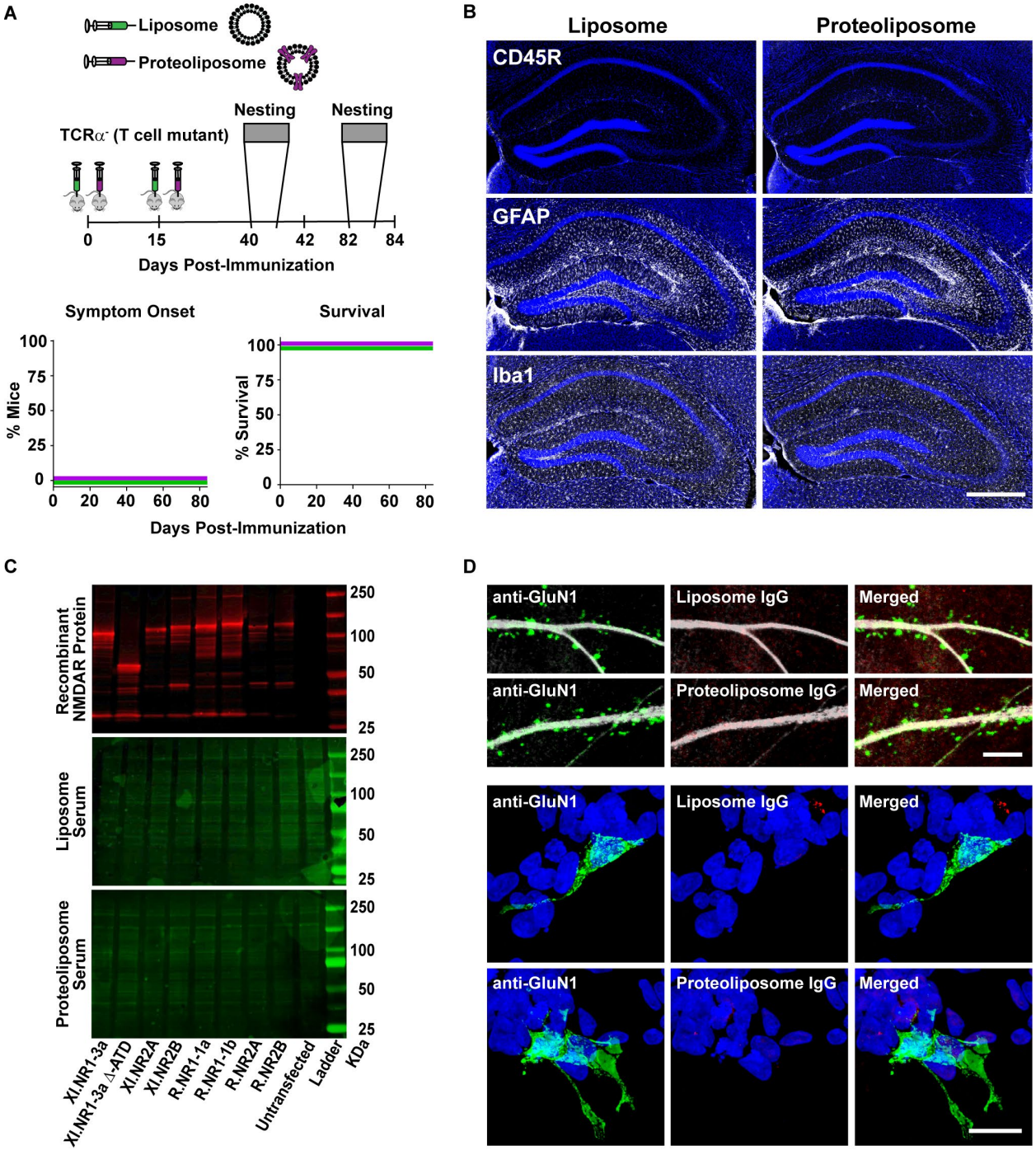
A
Liposome
Proteoliposome
Nesting
Nesting
TCRα- (T cell mutant)
0
15
40
42
82
84
Days Post-Immunization
Symptom Onset
Survival
% Mice
% Survival
100
75
50
25
0
0 20 40 60 80
Days Post-Immunization
B
Liposome
Proteoliposome
CD45R
GFAP
Iba1
C
Recombinant NMDAR Protein
Liposome Serum
Proteoliposome Serum
250
100
50
25
Xl.NR1-3a
Xl.NR1-3a Δ-ATD
Xl.NR2A
Xl.NR2B
R.NR1-1a
R.NR1-1b
R.NR2A
R.NR2B
Untransfected
Ladder
KDa
D
anti-GluN1
Liposome IgG
Merged
anti-GluN1
Proteoliposome IgG
Merged
anti-GluN1
Liposome IgG
Merged
anti-GluN1
Proteoliposome IgG
Merged

Figure 8. T cells are required to generate disease state in proteoliposome treated mice (A) Tcrα$^-$ mutant mice were immunized in parallel with a cohort of wildtype mice. None of the proteoliposome-treated mutant mice showed clinical or behavioral signs of encephalitis, or altered mortality rates by 12 weeks post-immunization (liposome = green; proteoliposome = purple). (B) Proteoliposome-treated TCRα$^-$ mice did not show increased labeling with CD45R (top panels), GFAP (middle panels) or Iba1 (bottom panels) compared to liposome-treated TCRα$^-$ mice. Scale bar: 500μm (C) A battery of recombinant GFP-tagged NMDA receptor subunits from *Xenopus* (Xl) and Rat (R) were blotted and detected with anti-GFP antibodies (red, top panel). Incubation with serum (1:100) derived from a liposome- and proteoliposome-treated mouse showed no specific labeling (green, middle & bottom panel). (D) Purified IgG from proteoliposome-treated TCRα$^-$ mice did not label synapses in mouse hippocampal neurons or HEK293FT cells expressing rat GluN1/2A subunits. The upper two rows show synapse with anti-GluN1 antibody (left, green) whereas IgG from liposome-treated mice (top middle, red) or IgG from proteoliposome treated-mice (bottom middle panel, red) showed no labeling. Scale bar = 5μm. The lower two rows show anti-GluN1 antibody labeling of HEK293FT cells expressing rat GluN1/2A subunits (left, green), but no labeling was detected using IgG from proteoliposome-treated or liposome-treated mice (bottom two rows, middle). Scale bar: 15μm.

List of Supplementary Materials:

Fig S1. IgG labeling in the CNS of proteoliposome treated-mice.

Fig S2. Confirmation of GluN1 specific antibodies in proteoliposome-treated mice.

Fig S3. Neuroinflammation and immune cell infiltrate at 3 weeks post-immunization.

Fig S4. Early detection of NMDA receptor immunoreactivity.

Fig S5. Autoimmune reaction to rat NMDA receptor holoprotein

Fig S6. B cells are required to generate disease state in proteoliposome treated mice.

Table S1. Individual value for all analyzes with N<20.

Movie S1-S5: Home cage video illustrating behavioral phenotype of proteoliposome-treated mice.

Fig. S1

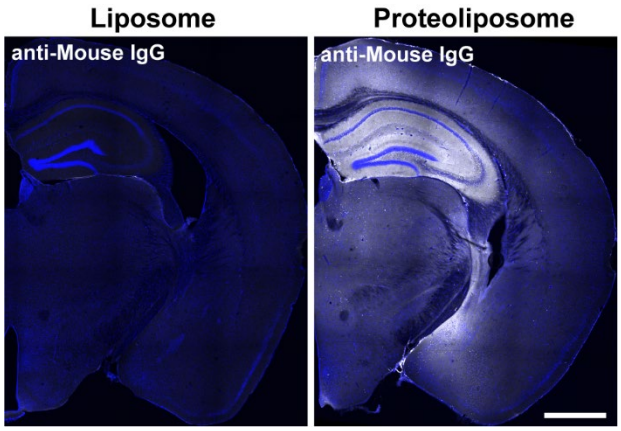

Figure S1. IgG labeling in the CNS of proteoliposome-treated mice

Representative image of mouse IgG labeling (anti-mouse heavy & light chain specific secondary antibody) in the brain of proteoliposome-treated (right) and the lack of IgG labeling in liposome-treated mice (right), [Scale bar = 1000μm].

Fig. S2

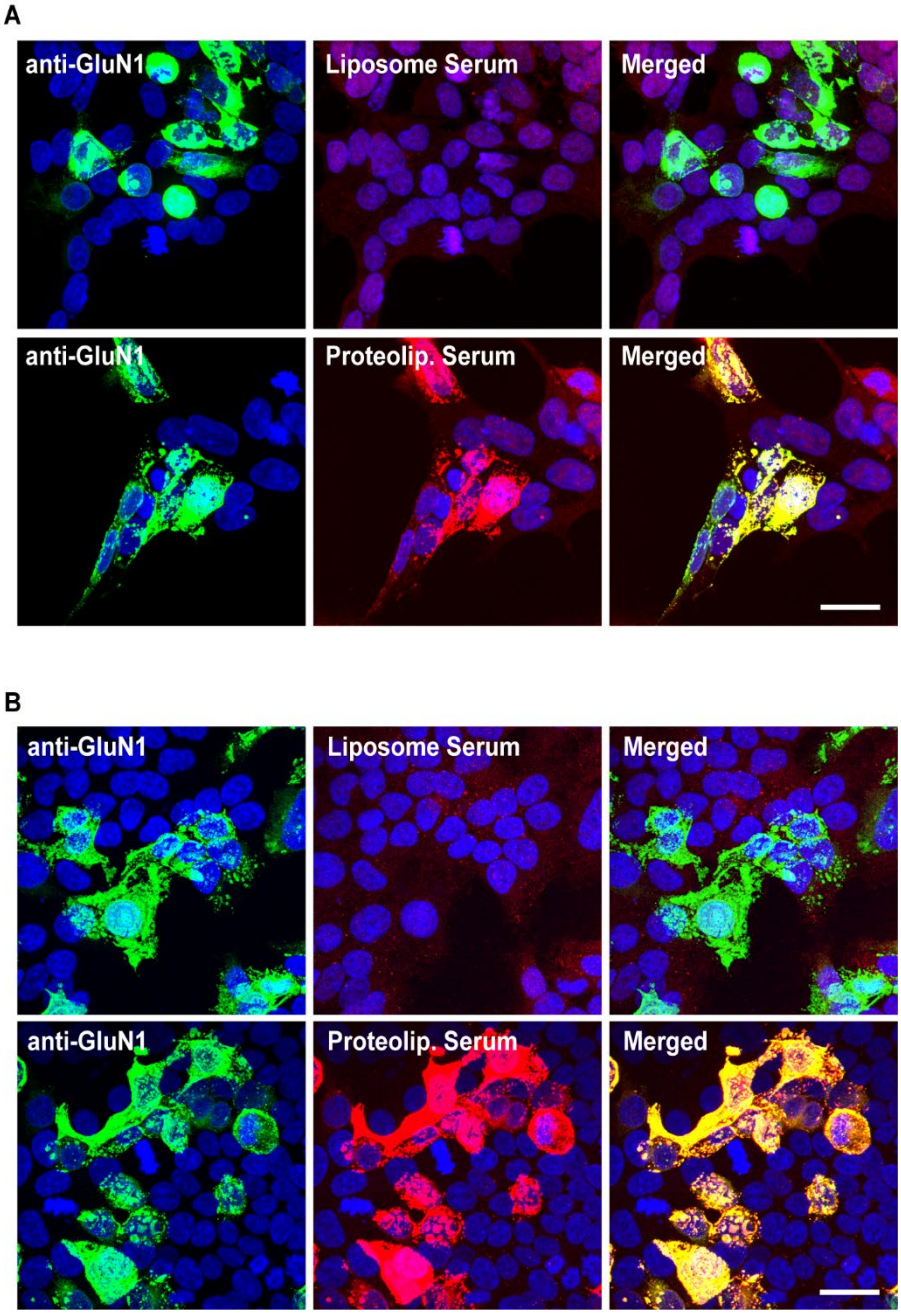
A
anti-GluN1
Liposome Serum
Merged
anti-GluN1
Proteolip. Serum
Merged
B
anti-GluN1
Liposome Serum
Merged
anti-GluN1
Proteolip. Serum
Merged

Figure S2. Confirmation of GluN1 specific antibodies in proteoliposome-treated mice

In both A and B, HEK293FT cells were transfected with rat GluN1 only. (A) HEK cells were labeled with anti-GluN1 antibody (left, top and bottom, green) and serum from mice treated with *X. laevis* NMDA receptor proteoliposomes (bottom, middle, red). Merge panel show colocalization (bottom, right, yellow) Serum from controls showed no staining (top middle panel, red). (B) GluN1 expressing HEK cells showed immunoreactivity to an anti-GluN1 antibody (left, top and bottom, green) and serum from mice treated with rat NMDA receptor proteoliposomes (bottom, middle, red). Colocalization is depicted in merged panel (bottom, right, yellow). No staining was observed in serum from control mice (top middle panel, red). Scale bar: 25μm.

Fig.S3

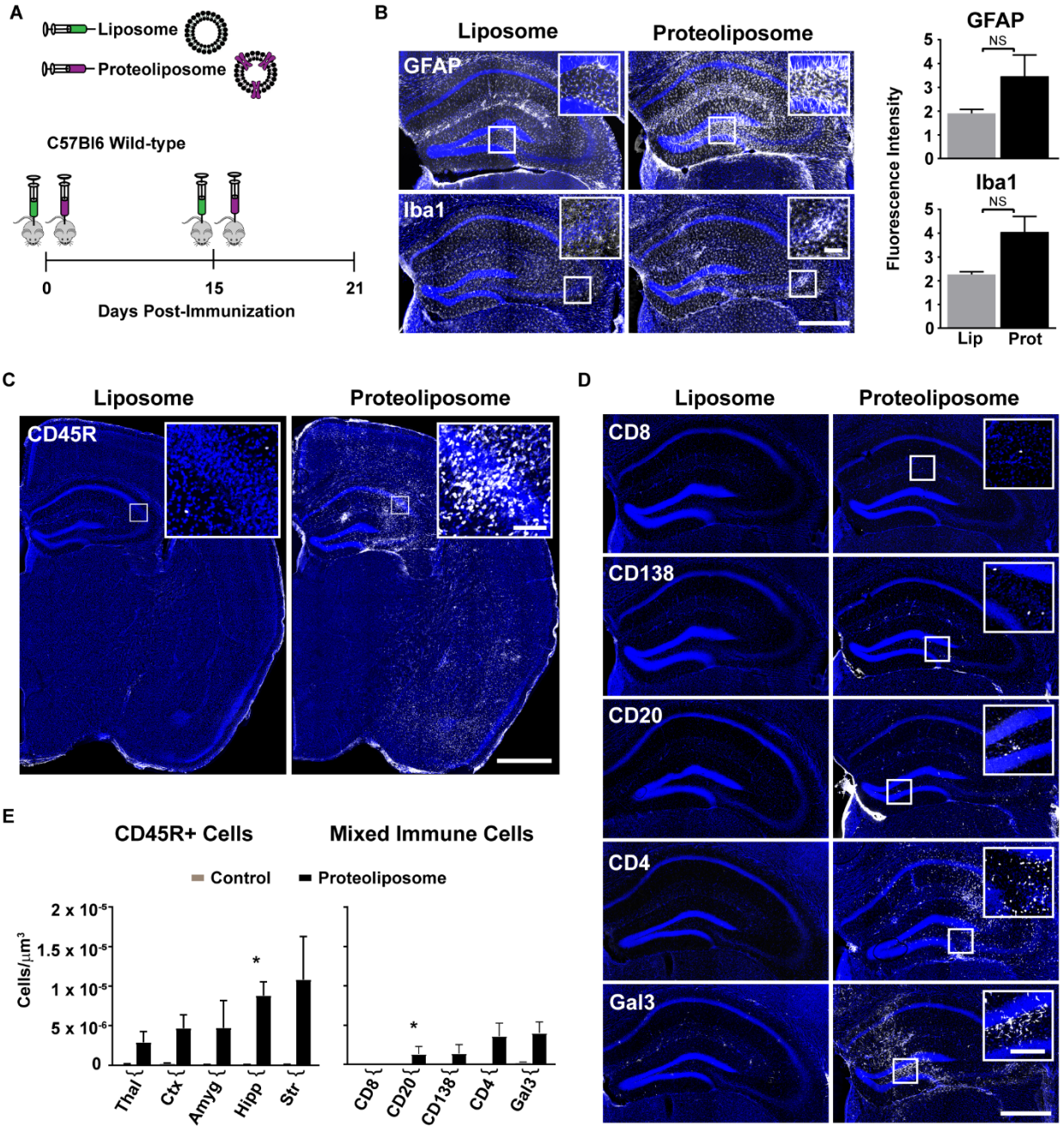
A
Liposome
Proteoliposome
C57Bl6 Wild-type
0
15
21
Days Post-Immunization
B
Liposome
Proteoliposome
GFAP
Iba1
GFAP
NS
Iba1
NS
Fluorescence Intensity
Lip
Prot
C
Liposome
Proteoliposome
CD45R
D
Liposome
Proteoliposome
CD8
CD138
CD20
CD4
Gal3
E
CD45R+ Cells
Mixed Immune Cells
Control
Proteoliposome
Cells/μm3
Thal
Ctx
Amyg
Hipp
Str
CD8
CD20
CD138
CD4
Gal3

Figure S3. Neuroinflammation and immune cell infiltrates at 3 weeks post-immunization (A) A separate cohort of two month old adult C57Bl6 wild-type mice received a subcutaneous injection on Day 0 and 15; proteoliposome (purple) or liposome (green). At three weeks post-immunization, one of the proteoliposome-treated mice had a clinical seizure, but no other overt behavioral changes or altered mortality rates were observed. (B) GFAP and Iba1 labeling in proteoliposome-treated mice (right panels; upper & lower, respectively) showed foci of increased immunofluorescence as compared to liposome-treated control mice (left). Insets show high magnification images of individual astrocytes and microglia in hippocampus. Scale bar: 500μm (inset: 100μm). GFAP and Iba1 fluorescence show no overall significant differences between proteoliposome-treated (black) and liposome-treated mice (gray) despite discrete foci of increased fluorescence in proteoliposome-treated mice (top and bottom histograms, respectively; GFAP: proteoliposome v. control. $p = 0.2857$; Iba1: proteoliposome v. control. $p = 0.0952$, Mann Whitney test; n=5 mice/group; y-axis units shown as x 10^7). (C) $CD45R^+$ cells were present in the brain of proteoliposome-treated mice (right), whereas liposome-treated mice had sparse or absent labeling (left). Inset: high magnification images show individual $CD45R^+$ cells in hippocampus; Scale bar: 1000 μm (inset: 100μm). (D) Representative immune cell labeling ($CD8^+$, $CD4^+$, $CD20^+$, $CD138^+$, $Galectin3^+$) in the hippocampus of a proteoliposome-treated mouse (right) and liposome-treated control mouse (left) with high magnification insets. Scale bar: 500μm (inset: 200μm). (E) Quantification of $CD45R^+$ cell densities (left histogram) in multiple brain regions and immune cell subtypes (right histogram) in the hippocampus only. See Table 1 for descriptive statistics and p values.

Fig. S4

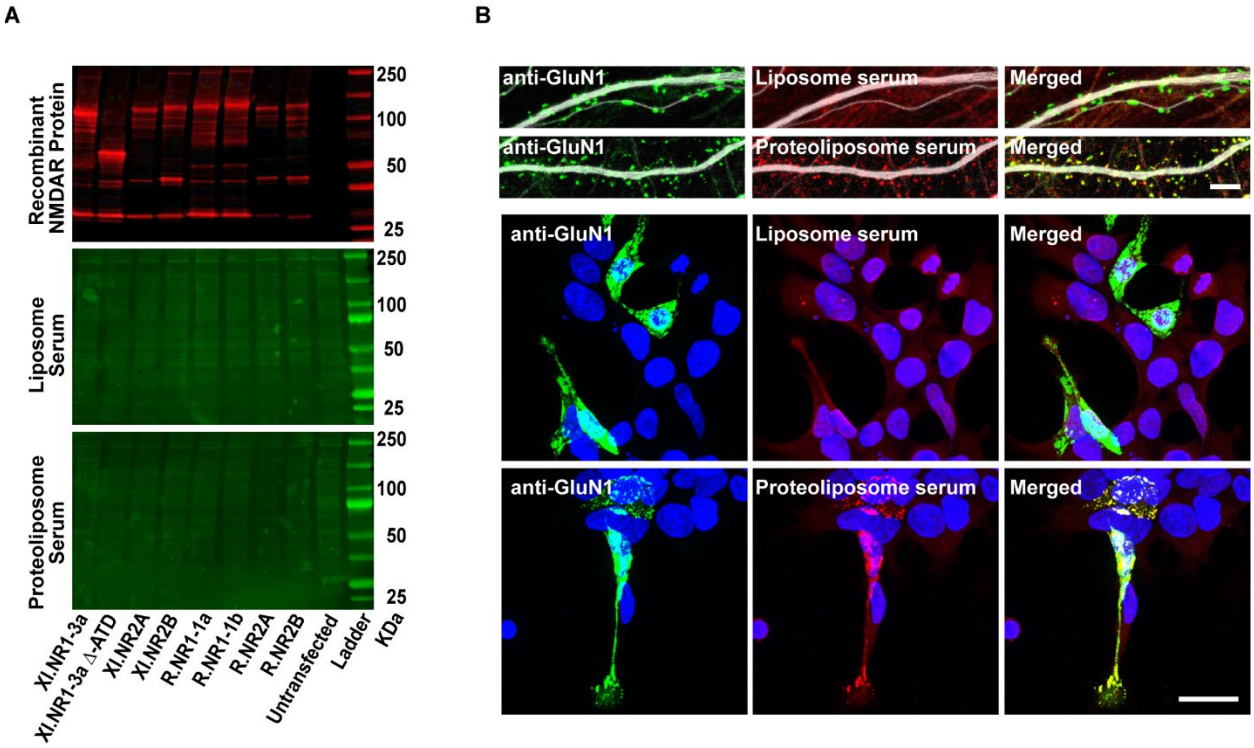
A
Recombinant NMDAR Protein
Liposome Serum
Proteoliposome Serum
250
100
50
25
Xl.NR1-3a
Xl.NR1-3a Δ-ATD
Xl.NR2A
Xl.NR2B
R.NR1-1a
R.NR1-1b
R.NR2A
R.NR2B
Untransfected
Ladder
KDa
B
anti-GluN1
Liposome serum
Merged
anti-GluN1
Proteoliposome serum
Merged
anti-GluN1
Liposome serum
Merged
anti-GluN1
Proteoliposome serum
Merged

Figure S4. Early detection of NMDA receptor immunoreactivity (A) Recombinant GFP-tagged NMDA receptor subunits from *Xenopus* (XI) and Rat (R) were blotted and detected with anti-GFP antibodies (red, top panel). Incubation with serum (1:100) derived from liposome- and proteoliposome treated mice showed no specific labeling at this early time point post-immunization (green, middle & bottom panels). (B) Dendrites of cultured hippocampal neurons showed the expected punctate pattern of synapses using an anti-GluN1 antibody (green, left). Higher concentrations of serum (1:10) from proteoliposome-treated mice were required to show punctate labeling along dendrites (bottom row, middle, red) that exactly matched anti-GluN1 labeling in the merge (bottom row, right, yellow). Serum (1:10) from liposome-treated mice showed no labeling (top row, middle) although synapses were present as labeled with anti-GluN1 (top row, left and right, green). Dendritic shafts were labeled with anti-MAP2 antibody (gray) to enhance visualization, Scale bar: 5μm. (C) HEK293FT cells transfected with rat GluN1/2A subunits were labeled with anti-GluN1 antibody (left, top and bottom, green) as did serum from proteoliposome-treated mice (bottom, middle, red). Merge panel shows colocalization (bottom, right, yellow). Serum derived from control mice (top middle panel, red) showed no labeling. Scale bar: 25μm.

Fig. S5

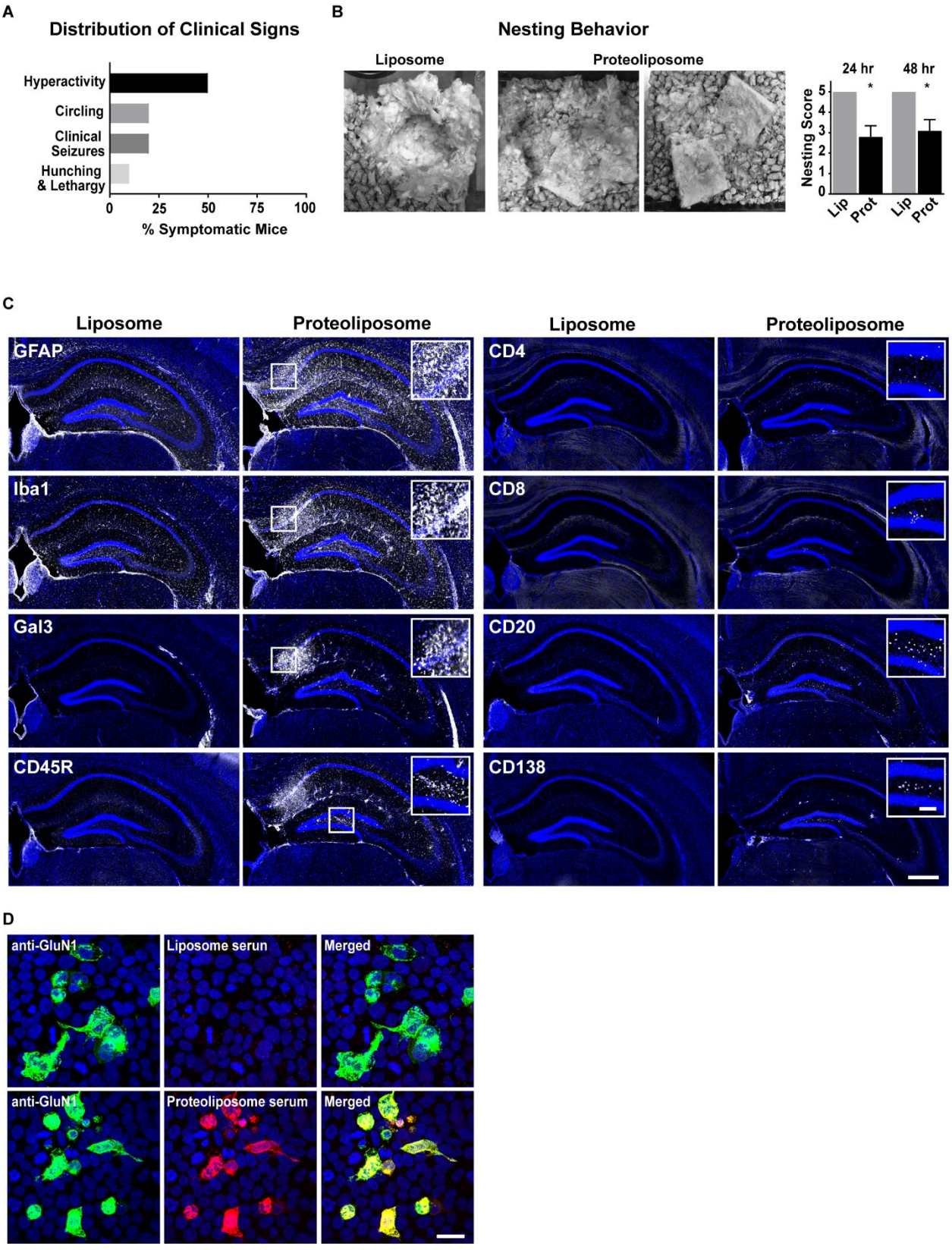
A
Distribution of Clinical Signs
Hyperactivity
Circling
Clinical Seizures
Hunching & Lethargy
0
25
50
75
100
% Symptomatic Mice
B
Nesting Behavior
Liposome
Proteoliposome
24 hr
48 hr
Nesting Score
Lip
Prot
Lip
Prot
C
Liposome
Proteoliposome
Liposome
Proteoliposome
GFAP
CD4
Iba1
CD8
Gal3
CD20
CD45R
CD138
D
anti-GluN1
Liposome serun
Merged
anti-GluN1
Proteoliposome serum
Merged

Figure S5. Autoimmune reaction to Rat NMDA receptor holoprotein Wild-type mice received subcutaneous injections at day 0 and day 15 with rat NMDA receptor GluN1/GluN2A subunit proteoliposomes (25µg NMDA receptor protein/200µl saline; n=10) or liposome only (n=8). (A) Home cage observations revealed 60% of mice displayed at least one sign of disease including locomotor hyperactivity, circling, seizures and/or abnormal posture. (B) Representative images of a normal nest created by a control mouse compared to the partial or incomplete nests in two proteoliposome treated-mice. Nests were scored at 24 and 48 hours and quantified as shown at right (24hr: liposome v. proteoliposome $p = 0.0178$; 48hr: liposome v. proteoliposome, $p = 0.0318$; Kruskal-Wallis test). (C) Immunofluorescence labeling of glial and leukocyte markers (GFAP, Iba1, Galectin3, CD45R, CD4, CD8, CD20, CD138) in the hippocampus rat proteoliposome-treated mice (right) compared to controls (left). In proteoliposome-treated mice regions of enhanced glial immunoreactivity and immune cell infiltrates were observed. Scale bar: 500µm. The insets are higher magnification images from the hippocampus to show individual cells. Scale bar: 100µm. (D) HEK293FT cells transfected with rat GluN1/2B subunits were labeled with anti-GluN1 antibody (top, left & right, green) and serum from proteoliposome-treated mice (middle, right, red; n = 10/10 mice). Merge panel shows colocalization (bottom, right, yellow). Serum derived from control mice (middle, left, red) showed no labeling (n=0/8). Scale bar: 25µm.

Fig. S6

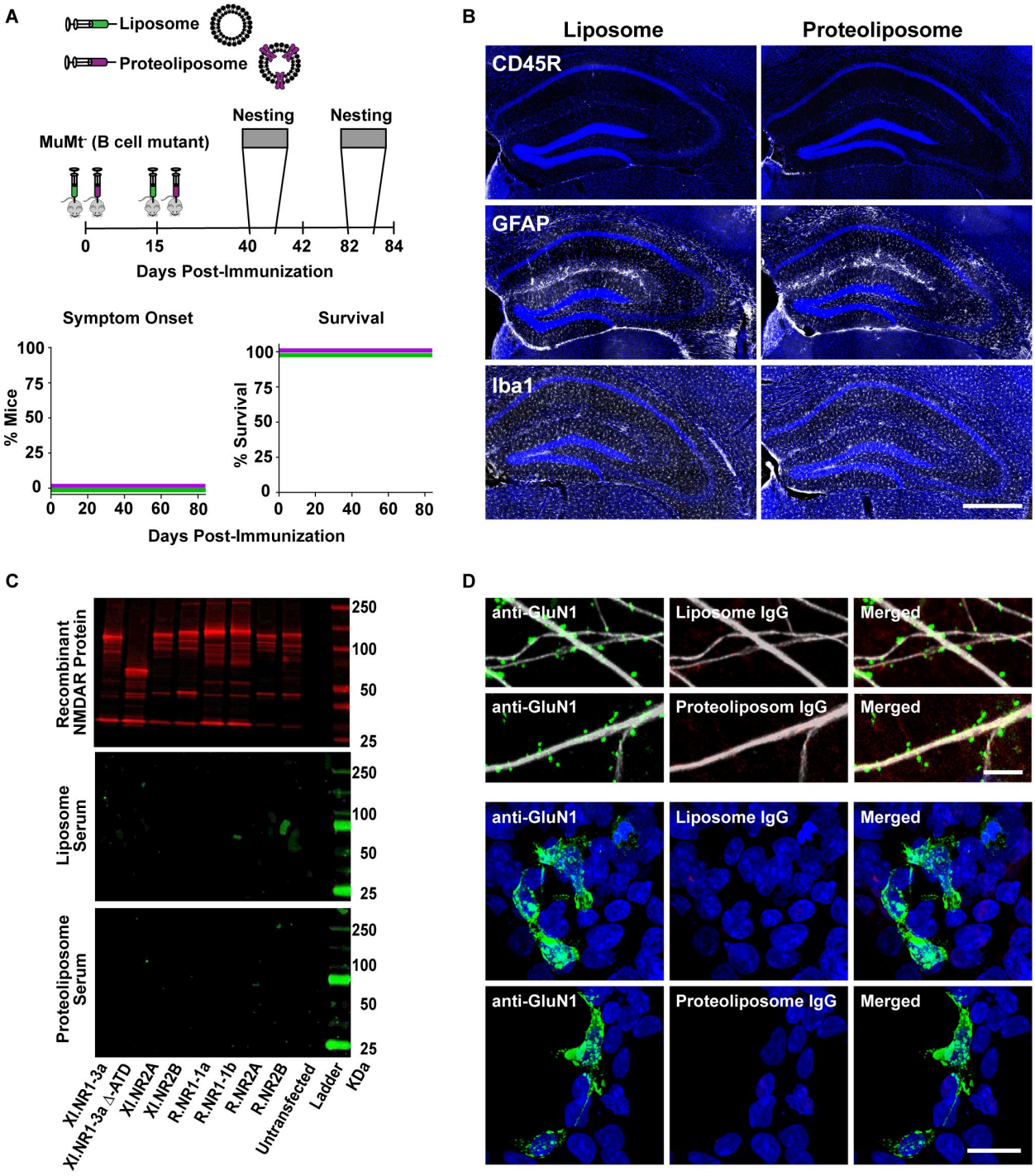
A
Liposome
Proteoliposome
MuMt⁻ (B cell mutant)
Nesting
Nesting
0
15
40
42
82
84
Days Post-Immunization
Symptom Onset
Survival
% Mice
% Survival
Days Post-Immunization
B
Liposome
Proteoliposome
CD45R
GFAP
Iba1
C
Recombinant NMDAR Protein
Liposome Serum
Proteoliposome Serum
250
100
50
25
Xl.NR1-3a
Xl.NR1-3a Δ-ATD
Xl.NR2A
Xl.NR2B
R.NR1-1a
R.NR1-1b
R.NR2A
R.NR2B
Untransfected
Ladder
KDa
D
anti-GluN1
Liposome IgG
Merged
anti-GluN1
Proteoliposom IgG
Merged
anti-GluN1
Liposome IgG
Merged
anti-GluN1
Proteoliposome IgG
Merged

Figure S6. B cells are required to generate disease state in proteoliposome treated mice (A) MuMt$^-$ mutant mice were immunized in parallel with a cohort of wildtype mice. Proteoliposome-treated mutant mice showed no clinical or behavioral signs of encephalitis, or altered mortality rates by 12 weeks post-immunization (liposome = green; proteoliposome = purple). (B) Proteoliposome-treated MuMt$^-$ mice did not show increased labeling with CD45R (top panels), GFAP (middle panels) or Iba1 (bottom panels) compared to liposome-treated MuMt$^-$ mice. Scale bar: 500μm (C) Recombinant GFP-tagged NMDA receptor subunits from *Xenopus* (XI) and Rat (R) were blotted and detected with anti-GFP antibodies (red, top panel). Incubation with serum (1:100) derived from a liposome- and proteoliposome-treated MuMt$^-$ mouse showed no specific labeling (green, middle & bottom panel). (D) Purified IgG from proteoliposome-treated MuMt$^-$ mice did not label synapses in mouse hippocampal neurons or HEK293FT cells expressing rat GluN1/2A subunits. The upper two rows show synapse with anti-GluN1 antibody (left, green) whereas IgG from liposome-treated mice (top middle, red) or IgG from proteoliposome treated-mice (bottom middle panel, red) showed no labeling. Scale bar = 5μm. The lower two rows show anti-GluN1 antibody labeling of HEK293FT cells expressing rat GluN1/2A subunits (left, green), but no labeling was detected using IgG from proteoliposome-treated or liposome-treated mice (bottom two rows, middle). Scale bar: 15μm.

Supplementary Table 1. Individual value for all analyzes with N<20

Fig. 4

GFAP Fluorescence Intensity: 6 weeks post-immunization (Fig. 4A)		
N	Control (10^9)	Proteolip. (10^9)
1	0.53	5.97
2	0.50	6.84
3	0.32	4.85
4	0.18	1.75
5	1.19	4.49
6	1.06	1.62

IBA1 Fluorescence Intensity: 6 weeks post-immunization (Fig. 4B)		
N	Control (10^9)	Proteolip. (10^9)
1	2.81	4.18
2	2.33	5.19
3	2.47	13.20
4	3.29	3.94
5	3.30	5.35
6	2.90	4.69

Fig. 5

$CD45R^+$ cell density: 6 weeks post-immunization (Fig. 5C)			
Striatum	N	Control (cells/μm^3; $x10^{-7}$)	Proteolip. (cells/μm^3; $x10^{-7}$)
	1	0.54	3.29
	2	0.38	16.70
	3	0.61	62.10
	4	0.73	8.60
	5	0.67	11.70
	6	0.47	7.49
Cortex	N	Control (cells/μm^3; $x10^{-7}$)	Proteolip. (cells/μm^3; $x10^{-7}$)
	1	0.88	10.70
	2	2.20	56.40
	3	2.55	61.50
	4	0.49	29.60
	5	1.80	11.10
	6	1.33	6.78
Amygdala	N	Control (cells/μm^3; $x10^{-7}$)	Proteolip. (cells/μm^3; $x10^{-7}$)

	1	1.79	26.10
	2	1.62	64.00
	3	1.28	50.40
	4	1.01	21.30
	5	0.96	15.80
	6	1.27	5.36
Hippocampus	N	Control (cells/μm^3; $x10^{-7}$)	Proteolip. (cells/μm^3; $x10^{-7}$)
	1	0.21	16.00
	2	0.17	45.68
	3	0.78	74.07
	4	0.43	22.56
	5	0.99	20.70
	6	0.99	15.11
Thalamus	N	Control (cells/μm^3; $x10^{-7}$)	Proteolip. (cells/μm^3; $x10^{-7}$)
	1	0.92	27.30
	2	1.32	68.11
	3	1.22	74.17
	4	1.18	13.88
	5	2.20	14.90
	6	0.97	5.25

Mixed immune cell density: 6 weeks post-immunization (Fig. 5C)			
CD8	N	Control (cells/μm^3; $x10^{-7}$)	Proteolip. (cells/μm^3; $x10^{-7}$)
	1	0	0.70
	2	0	1.87
	3	0	12.90
	4	0.083	0.26
	5	0.042	7.73
	6	0.037	4.99
CD20	N	Control (cells/μm^3; $x10^{-7}$)	Proteolip. (cells/μm^3; $x10^{-7}$)
	1	0	3.62
	2	0	8.93
	3	0	41.20
	4	0	14.10
	5	0	15.00
	6	0	12.70
CD4	N	Control (cells/μm^3; $x10^{-7}$)	Proteolip. (cells/μm^3; $x10^{-7}$)
	1	0	9.20
	2	0	31.60

	3	0	51.80
	4	0.039	7.79
	5	0	9.79
	6	0	3.67
CD138	N	Control (cells/μm^3; $x10^{-7}$)	Proteolip. (cells/μm^3; $x10^{-7}$)
	1	0	5.37
	2	0.041	16.20
	3	0	76.10
	4	0	17.10
	5	0	17.60
	6	0	7.81
Gal3	N	Control (cells/μm^3; $x10^{-7}$)	Proteolip. (cells/μm^3; $x10^{-7}$)
	1	2.86	24.00
	2	2.25	20.50
	3	3.73	41.70
	4	3.59	18.10
	5	2.91	27.20
	6	3.96	12.90

Fig. 7

Ephys: $I_{NMDAevoked}$ following acute serum application (Fig. 7B)			
N	Liposome serum ($I_{NMDAevoked}$) (nA)	Proteolip. serum ($I_{NMDAevoked}$) (nA)	% control
1	-5.09211	-5.18799	98.1519
2	-6.6769	-6.73101	99.1961
3	-7.0453	-7.22732	97.4815
4	-10.2169	-12.3023	83.0487
5	-4.54811	-4.63864	98.0484
6	-4.85956	-5.43507	89.4112
7	-9.47039	-8.98104	105.449
8	-5.97238	-6.19655	96.3823

Ephys: sEPSC DAPV sensitivity following chronic serum incubation (Fig. 7D)			
Liposome serum	$I_{cumulative}$ Baseline	$I_{cumulative}$ DAPV	% Baseline
1	-62.3551	-41.2035	66.0788
2	-22.364	-9.14722	40.9015

3	-26.675	-14.9295	55.9681
4	-25.2304	-4.36733	17.3098
5	-13.6142	-7.89848	58.0165
6	-29.5417	-7.78112	26.3394
Proteolip. serum	$I_{cumulative}$ Baseline	$I_{cumulative}$ DAPV	% Baseline
1	-31.8286	-27.5927	86.6915
2	-21.7316	-17.6507	81.2214
3	-8.72062	-9.37577	107.513
4	-27.9574	-19.8388	70.9608
5	-3.66914	-2.98848	81.4491

PSD-95$^+$ Puncta: 24hr incubation (Fig. 7E)		
N	Control (puncta/μm)	Proteolip. (puncta/μm)
1	0.43	0.57
2	0.75	0.45
3	0.7	0.53
4	0.67	0.53
5	0.79	0.55
6	0.79	0.56
7	0.43	0.50
8	0.41	0.63

PSD-95$^+$ + NR1$^+$ Puncta: 24hr incubation (Fig. 7E)		
N	Control (puncta/μm)	Proteolip. (puncta/μm)
1	0.34	0.12
2	0.68	0.10
3	0.62	0.10
4	0.52	0.27
5	0.61	0.08
6	0.90	0.17
7	0.43	0.26
8	0.39	0.34

Fig. S3

GFAP Fluorescence Intensity: 3 weeks post-immunization (Fig. S3B)		
N	Control (10^9)	Proteolip. (10^9)

1	2.17	5.84
2	1.44	5.42
3	1.88	2.15
4	1.71	2.15
5	2.36	1.81

IBA1 Fluorescence Intensity: 3 weeks post-immunization (Fig. S3B)		
N	Control (10^9)	Proteolip. (10^9)
1	2.51	4.84
2	2.45	5.58
3	2.2	4.73
4	2.27	3.05
5	1.90	2.08

$CD45R^+$ cell density: 3 weeks post-immunization (Fig. S3E)			
Striatum	N	Control (cells/μm^3; $x10^{-7}$)	Proteolip. (cells/μm^3; $x10^{-7}$)
	1	1.42	256.00
	2	1.25	61.12
	3	0.75	114.60
	4	1.25	0.88
Cortex	N	Control (cells/μm^3; $x10^{-7}$)	Proteolip. (cells/μm^3; $x10^{-7}$)
	1	2.23	43.30
	2	3.53	62.51
	3	2.19	80.03
	4	1.40	1.16
Amygdala	N	Control (cells/μm^3; $x10^{-7}$)	Proteolip. (cells/μm^3; $x10^{-7}$)
	1	0.81	16.20
	2	0.76	23.10
	3	0.46	149.80
	4	1.40	0.24
Hippocampus	N	Control (cells/μm^3; $x10^{-7}$)	Proteolip. (cells/μm^3; $x10^{-7}$)
	1	0.58	84.20
	2	1.29	83.34
	3	1.14	135.00
	4	0.85	49.89
Thalamus	N	Control (cells/μm^3; $x10^{-7}$)	Proteolip. (cells/μm^3; $x10^{-7}$)
	1	0.68	46.10
	2	1.64	58.38

	3	1.38	9.82
	4	2.44	1.47

Mixed immune cell density: 3 weeks post-immunization (Fig. S3E)			
CD8	N	Control (cells/μm^3; $x10^{-7}$)	Proteolip. (cells/μm^3; $x10^{-7}$)
	1	0.02	0.16
	2	0.028	0.12
	3	0	0.09
	4	0	0.14
	5	0	0
CD20	N	Control (cells/μm^3; $x10^{-7}$)	Proteolip. (cells/μm^3; $x10^{-7}$)
	1	0	50.80
	2	0	3.80
	3	0.16	8.31
	4	0	3.43
	5	0	0
CD4	N	Control (cells/μm^3; $x10^{-7}$)	Proteolip. (cells/μm^3; $x10^{-7}$)
	1	0.26	26.10
	2	0.15	35.10
	3	0.49	98.00
	4	0.75	20.60
	5	0.24	0.19
CD138	N	Control (cells/μm^3; $x10^{-7}$)	Proteolip. (cells/μm^3; $x10^{-7}$)
	1	0.03	59.40
	2	0.07	4.96
	3	0	3.06
	4	0.03	2.11
	5	0.21	0
Gal3	N	Control (cells/μm^3; $x10^{-7}$)	Proteolip. (cells/μm^3; $x10^{-7}$)
	1	2.47	38.70
	2	3.82	63.20
	3	2.92	78.30
	4	3.08	16.70
	5	1.77	2.30

Fig. S5

Nesting Behavior: Rat NMDA receptor proteoliposome preparation (Fig. S5B)					
N	24hr Liposome	24hr Rat NMDAR Proteoliposome		48hr Liposome	48hr Rat NMDAR Proteoliposome
1	5	1		5	1
2	5	3		5	3
3	5	5		5	5
4	5	2		5	4
5	5	5		5	5
6	5	5		5	5
7	5	1		5	1
8	5	1		5	1
9		3			4
10		2			2

Supplementary Table 1. Individual value for all analyzes with N<20. Raw data used in all statistical analyzes. Data presented by figure. Values are rounded to the nearest decimal point and expressed in format presented in corresponding histograms.

Movie S1-S5.

The videos illustrate the behavioral phenotype observed in home cage of proteoliposome-treated mice: movie S1. Representative liposome-treated control mouse showing normal activity in home cage; movie S2. Proteoliposome-treated mouse showing *locomotor hyperactivity*; movie S3. Proteoliposome-treated mouse displaying aberrant *circling*; movie S4. Proteoliposome-treated mouse during a *clinical seizure*; movie S5. Proteoliposome-treated mouse showing a prominent *hunched back & lethargy*.

Chapter 3*: Conclusions and future directions*

The central nervous system is an immunosuppressive environment with robust physical and biochemical barriers preventing easy access to pathogens as well as the panoply of peripheral immune cells charged with its defense. Despite such exquisite immunoregulatory mechanisms, autoimmune disorders of the CNS are not uncommon. Whatever their etiology, these conditions represent a breakdown in self-tolerance, derangement of immuno-protective machinery, and disruption of the delicate environs central to our unconscious and conscious experience.

The discovery of pathogenic antibodies in the context of autoimmune encephalitis has allowed clinicians to identify disorders that in the recent past were deemed idiopathic. The importance of these discoveries should not be understated as it facilitates better patient care and opens new research opportunities in the field of neuroimmunology. With both goals in mind, in this thesis work we generated a *de novo* mouse model of the most commonly reported variant of autoimmune encephalitis.

Model limitations and advantages

The model of autoimmune NMDA receptor encephalitis reported in this thesis recapitulates key clinical and pathophysiological aspects of the disorder (Graus et al., 2016a). However, as with any animal model there are certain limitations that should not be overlooked. For example, the histopathological signature in mice treated with NMDA receptor holoprotein includes significant infiltration of $CD4^+$ T cells. In the human condition, T cell involvement is not considered a major pathogenic component (Dalmau et al., 2017). This may of course represent an unintentional sampling bias as the tissue

available for pathological assessment is rare, and generally limited to the most severe cases. However, we cannot eliminate the possibility that the contribution of T cells in our animal model may be indicative of fundamental interspecies differences in immunity rather than reflecting the pathophysiology of the human disorder. Although worth considering, this seems less likely given reports of substantial levels of pro-inflammatory cytokines (IL-17A) and T_H17 cells in CSF of anti-NMDA receptor encephalitis patients.

In addition, unlike passive transfer studies our results to date cannot readily parse the pathophysiological contribution of autoantibodies from that of neuroinflammation. As mentioned above, intraventricular infusion of CSF from affected individuals has been shown to induce dose-dependent deficits to learning and memory with no concomitant inflammatory response. The observation that certain aspects of the human disorder are not recapitulated in these studies argues for the involvement of neuroinflammation. Thus, despite its shortcomings our model does offer certain advantages.

Furthermore, serum collected from mice in our studies treated with NMDA receptor proteoliposome contained polyclonal antibodies recognizing subunits other than GluN1. In anti-NMDA receptor encephalitis, *in vitro* studies of CSF or serum from human cases suggest that the conformationally intact GluN1 subunit is the primary immunogen with autoantibodies to this subunit representing a key pathogenic agent. Although this may prove correct, a study of antibodies produced by B cells isolated from patients indicate that only a small fraction produce GluN1 specific antibodies. In addition, B cells from these patients have been shown to produce antibodies to neuronal antigens other than the NMDA receptor (Kreye et al., 2016b). These findings raise the intriguing possibility that anti-NMDA receptor encephalitis pathophysiology may be more complicated than

previously suspected. That our model employs only NMDA receptor protein as the triggering immunogen and reproduces several of the behavioral and histopathological signatures argues against this possibility. Clearly however, more research is necessary to address such possibilities.

These are the most obvious shortcomings of our model; however, each is balanced in large part by its inherent strengths. The utility of our model is two-fold. First, we were able to generate a *de novo* autoimmune reaction using a well-defined immunogen. Thus, we can now trace the etiology of the autoimmune response. This may aid in our understanding of the mechanisms involved in loss of self-tolerance. Moreover, it allows us to manipulate conditions at various stages of disease progression to facilitate the study of different components of the immune response. The second advantage of our model is of course its potential contribution to translational medicine. A number of pharmacological interventions targeting specific components of the immune system can now be tested. We will discuss both points in the next section dedicated to future investigations.

Further model characterization

The first and most obvious question is the identity of the pathogenic epitope in our mouse model, and how it relates to human cases. In the human disorder an amino acid (N368) located on the ATD of the GluN1 subunit has been shown to regulate immunoreactivity (Gleichman et al., 2012a). In that study, point mutations that converted asparagine (N) to a glutamine (Q) nearly eliminated antibody binding in cell-based assays. This is curious as both amino acids are polar, differentiated by a single carbon

in their respective side chains. Substitution of amino-acids with vastly different side chains do not completely eliminate immunoreactivity (Gleichman et al., 2012a). This observation in addition to demonstrated anti-GluN2 antibodies in a subset of patients argues for multiple epitopes in the human disease. To disambiguate the pathogenic epitope(s) in the human condition as well as identify these epitope(s) in our mouse model, we propose a cryo-EM-based assay. Advances in this technology allow for the determination of three-dimensional states in protein complexes with atomic resolution (Bai et al., 2015). The strength of this technique is that native-like receptor complexes bound to either the human or mouse antibodies can be studied. Thus, one could pinpoint the exact epitope(s) bound by antibodies on conformationally intact receptors (Bai et al., 2015; Bianchi et al., 2018; Lü et al., 2017).

Further characterization of the immunopathology observed in our mouse model is another necessary next step. Our results indicate that CD4+ T cells contribute to the pathophysiology of autoimmune NMDA receptor encephalitis. Classically the ability of a specific immune cell subtype to induce, or independently contribute, to a disease has been studied by adoptive transfer. By isolating T cell populations from treated mice and transferring them to a naïve animal we can determine if activated T cells are capable of inducing pathological changes independent of antibody production (Miller et al., 2007). One could complement such studies by further examination of the immunopathology in our mouse model by conducting an immunohistochemical investigation of the T cell sub-populations composing the inflammatory infiltrates. For example, it would be interesting and informative to determine what percentage of the T cell infiltrates in our model are of the pro-infammatory T_H17^+ subtype .

A careful investigation of the development and progression of the autoimmune response in our model would be informative. In such a study, mice at predetermined post-immunization timepoints could be assessed for behavioral abnormalities indicative of the anatomical region involved (e.g., hippocampal dependent learning). Antibody composition and titer, along with neuropathology, could then be correlated with any abhorrent behavior. This would provide a more comprehensive understanding of the disease process and its impacts on behavior.

Translational medicine applications

Our model also offers a platform for the investigation of established and novel therapeutic interventions. The treatment of anti-NMDA receptor encephalitis is protracted, expensive, and often incomplete. Individuals may take years to recover to a degree deemed “full” by clinical evaluation. However, reports by former anti-NMDA receptor encephalitis patients said to have fully recovered, it becomes obvious that the disorder leaves an indelible mark (Cahalan, 2012). Add to this the significant number of relapse-remitting and treatment-refractory cases and the need for more efficacious therapies seems clear.

Examining the effects of a variety of on- and off-label monoclonal antibody (MAB)-based immunotherapies in our mouse model could aid in characterization of the autoimmune response and reveal novel applications of existing therapeutic agents. For example, rituximab, a chimeric (human-mouse) anti-CD20 monoclonal antibody that depletes B cells, is commonly used as a second-line immunotherapy in anti-NMDA receptor encephalitis (Graus et al., 2016a; Titulaer et al., 2013a). Introduction of this agent at

fixed post-immunization time-points could inform us regarding: 1) early contributions of B cells to induction of NMDA receptor autoimmunity; 2) the contribution of B cells to neuroinflammation. Belimumab is another monoclonal antibody worth investigation. This MAB is directed against B lymphocyte stimulator (BLyS), also known as B cell-activating factor (α). This member of the TNF family functions in B cell survival and chemotaxis and is currently a therapeutic target in systemic lupus erythematosus (SLE), (Dubey et al., 2011). In the context of SLE, dysfunction of BLyS has been implicated in the loss of self-tolerance, making it an especially interesting target at early time points of autoimmune pathogenesis in our model. Natalizumab is a monoclonal antibody currently used in the treatment of MS. This MAb targets α4-integrin, a CAM expressed by all leukocytes except neutrophils and essential for transmigration across the BBB. In our model, natalizumab could be used to prevent leukocyte infiltration. Thus, it could aid in parsing the pathogenic contribution of peripheral and CNS-resident immune cells. There are a number of MAbs in use or in development for the treatment T cell lymphoma and related T cell-mediated disorders (Latif and Morris, 2013). For example, Muromonab recognizes the CD3 receptor expressed by all T cell populations. It is currently approved for treatment of acute allograph rejection and has been shown to deplete T cell populations via complement-mediated lysis. Thus, muromonab and related agents could be used to dissect the relative contribution of T cells to early and late stages of the autoimmune reaction in our mice (Latif and Morris, 2013).

Microgliosis is a histopathological feature of anti-NMDA receptor encephalitis as well as in our mouse model. In the past decade fate-mapping studies have facilitated the development of genetic and pharmacological means of microglia ablation (Han et al.,

2017). The colony stimulating factor-1 receptor (CSF-1R) is tyrosine kinase receptor, regulating the differentiation and proliferation of microglia (Elmore et al., 2014). A number of CSF-1R specific tyrosine kinase inhibitors have been characterized in various CNS injury or disease models making them ideal candidates for use in our studies. For example, PLX5622, an orally delivered CSF-1R inhibitor, has been shown to ameliorate inflammation induced by neuronal lesion. Rice and colleagues (2017) demonstrated that a transient ablation of activated microglia following brain injury resolved chronic neuroinflammation (Rice et al., 2017). Interestingly, the astrocytic response to neural injury was not affected by microglial ablation. In our model, ablation of microglia prior to disease induction could provide valuable information regarding the role of microglia in facilitating peripheral immune cell infiltration; whereas, removing microglia after disease induction could address questions regarding the cells role in promoting neuroinflammation.

Finally, our model lends itself to exploration of antigen-specific immune tolerance induction. To this end, a number of strategies involving tolerogenic nanoparticles (tNPs) are currently under development for the treatment of autoimmune diseases. In broad terms, this approach can be divided into strategies aimed at triggering autoreactive immune cell anergy or deletion, tolerizing APCs to prevent induction of an autoimmune response, and expanding Treg cell populations to suppress autoimmunity (Kishimoto and Maldonado, 2018; Serra and Santamaria, 2018). Metal and metal-oxides, liposomes, and various polymers have been used to generate tNPs. The specific advantages and disadvantages of each material are beyond the scope of our discussion. Instead we will focus on a few examples of tNP application. One approach

to tolerizing the immune system is the conjugation of MHC class II-antigen complexes with tNPs to create artificial APCs. Such tNPs are capable of binding to $CD4^+$ T cell receptors; however, in the absence of costimulatory receptors (e.g. CD80) this "synthetic APC" induces T cell anergy or Treg differentiation (Kishimoto and Maldonado, 2018; Serra and Santamaria, 2018). Another approach is to use tNPs to mimic apoptotic cells and drive responding macrophages toward a tolergenic state. For example, by incorporating phoshatidylserine (PS) into liposomes loaded with antigenic material these tNPs are directed toward a macrophage's PS-specific scavenger receptors. Upon PS-tNP binding and phagocytosis, macrophages have been demonstrated to increase expression of pro-tolerance cytokines such as IL-10 and TGFβ while inhibiting pro-inflammatory NF-κB signaling. Using tNPs to target and destroy autoreactive immune effectors has also been explored. For example, pairing antigens with a CD22 receptor ligand, in a liposome-based tNP, has been shown to induce antigen-specific B cell deletion. These tNPS cause the co-localization of an antigen-specific B cell receptor with the CD22 co-inhibitory receptor to stimulate apoptosis. Finally, tNPs have been used to drive T cells toward a pro-tolerance regulatory phenotype. The Aryl Hydrocarbon Receptor (AHR) is a ligand-activated transcription factor controlling T cell differentiation. By targeting this receptor with a tNP containing an AHR ligand and a specific antigen, autoreactive T effector cells have been shifted to T regulatory cells in certain autoimmune disease models (Kishimoto and Maldonado, 2018; Serra and Santamaria, 2018). Any or all of these approaches to induction of antigen-specific immune tolerance could be tested using our mouse model.

References

Ajami, B., Bennett, J.L., Krieger, C., Tetzlaff, W., and Rossi, F.M.V. (2007). Local self-renewal can sustain CNS microglia maintenance and function throughout adult life. Nat. Neurosci. *10*, 1538–1543.

Albert, M.L., and Darnell, R.B. (2004). Paraneoplastic neurological degenerations: keys to tumour immunity. Nat. Rev. Cancer *4*, 36–44.

Amor, S., Groome, N., Linington, C., Morris, M.M., Dornmair, K., Gardinier, M.V., Matthieu, J.-M., and Baker, D. (1994). Identification of epitopes of myelin oligodendrocyte glycoprotein for the induction of experimental allergic encephalomyelitis in SJL and Biozzi AB/H mice. J. Immunol. *153*, 4349–4356.

Anglen, C.S., Truckenmiller, M.E., Schell, T.D., and Bonneau, R.H. (2003). The dual role of CD8+ T lymphocytes in the development of stress-induced herpes simplex encephalitis. J. Neuroimmunol. *140*, 13–27.

Aoto, J., Földy, C., Ilcus, S.M.C., Tabuchi, K., and Südhof, T.C. (2015). Distinct circuit-dependent functions of presynaptic neurexin-3 at GABAergic and glutamatergic synapses. Nat. Neurosci. *18*, 997–1007.

Arina, A., Tirapu, I., Alfaro, C., Rodríguez-Calvillo, M., Mazzolini, G., Inogés, S., López, A., Feijoo, E., Bendandi, M., and Melero, I. (2002). Clinical implications of antigen transfer mechanisms from malignant to dendritic cells. exploiting cross-priming. Exp. Hematol. *30*, 1355–1364.

Ariño, H., Armangué, T., Petit-Pedrol, M., Sabater, L., Martinez-Hernandez, E., Hara, M., Lancaster, E., Saiz, A., Dalmau, J., and Graus, F. (2016). Anti-LGI1–associated cognitive impairment. Neurology *87*, 759–765.

Armangue, T., Titulaer, M.J., Málaga, I., Bataller, L., Gabilondo, I., Graus, F., Dalmau, J., and Spanish Anti-N-methyl-D-Aspartate Receptor (NMDAR) Encephalitis Work Group (2013). Pediatric anti-N-methyl-D-aspartate receptor encephalitis-clinical analysis and novel findings in a series of 20 patients. J. Pediatr. *162*, 850-856.e2.

Bai, X., McMullan, G., and Scheres, S.H.W. (2015). How cryo-EM is revolutionizing structural biology. Trends Biochem. Sci. *40*, 49–57.

Banerjee, R.K., and Datta, A.G. (1983). Proteoliposome as the model for the study of membrane-bound enzymes and transport proteins. Mol. Cell. Biochem. *50*, 3–15.

Bartholomäus, I., Kawakami, N., Odoardi, F., Schläger, C., Miljkovic, D., Ellwart, J.W., Klinkert, W.E.F., Flügel-Koch, C., Issekutz, T.B., Wekerle, H., et al. (2009). Effector T cell interactions with meningeal vascular structures in nascent autoimmune CNS lesions. Nature *462*, 94–98.

Bauer, J., and Bien, C.G. (2016). Neuropathology of autoimmune encephalitides. Handb. Clin. Neurol. *133*, 107–120.

Beaulieu, J.-M., and Gainetdinov, R.R. (2011). The Physiology, Signaling, and Pharmacology of Dopamine Receptors. Pharmacol. Rev. *63*, 182–217.

Behr, R., Sackett, S.D., Bochkis, I.M., Le, P.P., and Kaestner, K.H. (2007). Impaired male fertility and atrophy of seminiferous tubules caused by haploinsufficiency for Foxa3. Dev. Biol. *306*, 636–645.

Bettler, B., Kaupmann, K., Mosbacher, J., and Gassmann, M. (2004). Molecular structure and physiological functions of GABA(B) receptors. Physiol. Rev. *84*, 835–867.

Bezzi, P., Domercq, M., Brambilla, L., Galli, R., Schols, D., De Clercq, E., Vescovi, A., Bagetta, G., Kollias, G., Meldolesi, J., et al. (2001). CXCR4-activated astrocyte glutamate release via TNFalpha: amplification by microglia triggers neurotoxicity. Nat. Neurosci. *4*, 702–710.

Bianchi, M., Turner, H.L., Nogal, B., Cottrell, C.A., Oyen, D., Pauthner, M., Bastidas, R., Nedellec, R., McCoy, L.E., Wilson, I.A., et al. (2018). Electron-Microscopy-Based Epitope Mapping Defines Specificities of Polyclonal Antibodies Elicited during HIV-1 BG505 Envelope Trimer Immunization. Immunity *49*, 288-300.e8.

Bien, C.G., Vincent, A., Barnett, M.H., Becker, A.J., Blümcke, I., Graus, F., Jellinger, K.A., Reuss, D.E., Ribalta, T., Schlegel, J., et al. (2012a). Immunopathology of autoantibody-associated encephalitides: clues for pathogenesis. Brain J. Neurol. *135*, 1622–1638.

Bien, C.G., Vincent, A., Barnett, M.H., Becker, A.J., Blümcke, I., Graus, F., Jellinger, K.A., Reuss, D.E., Ribalta, T., Schlegel, J., et al. (2012b). Immunopathology of autoantibody-associated encephalitides: clues for pathogenesis. Brain J. Neurol. *135*, 1622–1638.

Bjelobaba, I., Begovic-Kupresanin, V., Pekovic, S., and Lavrnja, I. (2018). Animal models of multiple sclerosis: Focus on experimental autoimmune encephalomyelitis. J. Neurosci. Res. *96*, 1021–1042.

Brambilla, R., Bracchi-Ricard, V., Hu, W.-H., Frydel, B., Bramwell, A., Karmally, S., Green, E.J., and Bethea, J.R. (2005). Inhibition of astroglial nuclear factor κB reduces inflammation and improves functional recovery after spinal cord injury. J. Exp. Med. *202*, 145–156.

de Bruijn, M.A.A.M., Aarsen, F.K., van Oosterhout, M.P., van der Knoop, M.M., Catsman-Berrevoets, C.E., Schreurs, M.W.J., Bastiaansen, D.E.M., Sillevis Smitt, P.A.E., Neuteboom, R.F., Titulaer, M.J., et al. (2018). Long-term neuropsychological outcome following pediatric anti-NMDAR encephalitis. Neurology *90*, e1997–e2005.

Byun, J.-I., Lee, S.-T., Moon, J., Jung, K.-H., Sunwoo, J.-S., Lim, J.-A., Kim, T.-J., Shin, Y.-W., Lee, K.-J., Jun, J.-S., et al. (2016). Distinct intrathecal interleukin-17/interleukin-6 activation in anti-N-methyl-d-aspartate receptor encephalitis. J. Neuroimmunol. *297*, 141–147.

Cahalan, S. (2012). Brain on Fire: My Month of Madness (Simon & Schuster).

Camdessanché, J.-P., Streichenberger, N., Cavillon, G., Rogemond, V., Jousserand, G., Honnorat, J., Convers, P., and Antoine, J.-C. (2011a). Brain immunohistopathological study in a patient with anti-NMDAR encephalitis. Eur. J. Neurol. *18*, 929–931.

Camdessanché, J.-P., Streichenberger, N., Cavillon, G., Rogemond, V., Jousserand, G., Honnorat, J., Convers, P., and Antoine, J.-C. (2011b). Brain immunohistopathological study in a patient with anti-NMDAR encephalitis. Eur. J. Neurol. *18*, 929–931.

Casad, R., and Volkova, T. (1999). N-methyl-D-aspartate receptor function observed by rate of ligand dialysis from proteoliposome solution. J. Biomol. Struct. Dyn. *16*, 969–975.

Coleman, J.A., Green, E.M., and Gouaux, E. (2016). Thermostabilization, Expression, Purification, and Crystallization of the Human Serotonin Transporter Bound to S-citalopram. J. Vis. Exp. JoVE.

Colombo, E., and Farina, C. (2016). Astrocytes: Key Regulators of Neuroinflammation. Trends Immunol. *37*, 608–620.

Croxford, A.L., Kurschus, F.C., and Waisman, A. (2011). Mouse models for multiple sclerosis: Historical facts and future implications. Biochim. Biophys. Acta BBA - Mol. Basis Dis. *1812*, 177–183.

Dale, R.C., Merheb, V., Pillai, S., Wang, D., Cantrill, L., Murphy, T.K., Ben-Pazi, H., Varadkar, S., Aumann, T.D., Horne, M.K., et al. (2012). Antibodies to surface dopamine-2 receptor in autoimmune movement and psychiatric disorders. Brain J. Neurol. *135*, 3453–3468.

Dalmau, J., and Rosenfeld, M.R. (2008). Paraneoplastic syndromes of the CNS. Lancet Neurol. *7*, 327–340.

Dalmau, J., Tüzün, E., Wu, H., Masjuan, J., Rossi, J.E., Voloschin, A., Baehring, J.M., Shimazaki, H., Koide, R., King, D., et al. (2007). Paraneoplastic anti-N-methyl-D-aspartate receptor encephalitis associated with ovarian teratoma. Ann. Neurol. *61*, 25–36.

Dalmau, J., Gleichman, A.J., Hughes, E.G., Rossi, J.E., Peng, X., Lai, M., Dessain, S.K., Rosenfeld, M.R., Balice-Gordon, R., and Lynch, D.R. (2008). Anti-NMDA-receptor

encephalitis: case series and analysis of the effects of antibodies. Lancet Neurol. *7*, 1091–1098.

Dalmau, J., Lancaster, E., Martinez-Hernandez, E., Rosenfeld, M.R., and Balice-Gordon, R. (2011). Clinical experience and laboratory investigations in patients with anti-NMDAR encephalitis. Lancet Neurol. *10*, 63–74.

Dalmau, J., Geis, C., and Graus, F. (2017). Autoantibodies to Synaptic Receptors and Neuronal Cell Surface Proteins in Autoimmune Diseases of the Central Nervous System. Physiol. Rev. *97*, 839–887.

Dando, S.J., Mackay-Sim, A., Norton, R., Currie, B.J., John, J.A.S., Ekberg, J.A.K., Batzloff, M., Ulett, G.C., and Beacham, I.R. (2014). Pathogens Penetrating the Central Nervous System: Infection Pathways and the Cellular and Molecular Mechanisms of Invasion. Clin. Microbiol. Rev. *27*, 691–726.

Daneman, R., and Prat, A. (2015). The Blood–Brain Barrier. Cold Spring Harb. Perspect. Biol. *7*.

Darnell, R.B., and DeAngelis, L.M. (1993). Regression of small-cell lung carcinoma in patients with paraneoplastic neuronal antibodies. Lancet Lond. Engl. *341*, 21–22.

Darnell, R.B., and Posner, J.B. (2006). Paraneoplastic Syndromes Affecting the Nervous System. Semin. Oncol. *33*, 270–298.

Davis, M.J., Haley, T., Duvoisin, R.M., and Raber, J. (2012). Measures of anxiety, sensorimotor function, and memory in male and female mGluR4−/− mice. Behav. Brain Res. *229*, 21–28.

Deacon, R.M.J. (2006). Assessing nest building in mice. Nat. Protoc. *1*, 1117–1119.

Dingledine, R., Borges, K., Bowie, D., and Traynelis, S.F. (1999). The glutamate receptor ion channels. Pharmacol. Rev. *51*, 7–61.

Drachev, L.A., Jasaitis, A.A., Kaulen, A.D., Kondrashin, A.A., Chu, L.V., Semenov, A.Y., Severina, I.I., and Skulachev, V.P. (1976). Reconstitution of biological molecular generators of electric current. Cytochrome oxidase. J. Biol. Chem. *251*, 7072–7076.

Drachman, D.B. (1994). Myasthenia Gravis. N. Engl. J. Med. *330*, 1797–1810.

Drachman, D.B., Adams, R.N., Josifek, L.F., and Self, S.G. (1982). Functional Activities of Autoantibodies to Acetylcholine Receptors and the Clinical Severity of Myasthenia Gravis. N. Engl. J. Med. *307*, 769–775.

Dubey, A.K., Handu, S.S., Dubey, S., Sharma, P., Sharma, K.K., and Ahmed, Q.M. (2011). Belimumab: First targeted biological treatment for systemic lupus erythematosus. J. Pharmacol. Pharmacother. *2*, 317–319.

Elmore, M.R.P., Najafi, A.R., Koike, M.A., Dagher, N.N., Spangenberg, E.E., Rice, R.A., Kitazawa, M., Matusow, B., Nguyen, H., West, B.L., et al. (2014). CSF1 receptor signaling is necessary for microglia viability, which unmasks a cell that rapidly repopulates the microglia-depleted adult brain. Neuron *82*, 380–397.

Engel, A.G., and Arahata, K. (1987). The Membrane Attack Complex of Complement at the Endplate in Myasthenia Gravisa. Ann. N. Y. Acad. Sci. *505*, 326–332.

Farina, C., Aloisi, F., and Meinl, E. (2007). Astrocytes are active players in cerebral innate immunity. Trends Immunol. *28*, 138–145.

Filatenkov, A., Richardson, T.E., Daoud, E., Johnson-Welch, S.F., Ramirez, D.M., Torrealba, J., Greenberg, B., Monson, N.L., and Rajaram, V. (2017). Persistence of parenchymal and perivascular T-cells in treatment-refractory anti-N-methyl-D-aspartate receptor encephalitis. Neuroreport *28*, 890–895.

Finke, C., Kopp, U.A., Scheel, M., Pech, L.-M., Soemmer, C., Schlichting, J., Leypoldt, F., Brandt, A.U., Wuerfel, J., Probst, C., et al. (2013). Functional and structural brain changes in anti-N-methyl-D-aspartate receptor encephalitis. Ann. Neurol. *74*, 284–296.

Finke, C., Kopp, U.A., Pajkert, A., Behrens, J.R., Leypoldt, F., Wuerfel, J.T., Ploner, C.J., Prüss, H., and Paul, F. (2016). Structural Hippocampal Damage Following Anti-N-Methyl-D-Aspartate Receptor Encephalitis. Biol. Psychiatry *79*, 727–734.

Franklin, K.B.J., and Paxinos, G. (2012). The Mouse Brain in Stereotaxic Coordinates (Academic Press).

Fukata, Y., Adesnik, H., Iwanaga, T., Bredt, D.S., Nicoll, R.A., and Fukata, M. (2006). Epilepsy-Related Ligand/Receptor Complex LGI1 and ADAM22 Regulate Synaptic Transmission. Science *313*, 1792–1795.

Fukuda, T., Motomura, M., Nakao, Y., Shiraishi, H., Yoshimura, T., Iwanaga, K., Tsujihata, M., and Eguchi, K. (2003). Reduction of P/Q-type calcium channels in the postmortem cerebellum of paraneoplastic cerebellar degeneration with Lambert-Eaton myasthenic syndrome. Ann. Neurol. *53*, 21–28.

Gable, M.S., Sheriff, H., Dalmau, J., Tilley, D.H., and Glaser, C.A. (2012). The frequency of autoimmune N-methyl-D-aspartate receptor encephalitis surpasses that of individual viral etiologies in young individuals enrolled in the California Encephalitis Project. Clin. Infect. Dis. Off. Publ. Infect. Dis. Soc. Am. *54*, 899–904.

Galea, I., Bechmann, I., and Perry, V.H. (2007). What is immune privilege (not)? Trends Immunol. *28*, 12–18.

Galli, S.J., and Tsai, M. (2012). IgE and mast cells in allergic disease. Nat. Med. *18*, 693–704.

Gleichman, A.J., Spruce, L.A., Dalmau, J., Seeholzer, S.H., and Lynch, D.R. (2012a). Anti-NMDA receptor encephalitis antibody binding is dependent on amino acid identity of a small region within the GluN1 amino terminal domain. J. Neurosci. Off. J. Soc. Neurosci. *32*, 11082–11094.

Gleichman, A.J., Spruce, L.A., Dalmau, J., Seeholzer, S.H., and Lynch, D.R. (2012b). Anti-NMDA receptor encephalitis antibody binding is dependent on amino acid identity of a small region within the GluN1 amino terminal domain. J. Neurosci. Off. J. Soc. Neurosci. *32*, 11082–11094.

Goehring, A., Lee, C.-H., Wang, K.H., Michel, J.C., Claxton, D.P., Baconguis, I., Althoff, T., Fischer, S., Garcia, K.C., and Gouaux, E. (2014). Screening and large-scale expression of membrane proteins in mammalian cells for structural studies. Nat. Protoc. *9*, 2574–2585.

Goldmann, T., and Prinz, M. (2013). Role of Microglia in CNS Autoimmunity. Clin. Dev. Immunol. *2013*.

Gouaux, E. (2004). Structure and function of AMPA receptors. J. Physiol. *554*, 249–253.

Goverman, J. (2009). Autoimmune T cell responses in the central nervous system. Nat. Rev. Immunol. *9*, 393.

Graus, F., Titulaer, M.J., Balu, R., Benseler, S., Bien, C.G., Cellucci, T., Cortese, I., Dale, R.C., Gelfand, J.M., Geschwind, M., et al. (2016a). A clinical approach to diagnosis of autoimmune encephalitis. Lancet Neurol. *15*, 391–404.

Graus, F., Titulaer, M.J., Balu, R., Benseler, S., Bien, C.G., Cellucci, T., Cortese, I., Dale, R.C., Gelfand, J.M., Geschwind, M., et al. (2016b). A clinical approach to diagnosis of autoimmune encephalitis. Lancet Neurol. *15*, 391–404.

Gresa-Arribas, N., Planagumà, J., Petit-Pedrol, M., Kawachi, I., Katada, S., Glaser, C.A., Simabukuro, M.M., Armangué, T., Martínez-Hernández, E., Graus, F., et al. (2016). Human neurexin-3α antibodies associate with encephalitis and alter synapse development. Neurology *86*, 2235–2242.

Han, J., Harris, R.A., and Zhang, X.-M. (2017). An updated assessment of microglia depletion: current concepts and future directions. Mol. Brain *10*.

Hansen, K.B., Ogden, K.K., Yuan, H., and Traynelis, S.F. (2014). Distinct functional and pharmacological properties of triheteromeric GluN1/GluN2A/GluN2B NMDA receptors. Neuron *81*, 1084–1096.

Hansen, K.B., Yi, F., Perszyk, R.E., Furukawa, H., Wollmuth, L.P., Gibb, A.J., and Traynelis, S.F. (2018). Structure, function, and allosteric modulation of NMDA receptors. J. Gen. Physiol. *150*, 1081–1105.

Hendriksen, E., van Bergeijk, D., Oosting, R.S., and Redegeld, F.A. (2017). Mast cells in neuroinflammation and brain disorders. Neurosci. Biobehav. Rev. *79*, 119–133.

Höftberger, R., Titulaer, M.J., Sabater, L., Dome, B., Rózsás, A., Hegedus, B., Hoda, M.A., Laszlo, V., Ankersmit, H.J., Harms, L., et al. (2013). Encephalitis and GABAB receptor antibodies: novel findings in a new case series of 20 patients. Neurology *81*, 1500–1506.

Howard, F.M., Lennon, V.A., Finley, J., Matsumoto, J., and Elveback, L.R. (1987). Clinical Correlations of Antibodies That Bind, Block, or Modulate Human Acetylcholine Receptors in Myasthenia Gravisa. Ann. N. Y. Acad. Sci. *505*, 526–538.

Hughes, E.G., Peng, X., Gleichman, A.J., Lai, M., Zhou, L., Tsou, R., Parsons, T.D., Lynch, D.R., Dalmau, J., and Balice-Gordon, R.J. (2010a). Cellular and synaptic mechanisms of anti-NMDA receptor encephalitis. J. Neurosci. Off. J. Soc. Neurosci. *30*, 5866–5875.

Hughes, E.G., Peng, X., Gleichman, A.J., Lai, M., Zhou, L., Tsou, R., Parsons, T.D., Lynch, D.R., Dalmau, J., and Balice-Gordon, R.J. (2010b). Cellular and synaptic mechanisms of anti-NMDA receptor encephalitis. J. Neurosci. Off. J. Soc. Neurosci. *30*, 5866–5875.

Huppert, J., Closhen, D., Croxford, A., White, R., Kulig, P., Pietrowski, E., Bechmann, I., Becher, B., Luhmann, H.J., Waisman, A., et al. (2010). Cellular mechanisms of IL-17-induced blood-brain barrier disruption. FASEB J. Off. Publ. Fed. Am. Soc. Exp. Biol. *24*, 1023–1034.

Husebye, E.S., Sthoeger, Z.M., Dayan, M., Zinger, H., Elbirt, D., Levite, M., and Mozes, E. (2005). Autoantibodies to a NR2A peptide of the glutamate/NMDA receptor in sera of patients with systemic lupus erythematosus. Ann. Rheum. Dis. *64*, 1210–1213.

Irani, S.R., Alexander, S., Waters, P., Kleopa, K.A., Pettingill, P., Zuliani, L., Peles, E., Buckley, C., Lang, B., and Vincent, A. (2010). Antibodies to Kv1 potassium channel-complex proteins leucine-rich, glioma inactivated 1 protein and contactin-associated protein-2 in limbic encephalitis, Morvan's syndrome and acquired neuromyotonia. Brain *133*, 2734–2748.

Irani, S.R., Michell, A.W., Lang, B., Pettingill, P., Waters, P., Johnson, M.R., Schott, J.M., Armstrong, R.J.E., S Zagami, A., Bleasel, A., et al. (2011). Faciobrachial dystonic seizures precede Lgi1 antibody limbic encephalitis. Ann. Neurol. *69*, 892–900.

Jaber, M., Robinson, S.W., Missale, C., and Caron, M.G. (1996). Dopamine receptors and brain function. Neuropharmacology *35*, 1503–1519.

Jain, A. (2015). From receptor to brain: Synaptic, cellular and behavioral pathophysiology in anti-GABAB receptor and anti-NMDA receptor encephalitides. Dissertation. University of Pennsylvania.

Kaltsas, G., Androulakis, I.I., de Herder, W.W., and Grossman, A.B. (2010). Paraneoplastic syndromes secondary to neuroendocrine tumours. Endocr. Relat. Cancer *17*, R173-193.

Kebir, H., Kreymborg, K., Ifergan, I., Dodelet-Devillers, A., Cayrol, R., Bernard, M., Giuliani, F., Arbour, N., Becher, B., and Prat, A. (2007). Human TH17 lymphocytes promote blood-brain barrier disruption and central nervous system inflammation. Nat. Med. *13*, 1173–1175.

Kesner, V.G., Oh, S.J., Dimachkie, M.M., and Barohn, R.J. (2018). Lambert-Eaton Myasthenic Syndrome. Neurol. Clin. *36*, 379–394.

Kipnis, J. (2016). Multifaceted interactions between adaptive immunity and the central nervous system. Science *353*, 766–771.

Kishimoto, T.K., and Maldonado, R.A. (2018). Nanoparticles for the Induction of Antigen-Specific Immunological Tolerance. Front. Immunol. *9*.

Kitamura, D., Roes, J., Kühn, R., and Rajewsky, K. (1991). A B cell-deficient mouse by targeted disruption of the membrane exon of the immunoglobulin mu chain gene. Nature *350*, 423–426.

Kivisäkk, P., Imitola, J., Rasmussen, S., Elyaman, W., Zhu, B., Ransohoff, R.M., and Khoury, S.J. (2009). Localizing central nervous system immune surveillance: meningeal antigen-presenting cells activate T cells during experimental autoimmune encephalomyelitis. Ann. Neurol. *65*, 457–469.

Koob, G.F., and Volkow, N.D. (2016). Neurobiology of addiction: a neurocircuitry analysis. Lancet Psychiatry *3*, 760–773.

Korn, T., and Kallies, A. (2017). T cell responses in the central nervous system. Nat. Rev. Immunol. *17*, 179–194.

Kothur, K., Wienholt, L., Mohammad, S.S., Tantsis, E.M., Pillai, S., Britton, P.N., Jones, C.A., Angiti, R.R., Barnes, E.H., Schlub, T., et al. (2016). Utility of CSF Cytokine/Chemokines as Markers of Active Intrathecal Inflammation: Comparison of Demyelinating, Anti-NMDAR and Enteroviral Encephalitis. PloS One *11*, e0161656.

Kreye, J., Wenke, N.K., Chayka, M., Leubner, J., Murugan, R., Maier, N., Jurek, B., Ly, L.-T., Brandl, D., Rost, B.R., et al. (2016a). Human cerebrospinal fluid monoclonal N-methyl-D-aspartate receptor autoantibodies are sufficient for encephalitis pathogenesis. Brain J. Neurol. *139*, 2641–2652.

Kreye, J., Wenke, N.K., Chayka, M., Leubner, J., Murugan, R., Maier, N., Jurek, B., Ly, L.-T., Brandl, D., Rost, B.R., et al. (2016b). Human cerebrospinal fluid monoclonal N-methyl-D-aspartate receptor autoantibodies are sufficient for encephalitis pathogenesis. Brain J. Neurol. *139*, 2641–2652.

Krueger, D.D., Tuffy, L.P., Papadopoulos, T., and Brose, N. (2012). The role of neurexins and neuroligins in the formation, maturation, and function of vertebrate synapses. Curr. Opin. Neurobiol. *22*, 412–422.

Krumbholz, M., Theil, D., Derfuss, T., Rosenwald, A., Schrader, F., Monoranu, C.-M., Kalled, S.L., Hess, D.M., Serafini, B., Aloisi, F., et al. (2005). BAFF is produced by astrocytes and up-regulated in multiple sclerosis lesions and primary central nervous system lymphoma. J. Exp. Med. *201*, 195–200.

Ladépêche, L., Planagumà, J., Thakur, S., Suárez, I., Hara, M., Borbely, J.S., Sandoval, A., Laparra-Cuervo, L., Dalmau, J., and Lakadamyali, M. (2018). NMDA Receptor Autoantibodies in Autoimmune Encephalitis Cause a Subunit-Specific Nanoscale Redistribution of NMDA Receptors. Cell Rep. *23*, 3759–3768.

Lai, M., Hughes, E.G., Peng, X., Zhou, L., Gleichman, A.J., Shu, H., Matà, S., Kremens, D., Vitaliani, R., Geschwind, M.D., et al. (2009). AMPA receptor antibodies in limbic encephalitis alter synaptic receptor location. Ann. Neurol. *65*, 424–434.

Lai, M., Huijbers, M.G.M., Lancaster, E., Graus, F., Bataller, L., Balice-Gordon, R., Cowell, J.K., and Dalmau, J. (2010). Investigation of LGI1 as the antigen in limbic encephalitis previously attributed to potassium channels: a case series. Lancet Neurol. *9*, 776–785.

Lampron, A., ElAli, A., and Rivest, S. (2013). Innate Immunity in the CNS: Redefining the Relationship between the CNS and Its Environment. Neuron *78*, 214–232.

Lancaster, E., and Dalmau, J. (2012). Neuronal autoantigens—pathogenesis, associated disorders and antibody testing. Nat. Rev. Neurol. *8*, 380–390.

Lancaster, E., Lai, M., Peng, X., Hughes, E., Constantinescu, R., Raizer, J., Friedman, D., Skeen, M.B., Grisold, W., Kimura, A., et al. (2010). Antibodies to the GABA(B) receptor in limbic encephalitis with seizures: case series and characterisation of the antigen. Lancet Neurol. *9*, 67–76.

Latif, T., and Morris, J.C. (2013). Monoclonal Antibody Therapy of T-Cell Leukemia and Lymphoma. T-Cell Leuk. - Charact. Treat. Prev.

Lee, C.-H., Lü, W., Michel, J.C., Goehring, A., Du, J., Song, X., and Gouaux, E. (2014a). NMDA receptor structures reveal subunit arrangement and pore architecture. Nature *511*, 191–197.

Lee, C.-H., Lü, W., Michel, J.C., Goehring, A., Du, J., Song, X., and Gouaux, E. (2014b). NMDA receptor structures reveal subunit arrangement and pore architecture. Nature *511*, 191–197.

Lepeta, K., Lourenco, M.V., Schweitzer, B.C., Martino Adami, P.V., Banerjee, P., Catuara-Solarz, S., de La Fuente Revenga, M., Guillem, A.M., Haidar, M., Ijomone,

O.M., et al. (2016). Synaptopathies: synaptic dysfunction in neurological disorders – A review from students to students. J. Neurochem. *138*, 785–805.

Liba, Z., Kayserova, J., Elisak, M., Marusic, P., Nohejlova, H., Hanzalova, J., Komarek, V., and Sediva, A. (2016). Anti-N-methyl-D-aspartate receptor encephalitis: the clinical course in light of the chemokine and cytokine levels in cerebrospinal fluid. J. Neuroinflammation *13*, 55.

Liddelow, S.A., and Barres, B.A. (2017). Reactive Astrocytes: Production, Function, and Therapeutic Potential. Immunity *46*, 957–967.

van Loo, G., De Lorenzi, R., Schmidt, H., Huth, M., Mildner, A., Schmidt-Supprian, M., Lassmann, H., Prinz, M.R., and Pasparakis, M. (2006). Inhibition of transcription factor NF-κB in the central nervous system ameliorates autoimmune encephalomyelitis in mice. Nat. Immunol. *7*, 954–961.

López Chiriboga, A.S., Siegel, J.L., Tatum, W.O., Shih, J.J., and Flanagan, E.P. (2017). Striking basal ganglia imaging abnormalities in LGI1 ab faciobrachial dystonic seizures. Neurol. Neuroimmunol. Neuroinflammation *4*.

Lü, W., Du, J., Goehring, A., and Gouaux, E. (2017). Cryo-EM structures of the triheteromeric NMDA receptor and its allosteric modulation. Science *355*.

Malviya, M., Barman, S., Golombeck, K.S., Planagumà, J., Mannara, F., Strutz-Seebohm, N., Wrzos, C., Demir, F., Baksmeier, C., Steckel, J., et al. (2017). NMDAR encephalitis: passive transfer from man to mouse by a recombinant antibody. Ann. Clin. Transl. Neurol. *4*, 768–783.

Martinez-Hernandez, E., Horvath, J., Shiloh-Malawsky, Y., Sangha, N., Martinez-Lage, M., and Dalmau, J. (2011a). Analysis of complement and plasma cells in the brain of patients with anti-NMDAR encephalitis. Neurology *77*, 589–593.

Martinez-Hernandez, E., Horvath, J., Shiloh-Malawsky, Y., Sangha, N., Martinez-Lage, M., and Dalmau, J. (2011b). Analysis of complement and plasma cells in the brain of patients with anti-NMDAR encephalitis. Neurology *77*, 589–593.

Mayford, M., Siegelbaum, S.A., and Kandel, E.R. (2012). Synapses and Memory Storage. Cold Spring Harb. Perspect. Biol. *4*.

Meeker, R.B., Williams, K., Killebrew, D.A., and Hudson, L.C. (2012). Cell trafficking through the choroid plexus. Cell Adhes. Migr. *6*, 390–396.

Miller, S.D., Karpus, W.J., and Davidson, T.S. (2007). Experimental Autoimmune Encephalomyelitis in the Mouse. Curr. Protoc. Immunol. Ed. John E Coligan Al *CHAPTER*, Unit-15.1.

Mombaerts, P., Clarke, A.R., Rudnicki, M.A., Iacomini, J., Itohara, S., Lafaille, J.J., Wang, L., Ichikawa, Y., Jaenisch, R., and Hooper, M.L. (1992). Mutations in T-cell

antigen receptor genes alpha and beta block thymocyte development at different stages. Nature *360*, 225–231.

Monso-Hinard, C., Lou, J.N., Behr, C., Juillard, P., and Grau, G.E. (1997). Expression of major histocompatibility complex antigens on mouse brain microvascular endothelial cells in relation to susceptibility to cerebral malaria. Immunology *92*, 53–59.

Morante-Redolat, J.M., Gorostidi-Pagola, A., Piquer-Sirerol, S., Sáenz, A., Poza, J.J., Galán, J., Gesk, S., Sarafidou, T., Mautner, V.-F., Binelli, S., et al. (2002). Mutations in the LGI1/Epitempin gene on 10q24 cause autosomal dominant lateral temporal epilepsy. Hum. Mol. Genet. *11*, 1119–1128.

Moscato, E.H., Peng, X., Jain, A., Parsons, T.D., Dalmau, J., and Balice-Gordon, R.J. (2014). Acute mechanisms underlying antibody effects in anti-N-methyl-D-aspartate receptor encephalitis. Ann. Neurol. *76*, 108–119.

Motomura, M., and Fukuda, T. (2011). [Lambert-Eaton myasthenic syndrome]. Brain Nerve Shinkei Kenkyu No Shinpo *63*, 745–754.

Nagel, A., Engel, A.G., Lang, B., Newsom-Davis, J., and Fukuoka, T. (1988). Lambert-eaton myasthenic syndrome IgG depletes presynaptic membrane active zone particles by antigenic modulation. Ann. Neurol. *24*, 552–558.

Navarro, V., Kas, A., Apartis, E., Chami, L., Rogemond, V., Levy, P., Psimaras, D., Habert, M.-O., Baulac, M., Delattre, J.-Y., et al. (2016). Motor cortex and hippocampus are the two main cortical targets in LGI1-antibody encephalitis. Brain J. Neurol. *139*, 1079–1093.

Naylor, D.E., Liu, H., and Wasterlain, C.G. (2005). Trafficking of GABA(A) receptors, loss of inhibition, and a mechanism for pharmacoresistance in status epilepticus. J. Neurosci. Off. J. Soc. Neurosci. *25*, 7724–7733.

Nelissen, S., Lemmens, E., Geurts, N., Kramer, P., Maurer, M., Hendriks, J., and Hendrix, S. (2013). The role of mast cells in neuroinflammation. Acta Neuropathol. (Berl.) *125*, 637–650.

Newcomer, J.W., and Krystal, J.H. (2001). NMDA receptor regulation of memory and behavior in humans. Hippocampus *11*, 529–542.

Nichols, M.J., and Newsome, W.T. (1999). The neurobiology of cognition. Nature *402*, C35–C38.

Ohguro, H., and Nakazawa, M. (2002). Pathological roles of recoverin in cancer-associated retinopathy. Adv. Exp. Med. Biol. *514*, 109–124.

Owuor, K., Harel, N.Y., Englot, D.C., Hisama, F., Blumenfeld, H., and Strittmatter, S.M. (2009). LGI1-associated epilepsy through altered ADAM23-dependent neuronal morphology. Mol. Cell. Neurosci. *42*, 448–457.

Pachernegg, S., Strutz-Seebohm, N., and Hollmann, M. (2012). GluN3 subunit-containing NMDA receptors: not just one-trick ponies. Trends Neurosci. *35*, 240–249.

Pan, H., Oliveira, B., Saher, G., Dere, E., Tapken, D., Mitjans, M., Seidel, J., Wesolowski, J., Wakhloo, D., Klein-Schmidt, C., et al. (2018). Uncoupling the widespread occurrence of anti-NMDAR1 autoantibodies from neuropsychiatric disease in a novel autoimmune model. Mol. Psychiatry.

Paoletti, P., Bellone, C., and Zhou, Q. (2013). NMDA receptor subunit diversity: impact on receptor properties, synaptic plasticity and disease. Nat. Rev. Neurosci. *14*, 383–400.

Pathmanandavel, K., Starling, J., Merheb, V., Ramanathan, S., Sinmaz, N., Dale, R.C., and Brilot, F. (2015). Antibodies to surface dopamine-2 receptor and N-methyl-D-aspartate receptor in the first episode of acute psychosis in children. Biol. Psychiatry *77*, 537–547.

Patrick, J., and Lindstrom, J. (1973). Autoimmune response to acetylcholine receptor. Science *180*, 871–872.

Pelosof, L.C., and Gerber, D.E. (2010). Paraneoplastic Syndromes: An Approach to Diagnosis and Treatment. Mayo Clin. Proc. *85*, 838–854.

Peng, X., Hughes, E.G., Moscato, E.H., Parsons, T.D., Dalmau, J., and Balice-Gordon, R.J. (2015). Cellular plasticity induced by anti-α-amino-3-hydroxy-5-methyl-4-isoxazolepropionic acid (AMPA) receptor encephalitis antibodies. Ann. Neurol. *77*, 381–398.

Pérez, O., Bracho, G., Lastre, M., Mora, N., del Campo, J., Gil, D., Zayas, C., Acevedo, R., González, D., López, J.A., et al. (2004). Novel adjuvant based on a proteoliposome-derived cochleate structure containing native lipopolysaccharide as a pathogen-associated molecular pattern. Immunol. Cell Biol. *82*, 603–610.

Petit-Pedrol, M., Armangue, T., Peng, X., Bataller, L., Cellucci, T., Davis, R., McCracken, L., Martinez-Hernandez, E., Mason, W.P., Kruer, M.C., et al. (2014). Encephalitis with refractory seizures, status epilepticus, and antibodies to the GABAA receptor: a case series, characterisation of the antigen, and analysis of the effects of antibodies. Lancet Neurol. *13*, 276–286.

Pilli, D., Zou, A., Tea, F., Dale, R.C., and Brilot, F. (2017). Expanding Role of T Cells in Human Autoimmune Diseases of the Central Nervous System. Front. Immunol. *8*, 652.

Planagumà, J., Leypoldt, F., Mannara, F., Gutiérrez-Cuesta, J., Martín-García, E., Aguilar, E., Titulaer, M.J., Petit-Pedrol, M., Jain, A., Balice-Gordon, R., et al. (2015a). Human N-methyl D-aspartate receptor antibodies alter memory and behaviour in mice. Brain J. Neurol. *138*, 94–109.

Planagumà, J., Leypoldt, F., Mannara, F., Gutiérrez-Cuesta, J., Martín-García, E., Aguilar, E., Titulaer, M.J., Petit-Pedrol, M., Jain, A., Balice-Gordon, R., et al. (2015b). Human N-methyl D-aspartate receptor antibodies alter memory and behaviour in mice. Brain J. Neurol. *138*, 94–109.

Prinz, M., and Priller, J. (2017). The role of peripheral immune cells in the CNS in steady state and disease. Nat. Neurosci. *20*, 136–144.

Prinz, M., Erny, D., and Hagemeyer, N. (2017). Ontogeny and homeostasis of CNS myeloid cells. Nat. Immunol. *18*, 385–392.

Probert, L., Akassoglou, K., Kassiotis, G., Pasparakis, M., Alexopoulou, L., and Kollias, G. (1997). TNF-alpha transgenic and knockout models of CNS inflammation and degeneration. J. Neuroimmunol. *72*, 137–141.

Prüss, H., Leubner, J., Wenke, N.K., Czirják, G.Á., Szentiks, C.A., and Greenwood, A.D. (2015). Anti-NMDA Receptor Encephalitis in the Polar Bear (Ursus maritimus) Knut. Sci. Rep. *5*, 12805.

Qian, Y., Liu, C., Hartupee, J., Altuntas, C.Z., Gulen, M.F., Jane-wit, D., Xiao, J., Lu, Y., Giltiay, N., Liu, J., et al. (2007). The adaptor Act1 is required for interleukin 17–dependent signaling associated with autoimmune and inflammatory disease. Nat. Immunol. *8*, 247–256.

Ransohoff, R.M., and Brown, M.A. (2012). Innate immunity in the central nervous system. J. Clin. Invest. *122*, 1164–1171.

Ransohoff, R.M., and Cardona, A.E. (2010). The myeloid cells of the central nervous system parenchyma. Nature *468*, 253–262.

Ransohoff, R.M., and Perry, V.H. (2009). Microglial Physiology: Unique Stimuli, Specialized Responses. Annu. Rev. Immunol. *27*, 119–145.

Ribatti, D. (2015). The crucial role of mast cells in blood–brain barrier alterations. Exp. Cell Res. *338*, 119–125.

Rice, R.A., Pham, J., Lee, R.J., Najafi, A.R., West, B.L., and Green, K.N. (2017). Microglial repopulation resolves inflammation and promotes brain recovery after injury. Glia *65*, 931–944.

Rosch, R.E., Wright, S., Cooray, G., Papadopoulou, M., Goyal, S., Lim, M., Vincent, A., Upton, A.L., Baldeweg, T., and Friston, K.J. (2018). NMDA-receptor antibodies alter cortical microcircuit dynamics. Proc. Natl. Acad. Sci. *115*, E9916–E9925.

Rudolph, U., and Knoflach, F. (2011). Beyond classical benzodiazepines: Novel therapeutic potential of GABAA receptor subtypes. Nat. Rev. Drug Discov. *10*, 685–697.

Salovin, A., Glanzman, J., Roslin, K., Armangue, T., Lynch, D.R., and Panzer, J.A. (2018). Anti-NMDA receptor encephalitis and nonencephalitic HSV-1 infection. Neurol. Neuroimmunol. Neuroinflammation *5*.

Sansing, L.H., Tüzün, E., Ko, M.W., Baccon, J., Lynch, D.R., and Dalmau, J. (2007). A patient with encephalitis associated with NMDA receptor antibodies. Nat. Clin. Pract. Neurol. *3*, 291–296.

Schulte, U., Thumfart, J.-O., Klöcker, N., Sailer, C.A., Bildl, W., Biniossek, M., Dehn, D., Deller, T., Eble, S., Abbass, K., et al. (2006). The epilepsy-linked Lgi1 protein assembles into presynaptic Kv1 channels and inhibits inactivation by Kvbeta1. Neuron *49*, 697–706.

Seagar, M., Russier, M., Caillard, O., Maulet, Y., Fronzaroli-Molinieres, L., De San Feliciano, M., Boumedine-Guignon, N., Rodriguez, L., Zbili, M., Usseglio, F., et al. (2017). LGI1 tunes intrinsic excitability by regulating the density of axonal Kv1 channels. Proc. Natl. Acad. Sci. U. S. A. *114*, 7719–7724.

Sellner, J., Dvorak, F., Zhou, Y., Haas, J., Kehm, R., Wildemann, B., and Meyding-Lamadè, U. (2005). Acute and long-term alteration of chemokine mRNA expression after anti-viral and anti-inflammatory treatment in herpes simplex virus encephalitis. Neurosci. Lett. *374*, 197–202.

Serra, P., and Santamaria, P. (2018). Nanoparticle-based approaches to immune tolerance for the treatment of autoimmune diseases. Eur. J. Immunol. *48*, 751–756.

Shepherd, J.D., and Huganir, R.L. (2007). The Cell Biology of Synaptic Plasticity: AMPA Receptor Trafficking. Annu. Rev. Cell Dev. Biol. *23*, 613–643.

Shillito, P., Molenaar, P.C., Vincent, A., Leys, K., Zheng, W., van den Berg, R.J., Plomp, J.J., van Kempen, G.T., Chauplannaz, G., and Wintzen, A.R. (1995). Acquired neuromyotonia: evidence for autoantibodies directed against K+ channels of peripheral nerves. Ann. Neurol. *38*, 714–722.

Sibilano, R., Frossi, B., and Pucillo, C.E. (2014). Mast cell activation: A complex interplay of positive and negative signaling pathways. Eur. J. Immunol. *44*, 2558–2566.

Sigel, E., and Steinmann, M.E. (2012). Structure, Function, and Modulation of GABAA Receptors. J. Biol. Chem. *287*, 40224–40231.

Smart, S.L., Lopantsev, V., Zhang, C.L., Robbins, C.A., Wang, H., Chiu, S.Y., Schwartzkroin, P.A., Messing, A., and Tempel, B.L. (1998). Deletion of the K(V)1.1 potassium channel causes epilepsy in mice. Neuron *20*, 809–819.

van Sonderen, A., Thijs, R.D., Coenders, E.C., Jiskoot, L.C., Sanchez, E., de Bruijn, M.A.A.M., van Coevorden-Hameete, M.H., Wirtz, P.W., Schreurs, M.W.J., Sillevis Smitt, P.A.E., et al. (2016). Anti-LGI1 encephalitis: Clinical syndrome and long-term follow-up. Neurology *87*, 1449–1456.

Song, X., Jensen, M.Ø., Jogini, V., Stein, R.A., Lee, C.-H., Mchaourab, H.S., Shaw, D.E., and Gouaux, E. (2018). Mechanism of NMDA receptor channel block by MK-801 and memantine. Nature *556*, 515–519.

Spatola, M., Petit-Pedrol, M., Simabukuro, M.M., Armangue, T., Castro, F.J., Barcelo Artigues, M.I., Julià Benique, M.R., Benson, L., Gorman, M., Felipe, A., et al. (2017). Investigations in GABAA receptor antibody-associated encephalitis. Neurology *88*, 1012–1020.

Sprengel, R. (2006). Role of AMPA receptors in synaptic plasticity. Cell Tissue Res. *326*, 447–455.

van Spronsen, M., and Hoogenraad, C.C. (2010). Synapse Pathology in Psychiatric and Neurologic Disease. Curr. Neurol. Neurosci. Rep. *10*, 207–214.

Suharni, null, Nomura, Y., Arakawa, T., Hino, T., Abe, H., Nakada-Nakura, Y., Sato, Y., Iwanari, H., Shiroishi, M., Asada, H., et al. (2014). Proteoliposome-based selection of a recombinant antibody fragment against the human M2 muscarinic acetylcholine receptor. Monoclon. Antibodies Immunodiagn. Immunother. *33*, 378–385.

Sun, W., Hansen, K.B., and Jahr, C.E. (2017). Allosteric Interactions between NMDA Receptor Subunits Shape the Developmental Shift in Channel Properties. Neuron *94*, 58-64.e3.

Takeshita, Y., and Ransohoff, R.M. (2012). Inflammatory cell trafficking across the blood-brain barrier (BBB): Chemokine regulation and in vitro models. Immunol. Rev. *248*, 228–239.

Tan, K.O., Tan, K.M.L., Chan, S.-L., Yee, K.S.Y., Bévort, M., Ang, K.C., and Yu, V.C. (2001). MAP-1, a Novel Proapoptotic Protein Containing a BH3-like Motif That Associates with Bax through Its Bcl-2 Homology Domains. J. Biol. Chem. *276*, 2802–2807.

Tanaka, K., Tanaka, M., Onodera, O., and Tsuji, S. (1995). [Paraneoplastic cerebellar degeneration--characterization of anti-Yo antibody and underlying cancer]. Rinsho Shinkeigaku *35*, 770–774.

Tanaka, M., Tanaka, K., Shinozawa, K., Idezuka, J., and Tsuji, S. (1998). Cytotoxic T cells react with recombinant Yo protein from a patient with paraneoplastic cerebellar degeneration and anti-Yo antibody. J. Neurol. Sci. *161*, 88–90.

Tay, S.H., and Mak, A. (2015). Anti-NR2A/B Antibodies and Other Major Molecular Mechanisms in the Pathogenesis of Cognitive Dysfunction in Systemic Lupus Erythematosus. Int. J. Mol. Sci. *16*, 10281–10300.

Titulaer, M.J., McCracken, L., Gabilondo, I., Armangué, T., Glaser, C., Iizuka, T., Honig, L.S., Benseler, S.M., Kawachi, I., Martinez-Hernandez, E., et al. (2013a). Treatment and

prognostic factors for long-term outcome in patients with anti-NMDA receptor encephalitis: an observational cohort study. Lancet Neurol. *12*, 157–165.

Titulaer, M.J., McCracken, L., Gabilondo, I., Armangué, T., Glaser, C., Iizuka, T., Honig, L.S., Benseler, S.M., Kawachi, I., Martinez-Hernandez, E., et al. (2013b). Treatment and prognostic factors for long-term outcome in patients with anti-NMDA receptor encephalitis: an observational cohort study. Lancet Neurol. *12*, 157–165.

Tovar, K.R., and Westbrook, G.L. (2017). Modulating synaptic NMDA receptors. Neuropharmacology *112*, 29–33.

Tovar, K.R., McGinley, M.J., and Westbrook, G.L. (2013). Triheteromeric NMDA receptors at hippocampal synapses. J. Neurosci. Off. J. Soc. Neurosci. *33*, 9150–9160.

Trajkovic, V., Stosic-Grujicic, S., Samardzic, T., Markovic, M., Miljkovic, D., Ramic, Z., and Mostarica Stojkovic, M. (2001). Interleukin-17 stimulates inducible nitric oxide synthase activation in rodent astrocytes. J. Neuroimmunol. *119*, 183–191.

Tüzün, E., and Dalmau, J. (2007). Limbic encephalitis and variants: classification, diagnosis and treatment. The Neurologist *13*, 261–271.

Tüzün, E., Zhou, L., Baehring, J.M., Bannykh, S., Rosenfeld, M.R., and Dalmau, J. (2009a). Evidence for antibody-mediated pathogenesis in anti-NMDAR encephalitis associated with ovarian teratoma. Acta Neuropathol. (Berl.) *118*, 737–743.

Tüzün, E., Zhou, L., Baehring, J.M., Bannykh, S., Rosenfeld, M.R., and Dalmau, J. (2009b). Evidence for antibody-mediated pathogenesis in anti-NMDAR encephalitis associated with ovarian teratoma. Acta Neuropathol. (Berl.) *118*, 737–743.

Ulusoy, C., Tüzün, E., Kürtüncü, M., Türkoğlu, R., Akman-Demir, G., and Eraksoy, M. (2012). Comparison of the Cytokine Profiles of Patients With Neuronal-Antibody-Associated Central Nervous System Disorders. Int. J. Neurosci. *122*, 284–289.

Urb, M., and Sheppard, D.C. (2012). The Role of Mast Cells in the Defence against Pathogens. PLoS Pathog. *8*.

Viegas, S., Jacobson, L., Waters, P., Cossins, J., Jacob, S., Leite, M.I., Webster, R., and Vincent, A. (2012). Passive and active immunization models of MuSK-Ab positive myasthenia: Electrophysiological evidence for pre and postsynaptic defects. Exp. Neurol. *234*, 506–512.

Vigot, R., Barbieri, S., Bräuner-Osborne, H., Turecek, R., Shigemoto, R., Zhang, Y.-P., Luján, R., Jacobson, L.H., Biermann, B., Fritschy, J.-M., et al. (2006). Differential compartmentalization and distinct functions of GABAB receptor variants. Neuron *50*, 589–601.

Werner, C., Pauli, M., Doose, S., Weishaupt, A., Haselmann, H., Grünewald, B., Sauer, M., Heckmann, M., Toyka, K.V., Asan, E., et al. (2016). Human autoantibodies to

amphiphysin induce defective presynaptic vesicle dynamics and composition. Brain *139*, 365–379.

Wheway, J., Obeid, S., Couraud, P.-O., Combes, V., and Grau, G.E.R. (2013). The Brain Microvascular Endothelium Supports T Cell Proliferation and Has Potential for Alloantigen Presentation. PLoS ONE *8*.

Wirtz, P.W., Nijnuis, M.G., Sotodeh, M., Willems, L.N.A., Brahim, J.J., Putter, H., Wintzen, A.R., Verschuuren, J.J., and for the Dutch Myasthenia Study Group (2003). The epidemiology of myasthenia gravis, Lambert-Eaton myasthenic syndrome and their associated tumours in the northern part of the province of South Holland. J. Neurol. *250*, 698–701.

Wright, S., Hashemi, K., Stasiak, L., Bartram, J., Lang, B., Vincent, A., and Upton, A.L. (2015). Epileptogenic effects of NMDAR antibodies in a passive transfer mouse model. Brain J. Neurol. *138*, 3159–3167.

Wu, G.F., and Alvarez, E. (2011). The immuno-pathophysiology of multiple sclerosis. Neurol. Clin. *29*, 257–278.

Yamagata, A., Miyazaki, Y., Yokoi, N., Shigematsu, H., Sato, Y., Goto-Ito, S., Maeda, A., Goto, T., Sanbo, M., Hirabayashi, M., et al. (2018). Structural basis of epilepsy-related ligand–receptor complex LGI1–ADAM22. Nat. Commun. *9*, 1546.

Zhang, N., and Bevan, M.J. (2011). CD8+ T Cells: Foot Soldiers of the Immune System. Immunity *35*, 161–168.

Zhou, Q., and Sheng, M. (2013). NMDA receptors in nervous system diseases. Neuropharmacology *74*, 69–75.

Zong, S., Hoffmann, C., Mané-Damas, M., Molenaar, P., Losen, M., and Martinez-Martinez, P. (2017). Neuronal Surface Autoantibodies in Neuropsychiatric Disorders: Are There Implications for Depression? Front. Immunol. *8*.